DYNAMIC MODELING AND CONTROL OF A HYDROGEN ENERGY SYSTEM

A Thesis

by

IORDANIS KESISOGLOU

Submitted to the Office of Graduate and Professional Studies of

Texas A&M University

in partial fulfillment of the requirements for the degree of

MASTER OF SCIENCE

Chair of Committee,	Stratos Pistikopoulos
Committee Members,	Rabi Mohtar
	M. Sam Mannan
Head of Department,	Stratos Pistikopoulos

August 2017

Major Subject: Energy

ABSTRACT

The population is expected to continue to rise in the future. A greater amount of automobile utilization is expected, leading to a rapid increase in the transportation sector, a sector heavily dependent on CO_2 emission fuels. It would be beneficial to introduce an alternative technology of high efficiency and low emission levels to mitigate the currently increasing GHG emissions to the environment.

Among the fossil fuels, hydrogen is the one with the highest energy density per unit volume when stored in solid form and has the highest abundance on earth. Hydrogen can be stored in solid form within metal hydrides. Due to the fact that hydrogen is initially obtained in very low densities, high pressure must be applied to be stored efficiently. Hence, a high pressure metal hydride, HPMH, tank is suggested for its storage.

The next step is the means of converting hydrogen into energy. Proton exchange membrane fuel cell, PEMFC, is the suggested technology. The major advantage of this technology is that it converts the fuel directly into energy electrochemically, allowing zero GHG emissions, making it sustainable and of high efficiency.

The main disadvantage of hydrogen storage is the long fueling time, which makes it challenging for automobile usage. The next issue is the rate of hydrogen supply to the fuel cell for energy production. As the fuel is initially in solid form it is hard to establish a desired steady flow rate to the engine when required. Finally, the absorption and desorption reactions of hydrogen are temperature-dependent, a variable that must be better analyzed due to its great impact to the system, making it a key component for the improvement of the safety and operability of the system.

This thesis combines pre-established detailed dynamic models of an HPMH tank and of a PEMFC system by utilizing the model building platform named gPROMS. The thesis investigates the filling time parameters, discharge rate parameters and the thermal management of an HPMH and PEMFC units. A PI controller is added for the automatization

of the system that regulates the water flow in the heat exchanger, depending on the hydrogen inflow in the HPMH and the energy output requirements from the PEMFC.

The model results provide a clear visualization of the impact of flow rate, pressure and temperature in the operability of the system. It is concluded that one of the most significant variables in the system is the temperature that can be controlled by the flow rate of the water in the heat exchanger. That variable can lead to a higher fueling rate and steadier desorption rate. Furthermore, the PI control is able to efficiently manage the flow rate of water in the heat exchanger and enhance the operability of the system, allowing higher fidelity and safety. The overall outcome of the thesis supports the claim that the future utilization of this system has potential to mitigate the GHG emissions in the transportation sector as well as introduce higher energy efficiencies compared to the current commercial technology and fuel.

ACKNOWLEDGMENTS

During my interesting work towards the fulfillment of this Master's thesis, a number of people played an important role on my work.

I would like to express my sincere thanks to my advisor, Professor Efstratios Pistikopoulos, for his stimulating suggestions that allowed a more in depth representation of my work. Furthermore, I would like to express my gratitude to my committee members Professor Rabi Mohtar and Professor M. Sam Mannan for their guidance and share of ideas regarding futuristic and safety aspects of the project.

I would like to thank Mr. Gerald Ogumerem and Dr. Nikolaos A. Diangelakis for their extended guidance, support and patience throughout the project.

I would like to thank all my Texas A&M lecturers for their great influence and knowledge that allowed a more spherical analysis of this thesis.

Finally yet importantly, I would like to thank my family for their support, faith and love.

CONTRIBUTORS AND FUNDING SOURCES

Contributors

This work was supervised by a thesis committee consisting of Professor Efstratios Pistikopoulos (advisor) and Professor Rabi Mohtar of the Department of Biological and Agricultural Engineering and Professor M. Sam Mannan of the Department of Chemical Engineering.

All work for the thesis was completed independently by the student.

Funding Sources

There are no outside funding contributions to acknowledge related to the research and complication of this document.

TABLE OF CONTENTS

LIST OF TABLES

LIST OF FIGURES

1. INTRODUCTION

The growing demand for energy and the seasonal variabilities in energy supply and demand has engendered the need for a more efficient energy storage system (EnergyEIA, 2013). Energy storage as hydrogen has a high potential of being the major energy option because of its energy density and energy retention. Hydrogen usage is not a new case, in fact various technologies have been used to produce, transport and store it. However, with the advent of fuel cell vehicles (FCV) there is a growing need for a safer, denser energy system. The purpose of this thesis is the representation and analysis of an integrated energy system, from storage to utilization of fuel reaching efficient operating conditions that would allow this technology to compete with the commercial internal combustion engine one.

Hydrogen can be stored in different states using different technologies and these technologies can be categorized into physical and chemical storage processes. Physical processes include all processes that do not change the hydrogen chemically; that means that hydrogen can be in the gaseous or liquid state as pressure or temperature fluctuates. Specifically, such hydrogen states and processes are: gas as in compressed gas storage, subcritical fluid as in cryo compressed (high pressure) or liquefied (low pressure), adsorbed in porous high surface area material. Chemical hydrogen storage is defined as the hydrogen storage in materials that form a strong covalent bond with hydrogen (ENERGY.GOV, 2016). Complex metal hydrides are a common example of chemical hydrogen storage where as in all chemical storage cases there are low binding energies among hydrogen atoms (Eberle, Felderhoff, & Ferdi, 2009). We shall further discuss the different advantages, disadvantages and alterations present.

1.1. Physical storage

Compressed hydrogen storage is the most widely known technique of hydrogen storage (Sandi, 2004). Yet, concerns arise related to weight and volume storage efficiency, high costs and irregularities on storage tanks and system integration. More specifically, in this case, the hydrogen is stored under high pressures in modified hydrogen tanks that can withstand pressures that vary from 350-700 bars. This introduces high costs of energy needed to pressurize the gas and creates financial concerns when pressure drops during operation. Finally, hydrogen's energy density even in 10,000 psi pressure is of 4.4 MJ/L compared to that of gasoline which is 31.6 MJ/L shows the low energy content of hydrogen in gas state (Sandi, 2004).

The process of liquid hydrogen is an operating process that keeps hydrogen in the liquid phase. In order to keep the hydrogen in liquid form due to its physical properties the process utilizes cryogenic temperatures, specifically hydrogen's boiling point at 1atm is $-252.8^{o}C$. In the case of cryo compressed processes the only addition is that the liquid hydrogen is stored under pressure. In the liquid form the hydrogen energy density is equal to 8.4 MJ/L which is almost double the previous case. Although this method acquires good volume and weight storage efficiency, long-term storage leads to fuel losses associated with elevated temperatures (boil-offs) and high costs of energy needed for the liquefaction of hydrogen (Sandi, 2004).

1.2. Chemical storage

In the metal hydride storage methodology, hydrogen can be stored within metal hydrides through the formation of a chemical bond in nanostructure materials. The advantage of metal hydrides is that it can absorb or desorb hydrogen with an appropriate change in temperature. In the MH storage system there are two kinds of processes; an exothermic process and an endothermic process. The exothermic reaction causes the hydrogen absorption and the endothermic causes the hydrogen desorption. It is assumed

that the flow rate of hydrogen in both processes is the same. (Endo, Matsumura, & Kawakami, 2016). Studies have shown that the hydrogen compression ratio decreases as the flow rate increases (Endo, Matsumura, & Kawakami, 2016).

Furthermore, carbon based materials with porous structures have considerable amounts of hydrogen storage capacities even at room temperature. This characteristic is based on the high surface area and sufficient amount of available pores. Limitation arises from the fact that the cycle mechanism of absorption and desorption is yet to be fully understood as well as their volume that they require (TZIMAS, PETEVES, & VEYRET, 2003).

In the cryo adsorption process the hydrogen can be stored on the surface or within solids with a process called absorption with operating conditions of $-193^{o}C$ & $0.2-0.5\ MPa$. These extreme conditions set limitations associated with heat losses to the environment (Energy, 2016).

Knowledge of the properties of hydrogen increases ones awareness of the hazards involved in handling it. Hydrogen is flammable and has a wide flammability range, with temperature reaching as high as $2045^{o}C$ compared to gasoline at $1247^{o}C$. The amount of energy required for its ignition is 20 μJ in air and the expansion volume of the gas is 850-1000 times its original volume depending on the outer pressure. In addition, hydrogen can reduce the performance of contaminated materials and piping materials such as carbon steel. Due to its small molecular size it can pass through porous or contaminated materials making them less elastic and more fragile. Thus material selection is a vital design consideration when using hydrogen. These characteristics make it a liability for all methodologies and especially if it is to be preferred as a fuel in automobiles that are parked in close small areas (Glass & Glass, 2000) (Flamberg & Denny, 2010). Table 1 lists some of the physical and chemical properties of hydrogen.

Table 1: Physical and chemical properties and characteristics of hydrogen. (Glass & Glass, 2000)

Property/Characteristic	Values (approximate)
Color	NONE
Odor	NONE
Toxicity	Nontoxic
Density, liquid (boiling point)	4.4 lb/ft^3 (0.07 g/cm^3)
Boiling point (1 atm)	-423.2 ^{o}F (-252.9^{o}C)
Critical temperature (188.2 psia)	-400.4 ^{o}F (-240.2^{o}C)
Stoichiometric mixture in air	29 vol%
Flammability limits in air	4-75 vol%
Detonation limits in air	18-60 vol%
Minimum ignition energy in air	20μJ
Auto ignition temperature	1,085^{o}F (585^{o}C)
Volume Exapansion: Liquid (-252.9^{o}C) to gas (-252.9^{o}C) Gas (from -252.9^{o}C to 20 ^{o}C) Liquid (-252.9^{o}C) to gas (-20^{o}C)	 1:53 1:16 1:848

When storing hydrogen in gas cylinders, they must be protected from corrosion and heat (direct sunlight). In most cases there are thermally activated Pressure Reducing Desuperheating valves and the only limitation is that there should be enough heat to activate them. Elevated temperature can cause the eruption of the tank and lead fragments of its cover over 82 meters from the tank, even for tanks as small as the ones of a car (Sandi, 2004). In addition, extra care must be taken with regard to the condition of the vessels; in cases that there is an onboard vessel, extra care must be placed as phenomenical insignificant issues can be fatal. For example, the car battery can weaken the vessel's wrap, leading to a point where the inner pressure becomes higher than the one that the container can withstand. Specifically, each storage method requires additional precautions to be taken due to the alternation of the storage processes.

In compressed hydrogen storage containers, "fast fueling" of hydrogen at elevated pressures can lead to extreme temperatures; this may damage the vessel, leading to rapture. In order to deal with this issue, the fuel's temperature is lowered before filling the container. Also, the materials used to store hydrogen should be taken under consideration

due to their embrittlement from long contact with hydrogen and their deterioration that can withstand as stated above (Sandi, 2004).

Liquid hydrogen is denser than gaseous thus it has a higher energy density. This means that a greater amount of hydrogen can be stored in liquid state compared to a gaseous one, and as Table 1 shows, the volume expansion would be even greater in case of a rapid increase of temperature. This comparison shows that although there are similar concerns and actions taken regarding the storage when storing liquid and gaseous hydrogen, in the case of an accident the outcome would be much more catastrophic for liquid hydrogen storage case. An additional issue regarding liquid hydrogen is that it must remain in low temperatures because if it is boiled off it must be vented out. For this reason, high volumetric cylinders must be used in order to minimize the heat losses (Flamberg & Denny, 2010). In addition, when the fuel tank is filled it must be sufficiently cooled down as there are major heat losses to the environment that can lead to increase in the temperature of the system and major boil offs, losses, of hydrogen to the environment. For this reason, although liquid hydrogen has a higher energy density than compressed hydrogen gas, liquid hydrogen has higher costs associated with the tank size and weight as well as hydrogen losses and energy required for the process (Flamberg & Denny, 2010).

In comparison to cooled liquid and compressed hydrogen gas, solid hydrogen storage in hydrides is preferred for stationary storage (Endo, Matsumura, & Kawakami, 2016). This is due to the more normal operating temperatures and pressures. It is a compact system which minimizes space consumption; in addition, it is safer than the other hydrogen storage systems due to its solid state and energy reliability (Endo, Matsumura, & Kawakami, 2016).

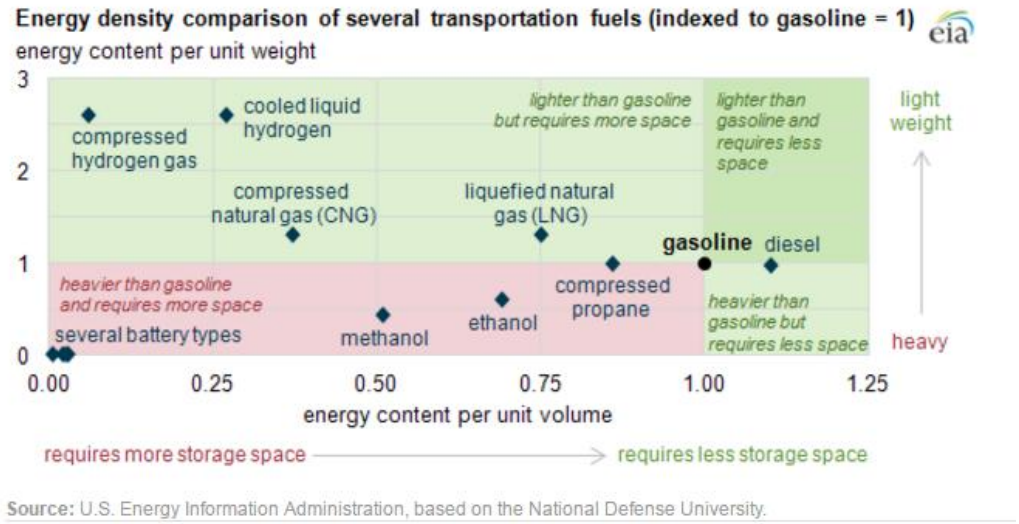

Figure 1: Energy density comparison of several transportation fuels (EIA, 2013).

Energy density is the amount of useful energy per volume of a substance. It is comparable to specific energy, which represents the amount of useful energy per mass of a substance (Dynamics, 2014). Hydrogen is the lightest fuel per energy unit (see Figure 1) and at the same time has a very low energy density due to its physical properties (see Table 1). However, in a condensed form, its energy density increases dramatically. Hydrogen as a fuel has a higher amount of energy per-weight when compared to gasoline. Essentially, various fuels require different kinds of equipment and storage tanks for the production of energy.

2. REVIEW OF METAL HYDRIDE (MH) SYSTEMS

2.1. Introduction to the properties of MH systems

Metal hydrides (MH) allow great amounts of hydrogen storage capacities and they are governed by two temperature driven processes: an absorption and a desorption reaction. Hydrogen absorption is an exothermic reaction, a chemical reaction that radiates energy in the form of heat. This heat produced inhibits the rate of reaction of the process. Hydrogen desorption is an endothermic reaction and heat is required for the process to take place; thus, the reaction absorbs heat from the surroundings (Valverdea, Rosaa, del Reala, & Arceb, 2013). In a pressurized metal hydride system, the temperature determines if the system absorbs or desorbs hydrogen, making heat transfer the most important parameter of the system. Figures 2 and 3 represent these processes of $LaNi_5$ MH (Berube, Radtke, & Gang, 2007).

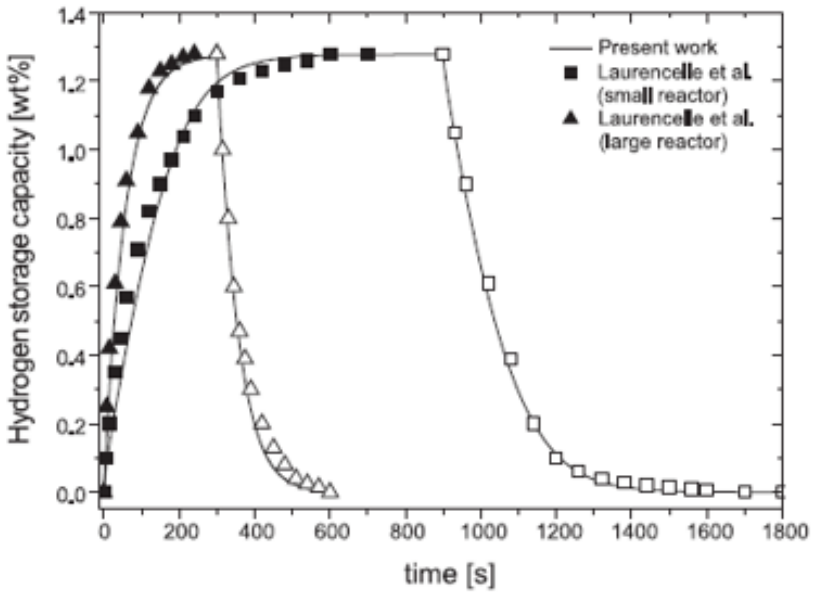

Figure 2: Hydrogen storage capacity with time of absorption (Full symbols) and desorption (hollow symbols) (Talagañisa & Meyerb, 2011).

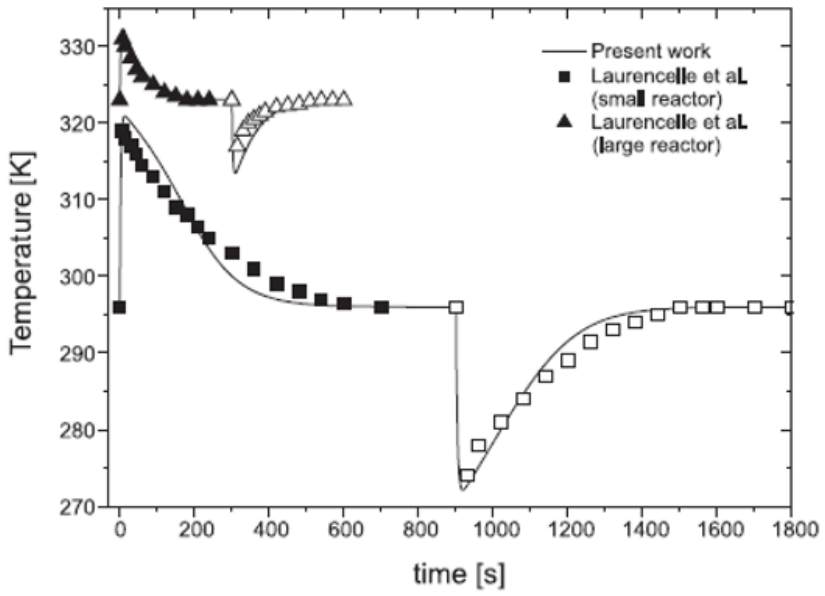

Figure 3: Temperature with time of absorption (Full symbols) and desorption (hollow symbols) (Talagañisa & Meyerb, 2011).

The graphs depict how the temperature and hydrogen capacity vary with time in the two processes. An extra comparison is made, showing that an increase in the reactor size allows higher operating temperatures, causing a decrease in the sorption time (Talagañisa & Meyerb, 2011).

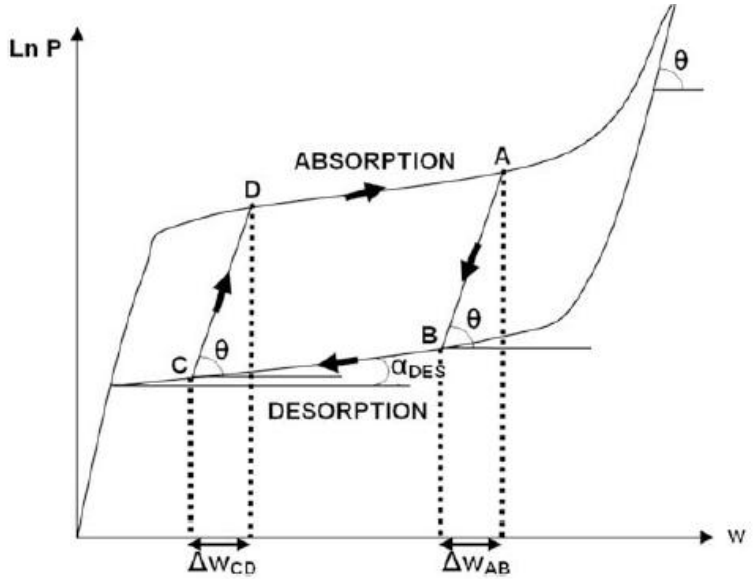

Figure 4: Hysteresis model of a MH system (Payáa, Linderb, Corberána, & Laurienb, 2009).

When pressure is plotted against hydrogen stored, it can better represent the cycling process that takes place, giving a better visualization of the system. In Figure 4, the two sorption processes are represented. AB is for absorption to desorption and CD is for desorption to absorption. An initial hydrogen concentration value is assigned for every sorption process. In the system, AB and CD include an alternation in the MH temperature, concentration, enthalpy of reaction and equilibrium pressure.

Pressure is well known for its effect on temperature and thus impact on the system. Specifically, pressure effects on the systems are studied in terms of hydrogen capacity, operability, and efficiency (Talagañisa & Meyerb, 2011).

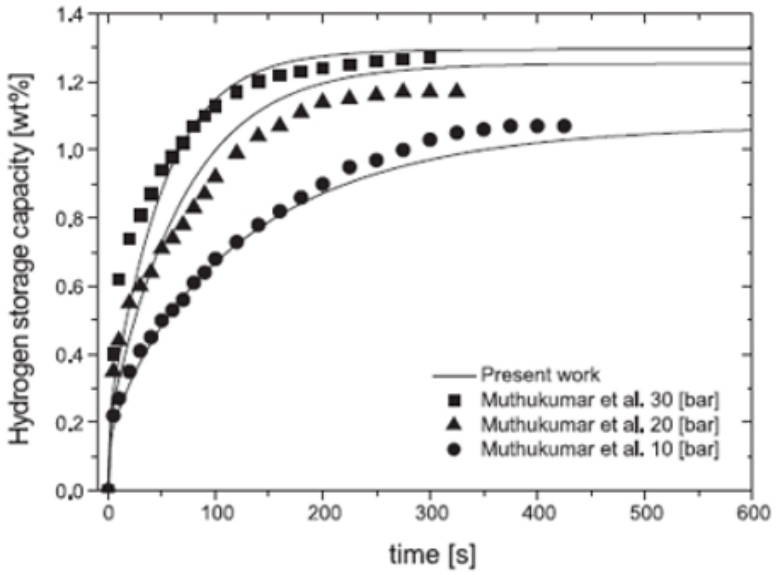

Figure 5: Pressure impact on the hydrogen absorption (Talagañisa & Meyerb, 2011).

Figure 5 suggests that as the operating pressure increases, the amount of hydrogen absorbed increases as well, which means that absorption rate is higher in higher pressures of the system.

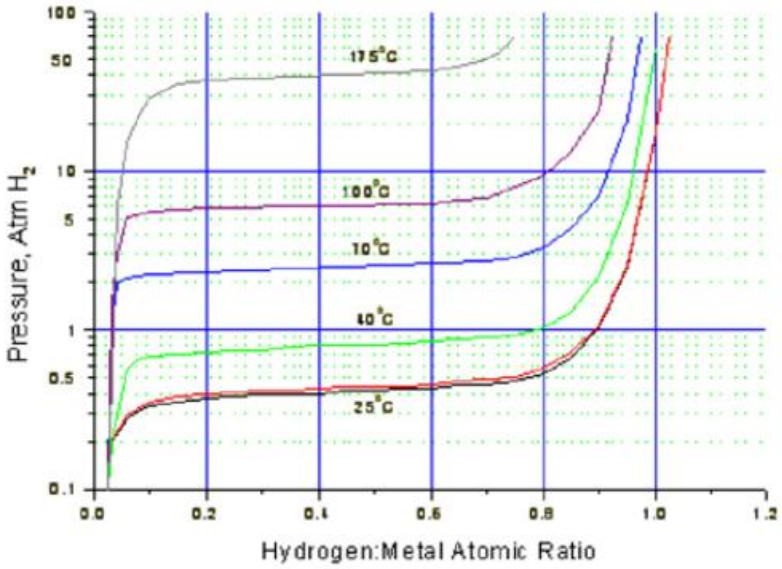

Figure 6: P-T-C equilibrium correlation (Ragheb, 2011).

Figure 6 represents another characteristic of pressure; higher operating temperature leads to higher equilibrium pressure and vice versa. The operability at different T and P is feasible by the modification of the alloy's production techniques and composition. Higher heat transfer allows higher sorption reaction rates. This allows higher flow rates to be processed (Ragheb, 2011).

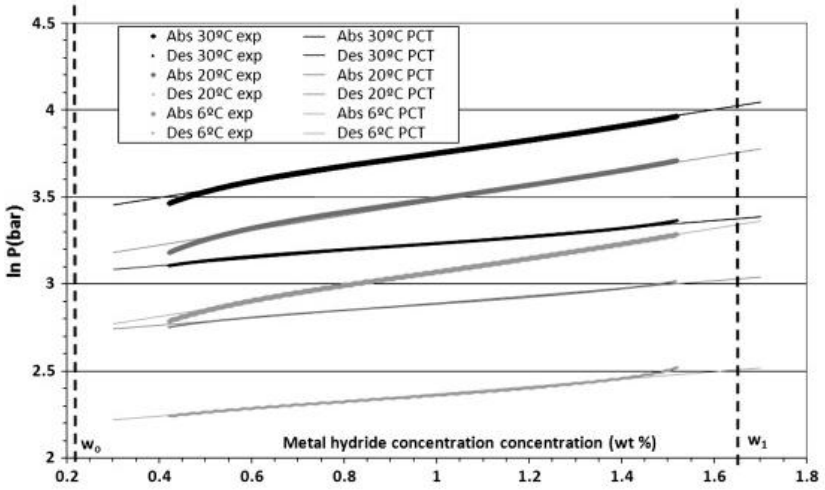

Figure 7: P-C-T equilibrium correlation (Payáa, Linderb, Corberána, & Laurienb, 2009).

In Figure 7, there is a noticeable difference between the absorbed and desorbed equilibrium pressures; the sorption processes do not follow the exact same root. Desorption takes place during the cooling period of the system, while absorption takes place during the heating. In Figure 7 there is a representation of a P-C-T graph for fixed temperatures at the pressure equilibrium. The transition between absorption and desorption takes place out of the plateau area in the β- phase (Payáa, Linderb, Corberána, & Laurienb, 2009).

2.2. Hydrogen absorption and desorption parameters among MH

Metal hydrides form metal atoms between hydrogen atoms and the host. There are two different types of metal hydrides that can be formed; the α-α phase where only a certain amount of hydrogen is absorbed and a β-β phase were a hydride is fully created, as shown in Figure 8 (Lamari-Darkrimb & Sakintunaa, 2007).

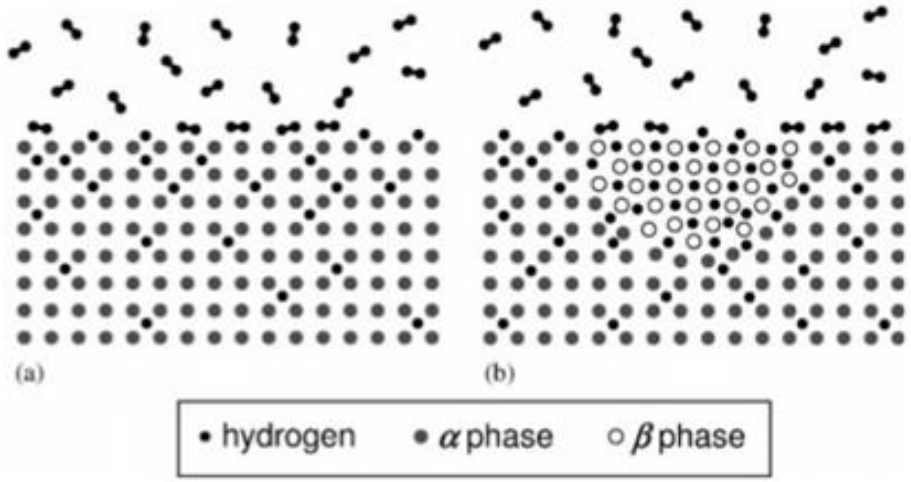

Figure 8: Phase cases representation followed by hydrogen in MH (Berube, Radtke, & Gang, 2007).

Hydrogen undertakes first physisorption, where the molecules are making contact with the metal surface without the formation of any chemical bonds through electrostatic attraction or van der Waals forces. Physisorption is a reversible process that is closely correlated to temperature and pressure.

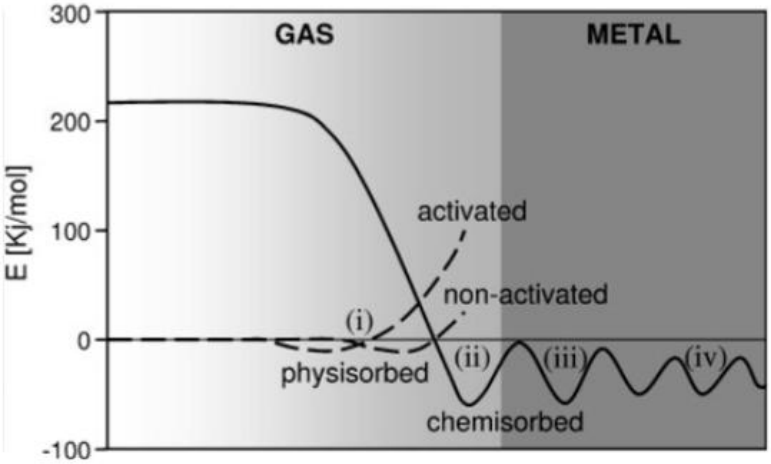

Figure 9: Potential energy curve for the Lennard Jones potential for hydrogen binding to a metal (Berube, Radtke, & Gang, 2007) .

Certain values of pressure and temperature allow the adhered hydrogen molecule to dissociate at the surface, forming new bonds in a process called chemisorption, Figure 9. The chemisorption process is followed by a movement of the hydrogen atoms to sites deeper in the metal, also known as the α phase. Increasing the concentration of hydrogen in the α phase increases the H-H interactions, which start to play an important role, leading to the next phase, named β- phase. This phase is associated with volumetric expansion, change of the crystalline structure and the formation of a nucleation energy barrier. This is a result of the energy between the two phases and the increase in volume (Berube, Radtke, & Gang, 2007).

Each metal has a different ability to dissociate hydrogen (Sakintunaa & Lamari-Darkrimb, 2007); the parameters that characterize this ability are: the purity, the surface structure and the morphology of the MH. A MH material is considered as an optimum material if it meets the following descriptions: medium dissociation pressure, high hydrogen capacity per unit mass as it determines the amount of energy that can be released, low heat of formation that minimizes the energy required to release hydrogen, low temperature of dissociation, low dissipation heat when an exothermic hydride is formed, fast kinetics, reversibility, cyclebility, low energy losses when hydrogen is charged and discharged, high stability on impurities (i.e. in oxygen and moisture) to be able to withstand a long life cycle, high safety and low cost of recycling (Lamari-Darkrimb & Sakintunaa, 2007).

For weight reasons and reasons regarding the number of hydrogen atoms per atom of metal there is a preference for light metals such as Be, B, Al, Na, Li, Mg that can form many different alloys. Heavier metals are used only as catalysts and to assist with alternating some of the properties of the light metals. Thus, different heavy metals have different impacts on MH. Among them magnesium alloys are the ones that are preferred due to their increased storage capacity by weight, inexpensiveness, good heat resistance, reversibility, vibration absorbing and recyclability. The hydride with the best energy density is MgH_2 but it requires a high temperature for hydrogen desorption and it is highly oxidized by impurities (i.e. oxygen and air) and has slow kinetics in hydrogen release. The

main concern has been reducing the desorption temperature which prohibits it for onboard usage. Increasing the kinetics of the two process reactions by different means is another important issue (Lamari-Darkrimb & Sakintunaa, 2007).

There are many MH with different characteristics. Complex aluminum hydrides acquire great hydrogen storage capacity but have poor kinetics and irreversibility. The only way that such a metal can be utilized is by the usage of catalysts and hydrides that will change its irreversible character (Lamari-Darkrimb & Sakintunaa, 2007). Lithium Alanates although very appealing for their high hydrogen content, they have a very high equilibrium pressure even in room temperature when they contain hydrogen. This class of MH is classified as unstable hydrides, which cannot be rehydrated again and have a high decomposition rate. Mg_2NiH_4 is the center of attention due to its high storage capacity, low weight, low cost, low toxicity, its bonding (chemical) properties and the unusual structure that it forms (Lamari-Darkrimb & Sakintunaa, 2007).

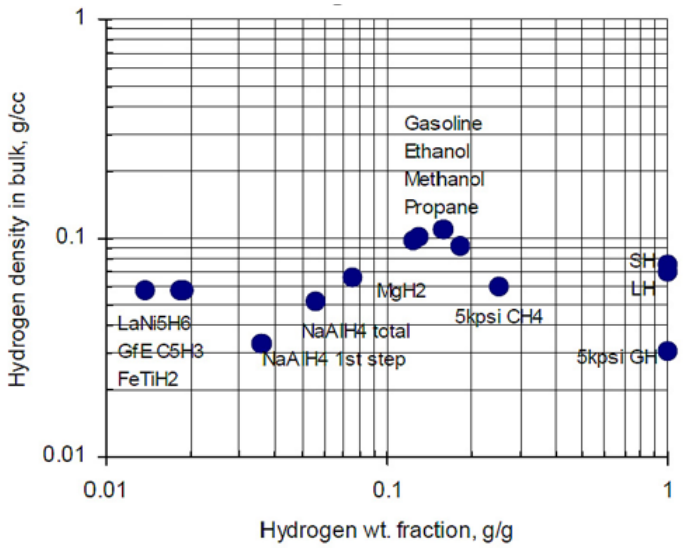

Figure 10: Graph of Hydrogen density in g/cc with Hydrogen wt fraction in g/g (Heung, 2003).

Figure 10 compares the hydrogen density of different MH in terms of weight that hydrogen adds to the material and in terms of density. Increasing the storage of hydrogen

depends heavily on the volume and weight parameters. In equivalent terms of weight and density, other energy fuels are included to provide information of how much better or worse each MH is comparably. From the graph, MgH_2 and $LaNi_5$ have the best descriptions with high hydrogen density and lower weight. These descriptions allow MgH_2 and $LaNi_5$ to compete with the commercial energy resources.

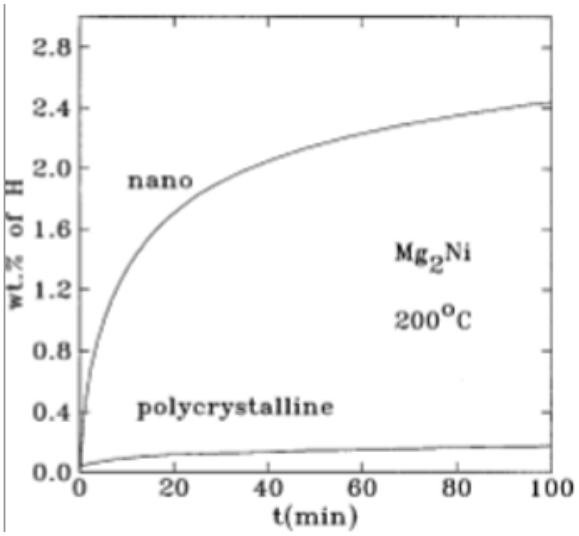

Figure 11: Rate of hydrogen absorption of polycrystalline with nano-crystalline Mg2Ni at 200 ^{0}C (Olsen & ZaluskiJ, 2001).

The structure affects the diffusion of the hydrogen within the alloy while the hydride is formed. Figure 11 suggests that nano-crystalline samples were able to store a good amount of hydrogen in a short period of time, where polycrystalline was not able to absorb much. Both metals were tested in their first cycle without any prior activation done on them (Olsen & ZaluskiJ, 2001) .

An alternation in the structure of the hydride can take place by a method called ball milling. This methodology uses elements that decrease its stability and at the same time uses a proper catalyst that improves the kinetics of the sorption processes. Ball-milling creates defects and micro structures on the already increased surface area inside the

material. The defects on the surface of the metal allow hydrogen to diffuse more easily due to the lower activation energies and the increased contact surface of the metal with the catalyst (Lamari-Darkrimb & Sakintunaa, 2007). The crystalline alloy that is created through ball milling has much better surface properties, in contrast to when it is created by a metallurgical method.

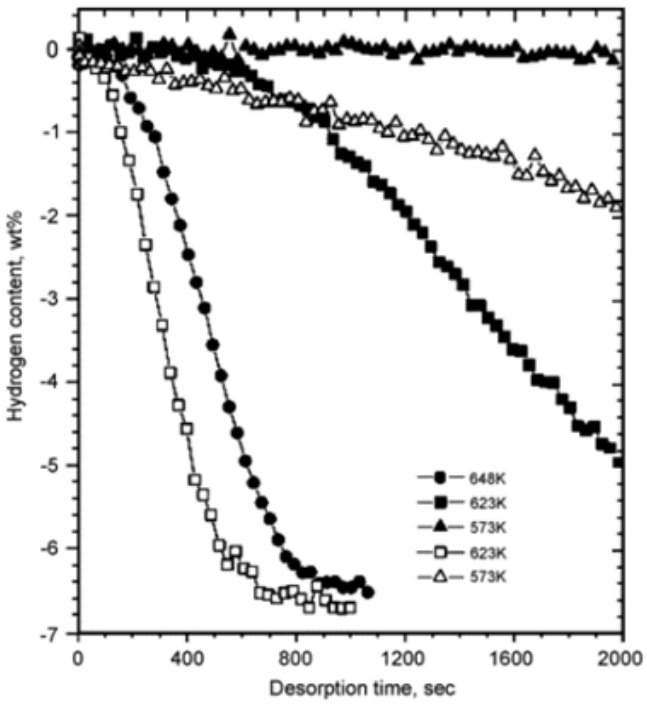

Figure 12: Hydrogen desorption curves of unmilled MgH_2 (solid symbols) and ball-milled (hollow symbols) MgH_2 under a hydrogen pressure of bar (Lamari-Darkrimb & Sakintunaa, 2007).

It has been noticed that milled MgH_2 has a faster desorption rate and reduced activation energy compared to the unmilled one as shown in Figure 12. Another characteristic is that ball milled alloys do not require to be activated in contrast to traditional methods. Milling reduces the pressure needed for hydrogen desorption by

decreasing the activation energy, allowing lower operating temperature conditions (Lamari-Darkrimb & Sakintunaa, 2007).

The milling time of the hydride is another parameter that can affect the efficiency of the metal.

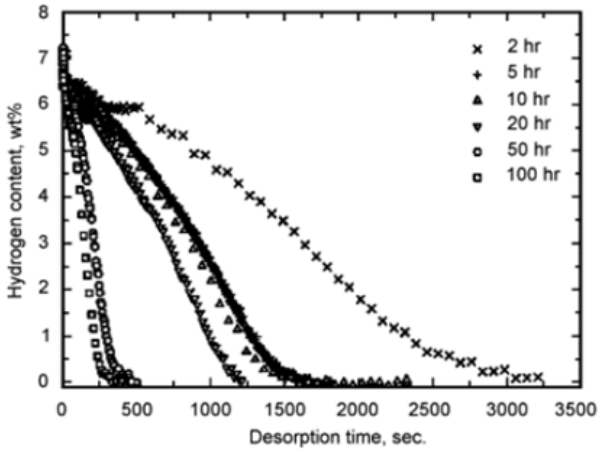

Figure 13: Desorption curves of magnesium catalyzed with 0.1 mol% Nb_2O_2 and milled for 2, 5, 10, 20, 50 and 100 hours at 573 K in vacuum (Lamari-Darkrimb & Sakintunaa, 2007).

Ball-milling enhances the creation of active sights, allowing hydrogen to penetrate the hydride more easily, but these powders are usually in the range of 60 to 100 μm. Figure 13 shows that the milling time of the MH increases the desorption rate. Enhancing ball-milling time produces smaller particles that decrease the formation of hydride layers greater than 50 μm (Lamari-Darkrimb & Sakintunaa, 2007).

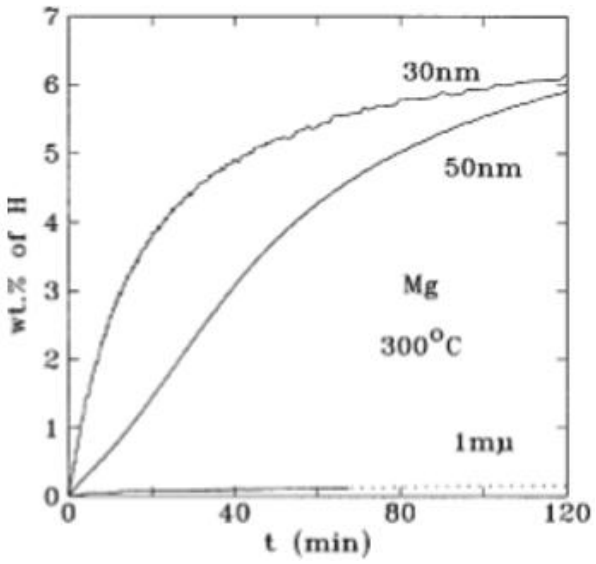

Figure 14: Effect of grain size on hydrogen absorption of ball-milled magnesium powder at 300 C on the first cycle without activation (Olsen & ZaluskiJ, 2001).

The size of the hydride grain after being ball milled plays a vital role in the efficiency of the system as Figure 14 shows. A decrease in the grain size increases surface contact area where hydrogen can be absorbed, leading to faster filling time and to higher uptake rate. The absorption rate is associated with the number of phase boundaries that exist as well as the porous surface structure of the alloy. Nano-crystalline alloys increase the kinetics of the system (hydrogenation and dehydrogenation), even at lower temperatures. The limitation in operating at reduced temperatures is the reduction of the hydrogen gaining capacity and the kinetics of the system (Lamari-Darkrimb & Sakintunaa, 2007).

In contrast, the advantage of having a sintered mass over loose powder is that there is a lower particle migration, higher safety, and more efficient gas distribution. The issue of low heat transfer can be solved with the creation of an efficient heat exchanger (Schüth & Felderhoff, 2004). Lower operating temperatures decreases the rate of the reaction and although it is good to have lower operating conditions, temperature should be high enough for the reaction to be carried on efficiently. Other techniques such as sputtering and vapor

condensations can be as good if not better than ball-milling for the initiation of nano-crystalline structures (Olsen & ZaluskiJ, 2001).

An optimum MH must withstand a long life cycle (Energizer, 2016) (Lamari-Darkrimb & Sakintunaa, 2007). Within 100 sorption cycles there is not much degradation of the MH properties as a result of the temperature alternations (Schüth & Felderhoff, 2004). After a greater number of cycles, the sorption processes can take up and release smaller amounts of hydrogen as a result of the agglomeration of the particles during the cycling. Mish metals as they are called, or Mm, are: Ce, La, Nd and Pr. They are important for these processes as they increase the cycle stability. The drawback is that as the concentration of these metals increases within the MH, the hydrogen capacity decreases, and the reaction rate decreases (Lamari-Darkrimb & Sakintunaa, 2007). Within the range of the first thousand cycles there was an increase in the uptake capacity and a higher desorption time as a result of crystallite growth and structural relaxation. To avoid any storage capacity loss there must be an increase in the operating temperature of the system. However, in the long run, there will be a decrease in the hydrogen capacity and increase of the filling time (Lamari-Darkrimb & Sakintunaa, 2007). In the case of magnesium hydride, the MH was able to withstand a great number of cycles because the larger grains were always taking back their nano-crystalline structure after desorption (Olsen & ZaluskiJ, 2001). The resistance of the alloys in decreasing capacities due to impurities is a very important factor especially for on board applications. These impurities are associated with the contact of a metal hydride with the following elements: N_2, O_2, CO_2 and CO.

Catalysts are used to increase the kinetics of the system by increasing the rate of hydrogen dissociation to the metal. Such a catalyst is palladium, but it is associated with high costs, making it unfavorable for grand scale applications (Lamari-Darkrimb & Sakintunaa, 2007). Catalysts can be effectively used in a reaction by enhancing the time and cost efficiency. Catalysts provide alternative roots with lower energy barriers. Different catalysts can be used to boost desorption, and other catalysts can be used to enhance the absorption or both processes depending on the nature of the MH and the operating conditions. In summary, the impact of the catalyst and structure on the rate of hydrogen absorption can increase the efficiency of the system. The nano catalysis allows

hydrides to eliminate any fear of poisoning when it comes in contact with oxygen, even for long time periods. There is no further need in operating in high temperatures prior to absorption to avoid impurities (Olsen & ZaluskiJ, 2001).

The creation of alloys with different characteristics than the pure metals can increase the plateau pressure values (Olsen & ZaluskiJ, 2001). In some cases, there is an increase in the instability of the system leading to higher reaction rates in lower temperatures, making it more efficient (Olsen & ZaluskiJ, 2001). In some other cases, the thermal conductivity of a MH is enhanced (Corgnale, Hardy, Tamburello, Garrison, & Anton, 2012). The conclusion is that each catalyst has a different impact on each MH.

Table 2 summarizes the reasons for performing different alternations to the MH before usage. Parameters that make a MH preferable are: a high storage capacity and kinetics; a decrease in the energy required to form it (enthalpy of formation); an increase of the heat transfer that it can operate, and thus be more energy efficient; the cyclability, which represents the ability of MH to withstand more sorption processes and a lower releasing temperature so that MH is not a liability, preventing from heating the system too much when desorption takes place.

Table 2: Summary of the benefits and detriments of Nano engineering on selected metal hydride properties. (Berube, Radtke, & Gang, 2007)

	Storage Capacity	Kinetics	Enthalpy of formation	Heat transfer	Cyclability	Release temperature
Increase surface area	Increase physisorption	Increased surface dissociation	Decreased (nano-gained materials)	Decreased	Potentially decreased	Potentially decreased
Increased grain boundaries	Decreased	Increased diffusion (a phase)	Potentially decreased	Decreased	Potentially decreased	Potentially decreased
Doping with catalysts	Decreased for excessive doping	Increased	No observed effect	Decreased	May help reversibility	Decreased
Increased porosity	Potentially increased physisorption	Faster gas diffusion	No observed effect	Decreased	No observed effect	No observed effect
Formation of nano-composites	Mean of the components	Increased	Potentially decreased	Decreased	Potentially increased or decreased	Decreased
Doping/ allying	Potentially increased or decreased	Potentially increased	Decreased	Potentially increased or decreased	Potentially increased or decreased	Decreased

2.3. Storage MH comparison

A comparison of different storage methods allows a better determination which should be preferred and which ones should not.

Table 3: Comparison of hydrogen storage technologies (Visaria, Mudawar, & Pourpoint, 2010)

	Compressed H2 Gas	Liquid H2	Chemical Hydride	Complex MH	HPMH	Physisorbing metarials
Storage / Charging pressure	Up to 700 bar	1-2 bar	1-2 bar	~150 bar	Up to 500 bar	20-40 bar
Storage temperature	Room temp.	20 K	Room temp.	~500 K	~350K	~77K
Material and system volumetric capacity (g/L)	40 Sys (25)	70.8 Sys (30-35)	100 Sys(30)	100(30-160) Sys (20-30)	50-150 Sys (40)	30-40
Material and system gravimetric capacity (wt%)	Sys (4.7 at 700 bar)	Sys (5-6)	10 Sys(3-4)	4-7 Sys (1-2)	2-3 Sys (1-2)	4-8 Sys (2-4)
Fill time (min)	5-10	7-9	N/A	8-12	5	10

Table 3 Continued: Comparison of hydrogen storage technologies (Visaria, Mudawar, & Pourpoint, 2010)

	Compressed H2 Gas	Liquid H2	Chemical Hydride	Complex MH	HPMH	Physisorbing metarials
Onboard reversible	Yes	Yes	No	Yes	Yes	Yes
Desorption temperature, pressure	Room temp., 3.5 bar	N/A	>500 K, 3.5 bar	400 K, 3.5 bar	Room temp., 3.5 bar	77-100 K, 3.5 bar
Durability and repeatability	N/A	N/A	Need to be regenerated for reuse	Sensitive to impurities	Sensitive to impurities	Sensitive to impurities
Reactivity to air and moisture	N/A	N/A	Stable, no	Pyrophoric materials, Yes	Pyrophoric materials	Yes
Heat of reaction	N/A	N/A	~55 kJ/mole H2	~40 kJ/mole H2	~15-25 kJ/mole	~4-6 kJ/mole

2.4. Pressurized MH "Hybrid" tanks

The HPMH as a storage technology is preferred due to its high hydrogen gas purity, safety, compact system, reliability, and absence of moving parts (Endo, Matsumura, & Kawakami, 2016). High pressure systems should be used to improve the capacity in tank

materials with low density and high withstanding stress, Figure 15. Low pressure systems for tank materials should be utilized with higher density, including MH with high hydrogen storage capacity (Hardy & Corgnale, 2012). Increased pressures allow the amount of hydrogen stored in the absorption process to increase as well. This makes the HPMH system have higher volumetric capacity compared to all other storage systems at 40 g/L. When storing hydrogen under high pressure (over 50 bars), the hydrogen is stored chemically within the MH and as compressed gas in between the empty space within the packed bed material. Such storages are called "Hybrid tank". The advantage of such a hydride system is that it decreases the filling time (increased absorption rate) and that hydrogen can be released very quickly as some of it is stored in the gaseous phase and it does not have to be released only through desorption (Hardy & Corgnale, 2012).

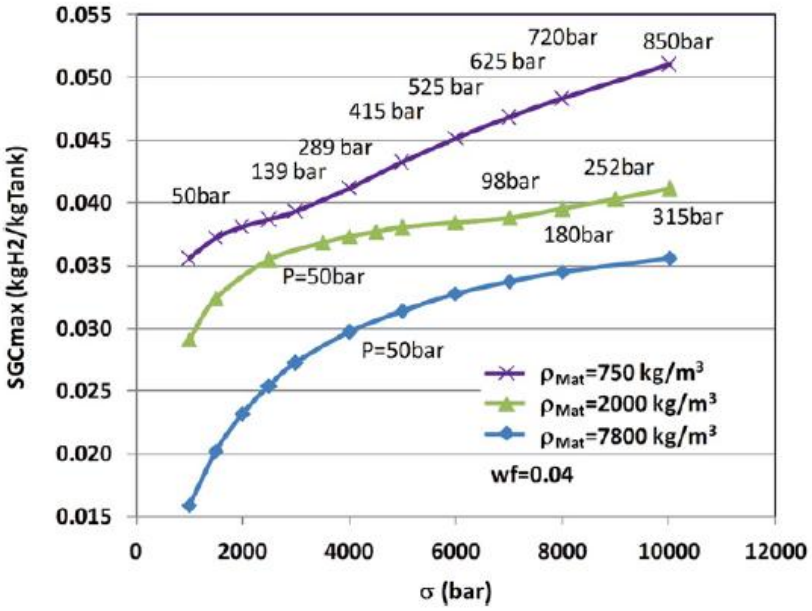

Figure 15: Optimum SGC for operating pressures of 50-850bars and alternating material properties (density and pressure) keeping the rest of the variables constant. (Claudio Corgnale B. J., 2012).

The disadvantage is that this process has low gravimetric capacities and increased weight due to the high pressure cylinders and the cooling system (Mudawar, Visaria, &

Pourpoint, 2010). They key parameter in a HPMH systems is the heat exchanger. For attaining a certain flow rate, the heat exchanger component must be taken under consideration (Visaria, Mudawar, & Pourpoint, 2010). One of the characteristics of HPMH is that the MH must be activated before it is capable of absorbing hydrogen. The size of the MH particles is too big to allow any hydrogen absorption. The activation process consists of high pressure repeating cycles and heating in vacuum. The particles break into smaller pieces that can now react with hydrogen. When the MH is activated, it can ignite when exposed to any oxidizer like air and the temperature of ignition can be as high as 1000 ^{o}C. The high pressure and the igniting nature of the activated MH causes safety issues related to this technique (Visaria, Mudawar, & Pourpoint, 2010). As the particle size decreases the hydrating time needed decreases and the reaction rate increases (Visaria, Mudawar, & Pourpoint, 2010). It is preferred to have particles as small as possible even in powder form, to be able to maximize the contact surface area. That will cause the sorption processes rates to increase, minimizing the filling time.

Heat transfer is one of the most important parameters in a temperature governed system. As the thermal conductivity increases, there will be more energy transfer allowing a lower filling time because the reactions can operate at higher rates. The lower the temperature conditions, the shorter the filling time is. For our system it will be preferred to attain high energy transfer and keep the temperature low. This allows to get rid of the heat released as fast as possible and keep a high rate of absorption.

To conclude, the heat exchanger is the most important component of the system as it is responsible for storing and releasing the H in and from the MH within a short period of time. The thickness of a MH is an important design parameter of the heat exchanger as it determines the filling time needed; the higher the surface area the shorter the filling time (Visaria, Mudawar, & Pourpoint, 2010). The cooling rate must be sufficient enough to decrease the temperature below the equilibrium point in order for the reaction to continue. Finally, the coolant's temperature and the thermal contact resistance are important parameters for the reason explained above (Visaria, Mudawar, & Pourpoint, 2010) .

2.5. On board hydrogen production system

Energy can be converted into hydrogen through the electrolysis process. This process further allows the storage and the conversion of hydrogen into energy whenever it is in need. This process produces highly purified hydrogen, excluding the need for a purification system, making it more economical money and space wise. The hydrogen is stored in a metal Hydride (MH), in this case, $LaNi_5$, through the process of absorption and released through desorption. Heating and cooling systems are required due to the exothermic and endothermic character of these processes accordingly (Rosaa, Valverdea, del Reala, & Arceb, 2013). The electrolyzer will operate when there is a surplus of the energy demand causing an increase of the stored hydrogen amount, but when there is an extra need for energy, the fuel cell will operate utilizing the already stored hydrogen (Rosaa, Valverdea, del Reala, & Arceb, 2013). Theoretically such a system is very appealing, yet it is not volumetrically and gravitationally efficient (Visaria, Mudawar, & Pourpoint, 2010). One of the problems of energy systems is that many times they operate under steady state conditions ignoring their dynamic character, leading to an overestimation of their energy output (Rosaa, Valverdea, del Reala, & Arceb, 2013).

3. REVIEW OF VARIOUS FUEL CELL SYSTEMS

3.1. Introduction to the properties of fuel cell systems

In 1839 W. Grove set the first fuel cell demonstration. By the usage of an electric current, water was electrolyzed into oxygen and hydrogen. When the power source is replaced by an ammeter, a certain amount of current was produced. During this process, the electrolysis phenomenon was reversed where oxygen and hydrogen were reuniting producing electricity. The described process can be seen in Figure 16 a and b (Larminie & Dicks, 2003).

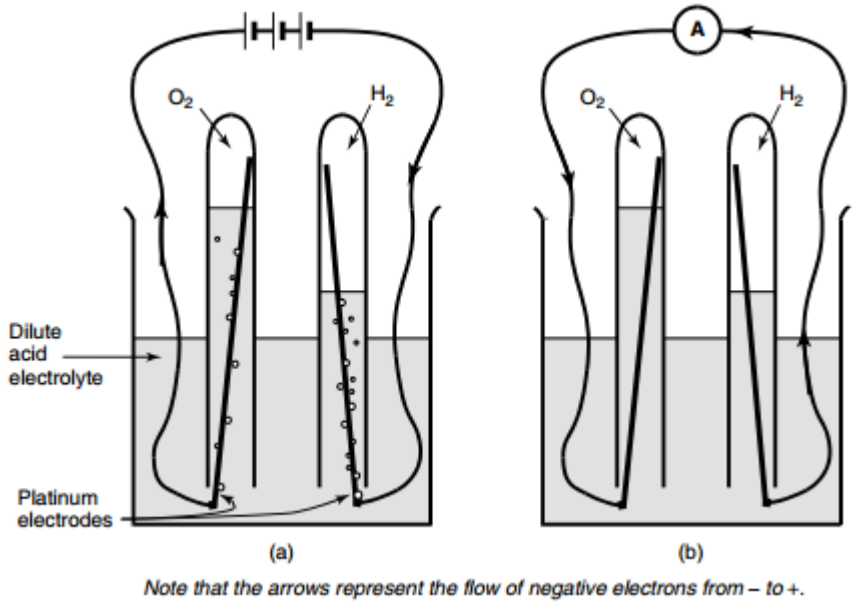

Figure 16: a) The electrolysis of water. The water is separated into hydrogen and oxygen by the passage of an electric current. b) A small current flows. The oxygen and hydrogen are recombining (Larminie & Dicks, 2003).

Combining hydrogen and fuel cell technology can be a very important step closer to sustainability and addressing the pollution of the environment. These are just a few

reasons why fuel cell technology is believed to be part of technologies to meet the energy needs of future generations (Mishra, Yang, & Pitchumani, 2005) (Ziogou, 2013) (Hart, 2016).

Fuel cells are defined as static energy conversion devices that allow the conversion of gaseous fuels mainly H_2 directly into electrical energy through a chemical reaction. The only by-product of this process is water and heat, where heat is sometimes utilized as well. Their process makes fuel cells a clean technology as it does not produce GHGs (Nehrir & Hashem, 2007), and in contrast to the rest of the conventional engine technologies, it does not require mechanical work to produce energy from a fuel (Pukrushpan, Peng, & Stefanopoulou, 2004), a mean that leads to greater energy losses and reduced efficiencies. Fuel cell is a combination of the characteristics of a battery and of an engine. They can operate as long as fuel and air (oxygen) are being provided, and they have similar behavior to that of a battery when load is available but not the "memory effect" yet degradation issues arise in the end (Cook, 2002).

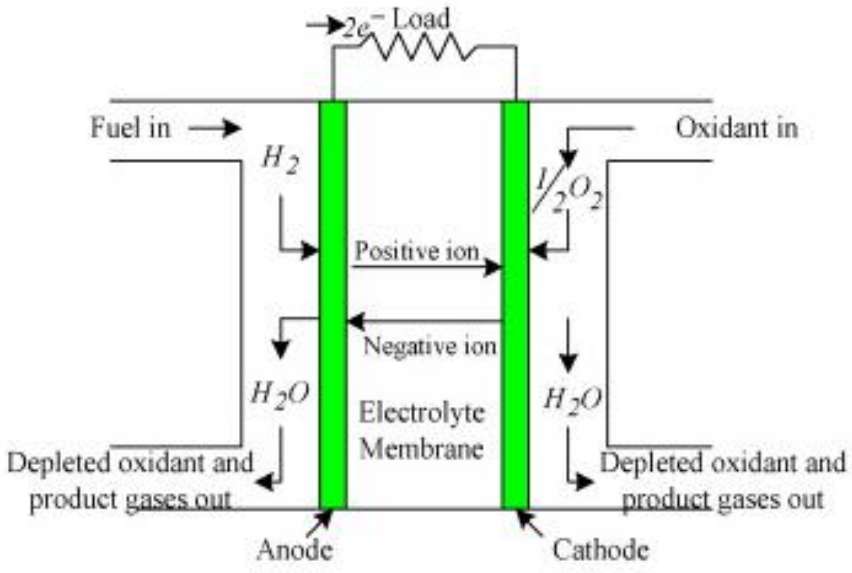

Figure 17: Fuel cell system where the electrolyte membrane is in between two electrodes (anode and cathode) (Kirubakaran, Shailendra, & Nema, 2009), (Huang, Zhang, & Jian, 2006) .

In the fuel cell system, hydrogen is supplied at the anode, and air is fed at the cathode. As it can be better depicted in Figure 17 and 18, at the anode electrode the hydrogen is separated into electrons and cations. Then, only the positive ions can diffuse through the membrane and towards the cathode electrode. In other words, the electrolyte prohibits the electrons to pass through. The electrons try to find a way to recombine with the ions at the cathode side and become stable. An electrical circuit provides this path for the electrons, and as electrons pass through, they produce electricity. At the cathode the oxygen from the air, the diffused hydrogen and electrons combine and form pure water.

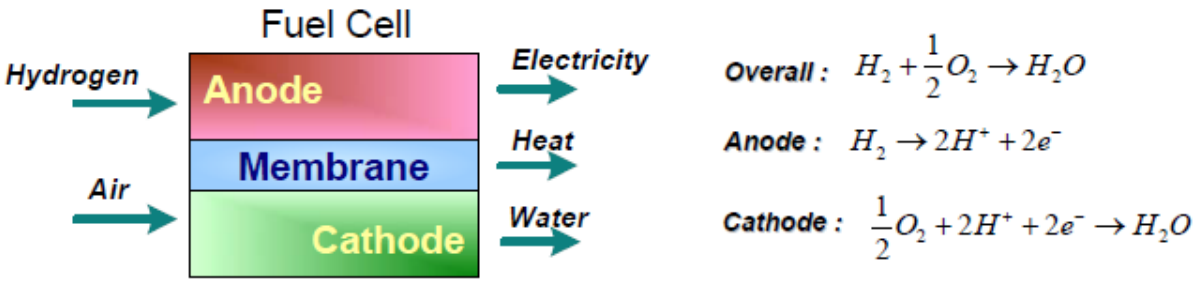

Figure 18: Fuel cell process (Ziogou, 2013).

3.2. Fuel cell technology comparison

In Table 4, various energy-generating systems are presented to compare their differences between efficiency and cost. The comparative advantage of the fuel cell is its high conversion efficiency as the energy is released electrocatalytically (Ziogou, 2013), but as the Table suggests it has much higher operating and capital costs compared to the commercial systems. Furthermore, full cells have additional advantages due to lack of fuel combustion: they produce zero emission rates and they are silent. In addition, they are scalable and allow a rapid installation, modularity that allow facile generation of electricity jointly (Xu, Kong, & Xuhui, 2004).

Table 4: Comparison of different generation systems (Kirubakaran, Shailendra, & Nema, 2009).

	Reciprocation engine: Diesel	Turbine generator	Photo voltaics	Wind turbine	Fuel cells
Capacity Range	500 kW to 5 MW	500 kW to 25 MW	1 kW to 1 MW	10 kW to 1 MW	200 kW to 2 MW
Efficiency	35%	29-42%	6-19%	25%	40-60%
Capital Cost ($/kW)	200-350	450-870	6600	1000	1500-3000
O&M Cost ($/kW)	0.005-0.015	0.005-0.0065	0.001-0.004	0.01	0.0019-0.0153

The performance of the system is associated with its electrical and thermodynamics efficiency. The electrical efficiency is based on the losses of the fuel cell in respect to ohmic, concentration and activation losses. The water vapor management, fuel process inflow and the control of the temperature of the system determine the thermodynamic efficiency. Each fuel cell has different characteristics based on the applications that they are used for and the materials that they are made of (EG&G Technical Services, 2004).

The characteristics of the main categories of different fuel cell technologies are compared on Table 5 so that to provide the comparative advantages and disadvantages of each case scenario. Although all these technologies operate under the same principal Table 5 presents that each type of fuel cell has different capabilities and is appropriate for distinct applications due to their diverse operating characteristics.

Fuel cells can be categorized into three main areas: stationary, transportation and portable.

- Stationary fuel cells main usage is as backup power generators for a fixed place. The power produced ranges from 0.5- few MW.
- Transportation fuel cells are used instead of engines from scooters to trucks with a power range from 1-100 kW.
- Portable fuel cells are used for the charge of small devices like laptops, phones and other everyday devices with a power range form 5-20 kW.

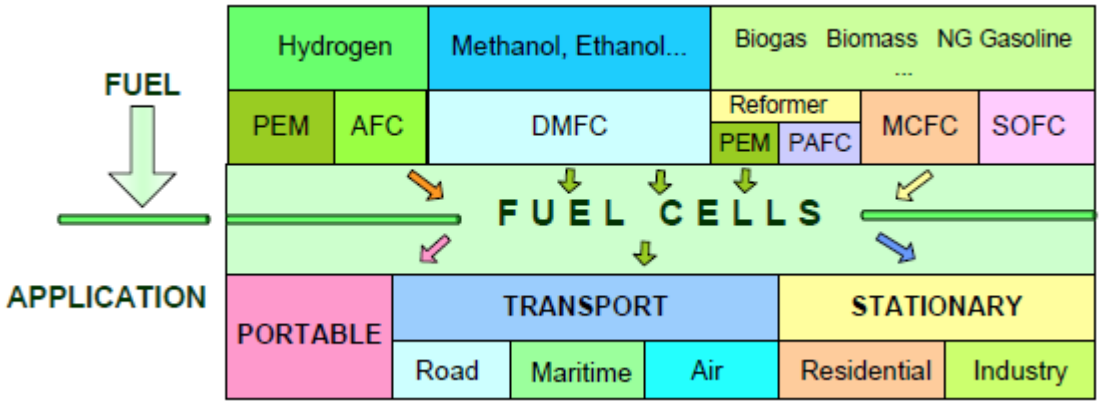

Figure 19: Fuels cells and applications (Ziogou, 2013).

Figure 19 allows a better visualization of different main types of fuel cells that in this Figure are distinguished based on the type of fuel they utilize and the type of application that they are used for.

Table 5: Comparison of different categories of fuel cells, (MICHAEL, VON SPAKOVSKY, & Nelson, 2001), (Maru & HANS, 2001), (Mozsgai, Yeom, Flachsbart, & Shannon, 2003), (EG&G Technical Services, 2004), (Coors, 2003), (Jamarda, Salomona, Martinent-Beaumonta, & Coutanceau, 2009), (Colominas, McLafferty, & Macdonald, 2009), (O'Sullivan, 1999), (Swider-Lyons, Carlin, Rosenfeld, & Nowak, 2002), (Yakabe, Sakurai, Sobue, Yamashita, & Hase, 2006), (Brenda, Vijay, & Wei, 2004), (Canha, Popov, & Farret, 2002), (Cheng, Sutanto, Ho, & Law, 2001), (Soltani & Bathaee, 2008).

Parameters	Fuel Cells					
	PEMFC	AFC	PAFC	MCFC	SOFC	DMFC
Electrolyte	Solid polymer membrane (Nafion)	Liquid solution of KOH	Phosphoric acid (H_3PO_4)	Lithium and potassium carbonate (LiAlO2)	Stabilized solid oxide electrolyte (Y_2O_3, ZrO_2)	Solid polymer membrane
Operating temperature (°C)	50–100	50–200	~200	~650	800–1000	60–200
Anode reaction	$H_2 \rightarrow 2H^+ + 2e^-$	$H_2 + 2(OH^-) \rightarrow 2H_2O + 2e^-$	$H_2 \rightarrow 2H^+ + 2e^-$	$H_2O + CO_3^{2-} \rightarrow H_2O + CO_2 + 2e^-$	$H_2 + O^2 \rightarrow H_2O + 2e^-$	$CH_3OH + H_2O \rightarrow CO_2 + 6H^+ + 6H^-$
Cathode reaction	$1/2O_2 + 2H^+ + 2e^- \rightarrow H_2O$	$1/2O_2 + H_2O + 2e^- \rightarrow 2(OH)^-$	$1/2O_2 + 2H^+ + 2e^- \rightarrow H_2O$	$1/2O_2 + CO_2 + 2e^- \rightarrow CO_3^{2-}$	$1/2O_2 + 2e^- \rightarrow O^{2-}$	$3O_2 + 12H^+ + 12H^- \rightarrow 6H_2O$
Charge carrier	H^+	OH^-	H^+	$CO_3^=$	$O^=$	H^+

Table 5 Continued: Comparison of different categories of fuel cells, (MICHAEL, VON SPAKOVSKY, & Nelson, 2001), (Maru & HANS, 2001), (Mozsgai, Yeom, Flachsbart, & Shannon, 2003), (EG&G Technical Services, 2004), (Coors, 2003), (Jamarda, Salomona, Martinent-Beaumonta, & Coutanceau, 2009), (Colominas, McLafferty, & Macdonald, 2009), (O'Sullivan, 1999), (Swider-Lyons, Carlin, Rosenfeld, & Nowak, 2002), (Yakabe, Sakurai, Sobue, Yamashita, & Hase, 2006), (Brenda, Vijay, & Wei, 2004), (Canha, Popov, & Farret, 2002), (Cheng, Sutanto, Ho, & Law, 2001), (Soltani & Bathaee, 2008).

Parameters	Fuel Cells					
	PEMFC	AFC	PAFC	MCFC	SOFC	DMFC
Fuel	Pure H_2	Pure H_2	Pure H_2	H_2, CO, CH_4, other hydrocarbons	H_2, CO, CH_4, other hydrocarbons	CH_3OH
Oxidant	O_2 in air	O_2 in air	O_2 in air	O_2 in air	O_2 in air	O_2 in air
Efficiency	40–50%	~50%	40%	>50%	>50%	40%
Cogeneration	–	–	Yes	Yes	Yes	No
Reformer is required	Yes	Yes	Yes	–	–	–
Cell Voltage	1.1	1.0	1.1	0.7–1.0	0.8–1.0	0.2–0.4
Power density (kW/m^3)	3.8–6.5	~1	0.8–1.9	1.5–2.6	0.1–1.5	~0.6

Table 5 Continued: Comparison of different categories of fuel cells, (MICHAEL, VON SPAKOVSKY, & Nelson, 2001), (Maru & HANS, 2001), (Mozsgai, Yeom, Flachsbart, & Shannon, 2003), (EG&G Technical Services, 2004), (Coors, 2003), (Jamarda, Salomona, Martinent-Beaumonta, & Coutanceau, 2009), (Colominas, McLafferty, & Macdonald, 2009), (O'Sullivan, 1999), (Swider-Lyons, Carlin, Rosenfeld, & Nowak, 2002), (Yakabe, Sakurai, Sobue, Yamashita, & Hase, 2006), (Brenda, Vijay, & Wei, 2004), (Canha, Popov, & Farret, 2002), (Cheng, Sutanto, Ho, & Law, 2001), (Soltani & Bathaee, 2008).

Parameters	Fuel Cells					
	PEMFC	AFC	PAFC	MCFC	SOFC	DMFC
Installation Cost (US $/kW)	<1500	~1800	2100	~2000–3000	3000	–
Capacity	30 W, 1 kW, 2 kW, 5 kW, 7 kW, 250 kW	10–100 kW	100 kW, 200 kW, 1.3 MW	155 kW, 200 kW, 250 kW 1 MW, 2 MW	1 kW, 25 kW, 5 kW, 100 kW, 250 kW, 1.7 MW	1 W to 1 kW, 100 kW to 1 MW (Research)
Applications	Residential; UPS; emergency services such as hospitals and banking; industry; transportation; commercial	Transportation; space shuttles; portable power	Transportation; commercial cogeneration; portable power	Transportations (e.g. marine-ships; naval vessels; rail); industries; utility power plants	Residential; utility power plants; commercial cogeneration; portable power.	It is used to replace batteries in mobiles; computers and other portable devices

Table 5 Continued: Comparison of different categories of fuel cells, (MICHAEL, VON SPAKOVSKY, & Nelson, 2001), (Maru & HANS, 2001), (Mozsgai, Yeom, Flachsbart, & Shannon, 2003), (EG&G Technical Services, 2004), (Coors, 2003), (Jamarda, Salomona, Martinent-Beaumonta, & Coutanceau, 2009), (Colominas, McLafferty, & Macdonald, 2009), (O'Sullivan, 1999), (Swider-Lyons, Carlin, Rosenfeld, & Nowak, 2002), (Yakabe, Sakurai, Sobue, Yamashita, & Hase, 2006), (Brenda, Vijay, & Wei, 2004), (Canha, Popov, & Farret, 2002), (Cheng, Sutanto, Ho, & Law, 2001), (Soltani & Bathaee, 2008).

Parameters	Fuel Cells					
	PEMFC	AFC	PAFC	MCFC	SOFC	DMFC
Advantages	High power density; quick start up; solid non-corrosive electrolyte	High power density; quick start up	Produce high grade waste heat; stable electrolyte characteristics	High efficiency; no metal catalysts needed	Solid electrolyte; high efficiency; generate high grade waste heat	Reduced cost due to absence of fuel reformer
Drawbacks	Expensive platinum catalyst; sensitive to fuel impurities (CO, H_2S)	Expensive platinum catalyst; sensitive to fuel impurities (CO, CO_2, CH_4, H_2S)	Corrosive liquid electrolyte; sensitive to fuel impurities (CO, H_2S)	High cost; corrosive liquid electrolyte; slow start up; intolerance to sulfur	High cost; slow start up; intolerance to sulfur	Lower efficiency and power density

For our case, as the fuel cell is intended to be applied in transportation, and substitute the commercial diesel engine, higher safety precautions must be taken under consideration. It was concluded from Table 5 that PEM fuel cell is the technology that best fits our requirements. Its low operating temperature of 50-100^0 C, high energy density, and rapid start up as well as its size and weight make it more applicable for commercial usages in vehicles (Ziogou, 2013). The main disadvantages of PEM fuel cell are: the low operating efficiency (40-45%), the high costs associated with the required platinum catalyst and its high sensitivity to CO.

So far, PEMFC of 3-7 kW and 50 kW are used, for residential and building usage accordingly, to provide heat and electricity. It is interesting to state that Ballard Power systems, in Canada, developed a 250 kW PEM system (Maru & HANS, 2001). A PEMFC system is expected to be part of the future automotive industry as the global goal reduction of greenhouse gas emissions in the automotive sector is 95% until 2050 (European, 2017).

4. REVIEW OF THE PROPORTIONAL INTEGRAL (PI) CONTROLS

Sensors are utilized to measure the different characteristics of a system. These values can be used as feedback to improve the performance of the system. An automatic control system is a closed loop system that does not require any operational input. The controller regulates the system so that it remains within a specified range. An automatic control system has two process variables: a manipulated variable and a controlled variable (TPUB).

- The manipulated variable is the process variable that is alternated by the control system to ensure that the controlled variable is at a desired value or within a desired range of values. (TPUB, 2017)
- The control variable is the process variable that is kept at a desired value or within a desired range of values(TPUB, 2017)

In an automatic control system, four functions take place. The control process initiates with a measurement of the controlled variable. The current measured values are then compared with the desired ones. Then, the control device computes the error created, which is the difference between the desired and the actual values. The controller then determines the magnitude of action that has to perform on the manipulated variable as to "correct" the system by minimizing the error (TPUB, 2017).

"Based on a survey of over eleven thousand controllers in the refining, chemicals and pulp and paper industries, 97% of regulatory controllers utilize PID feedback" (Honeywell, 2000) .

PID controller is a very common case among of its kind. A PID controller is described by the following formula:

$$u(t) = Kp \times e(t) + Ki \int_0^t e(t)dt + Kd \frac{de}{dt}$$

In the controller, u is defined as the manipulated variable and e as the error. The control signal is composed of three terms. The P-term is proportional to the present error,

the I-term is proportional to the integral error, error created from time zero to present time, and the D-term is proportional to the error derivative or future expected error. The K values stand for the individual gain of each case. Figure 20 represents the error created by the system, area between the line and the Time-axis, which the controller tries to penalize. An important parameter of the PID controller is that it takes under consideration the future prediction, the current and the past errors of the control (Honeywell, 2000).

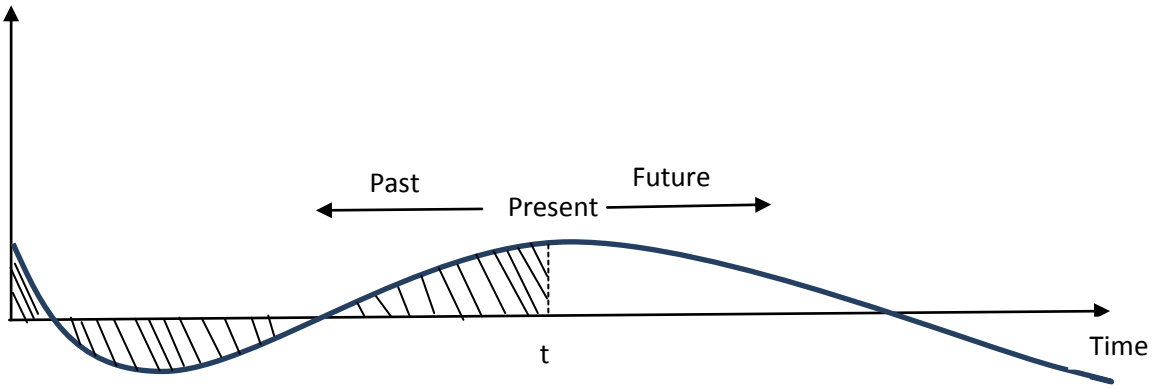

Figure 20: The PID controller operates utilizing information from the past, present and future prediction errors (Honeywell, 2000).

Each term has a different impact on the system, an impact that can better be represented in Figure 21. Figure 21 describes three different cases: the response to step changes for proportional command signal (P), proportional integral (PI), and proportional integral derivative action (PID).

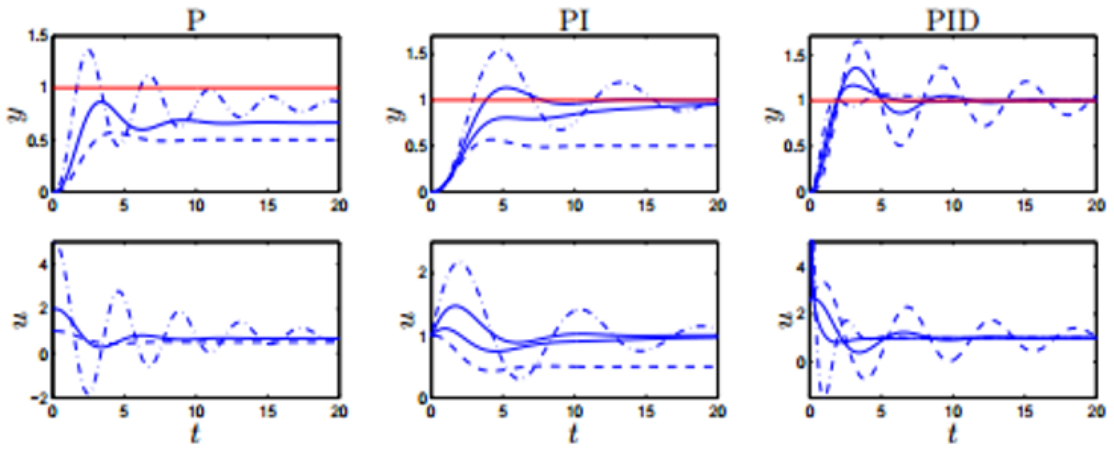

Figure 21: Response to step changes in the command signal for P, PI and PID controllers for a transfer function $P(s) = \frac{1}{(s+1)^3}$. *(Honeywell, 2000).*

The Kp values used in the P case are: 1 (dashed), 2 and 5 (dashed-dotted) lines. An increase in the gain-value decreases the steady state error, but at the same time it introduces more oscillations in the system, Figure 21. In the case of PI, the values used are: Kp=1, Ki=0 (dashed), Kp=1, Ki=0.2, 0.5 and 1 (dash-dotted). As the Ki gain value increases for the same Kp value, it causes an increase in the wavelength of oscillations that take place but they are of lower number compared to the Kp case. The PI control is able to get closer to set point value, decreasing the error further. For the PID case, the controller has the following values: Kp=2.5, Ki=1.5 and Kd=0 (dashed) and Kp=2.5, Ki=1.5, Kd=1, 2, 3, 4 (dash-dotted). The PID case can provide extra stability to the initially oscillatory PI system, but it is risky as the Kd values can create issues in the system. The derivative action extrapolates the error created by Kd times in a way to predict and avoid the future error (Honeywell, 2000). The issue with the D control is that if there is noise in the system, such as sudden peaks like in a dynamic system, the controller is confused and it cannot make a correct estimation of the future, messing up the control. For that reason D controller is not usually used (Control, 2016).

5. RESEARCH OBJECTIVES

The objective of this thesis is the operational analysis, the impact and control of the different variables of pre-established HPMH and PEMFC dynamic models individually and combined. The dynamic models are presented individually and combined through a model builder platform named gPROMS. The ultimate goal of the thesis is to regulate the filling time variables, discharge rate variables and the thermal management variables of the HPMH and PEMFC model to achieve improved combined operating conditions. More specifically, these are associated with higher fueling rates of hydrogen in the MH tank and steady hydrogen flow of sufficient amount from the MH tank to the fuel cell to meet the power demand of the vehicle. Finally, the thesis investigates the impact of a PI controller to the overall behavior of the system. This method is used to allow the automatization of the system and to investigate the controller's ability to sustain improved operating conditions in a safer manner.

6. MODELING

6.1. Outline

In a metal hydride tank and fuel cell modeled system, the materials have a variety of properties that must be taken under consideration. The idea of the modeled system is to keep it simple and yet detailed. The simplicity is associated with the prevention of any fatigue in the system through prolonged modeling time. A simple, fast operating and realistic model that simulates closely the behavior of the experiment, is feasible through the adoption of different assumptions. The modeled mathematical expressions are based on already established formulas provided by the literature. The values utilized by the newly established combined model are taken from literature and from the available experimental apparatus.

The model represents a MH tank connected in series with a fuel cell and a PI controller that regulates them both. First, there is the simulation of the absorption phase of the MH tank where hydrogen is absorbed. After the termination of the absorption process, the second phase that of desorption initiates that uses the data produced from the absorption process. Such data are associated with the amount of hydrogen stored and the amount of solid mass converted. The desorption process, converts the MH back into solid by emancipating the previously stored hydrogen. The MH tank is now connected with a fuel cell that is the third part of the modeling series. The desorbed hydrogen flows from the tank to the fuel cell and current is produced. An overview of the system is the following: The MH system is cooled down and hydrogen is fed to the MH tank during the absorption reaction phase. Then the system is heated up and hydrogen is desorbed to the fuel cell during the desorption reaction phase. Finally, the fuel cell utilizes the provided hydrogen to produce electric power that can be used to produce work. In the next part of the model a PI control is introduced to exclude the need of an operator in the system. The controller manipulates the water flow rate in the heat exchanger to control the rate of storage and outflow of hydrogen to and from the MH tank and the inflow of hydrogen in the fuel cell to meet the demanded amount of power by the automobile.

The software that is utilized to represent this model is gPROMS ModelBuilder version 4.2 copyright Process Systems Enterprise Limiter (1997-23013) (PSE, 1997). gPROMS is a powerful process modeling platform that can be thought as a mixture of Aspen Plus and MAT LAB. The importance of this software is that it allows the modeling and the solution programs to be under a single platform. Furthermore, it allows the interconnection of different models with one another providing the ability to decide which set of values and equations are desired to interact with each other. This allows the representation of different conditions and acquisition of more accurate results in a more rapid and facile manner (PSE, 1997).

6.2. Modeling

The model is based on the work done mainly by B.A. Talagan et al. (Talagañisa & Meyerb, 2011), and C. O. Ziogou (Ziogou, 2013). The metal hydride tank model represents a high pressure aluminum tank loaded with $LaNi_5$ material hydride (MH), where the fuel cell is a dynamic PEM model.

6.2.1. Metal hydride model

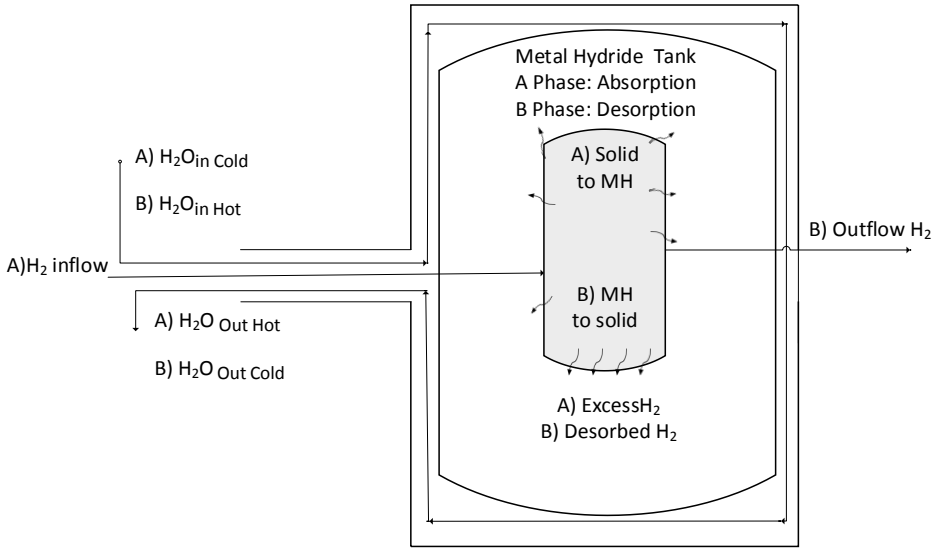

Figure 22: Structure of the Dynamic Model of MH hydrogen storage during absorption and desorption phase.

The MH tank model is utilized to better understand the dynamic character of the absorption and desorption processes and to further assist improve the performance of the system under various extreme conditions. To test the higher thermodynamic operability of the system, the model is tested under isothermal and equilibrium conditions.

This model utilizes a cylindrical tank filled with $LaNi_5$ metal hydride. Figure 22 can be used to better illustrate that system. In the model, both absorption and desorption processes are going to be investigated and the heat exchanger is responsible in regulating the temperature of the system. During the exothermic absorption reaction, the temperature of the water is set at 298 K and during the endothermic desorption reaction the water temperature is set at 340 K.

To establish a mathematical model a number of assumptions were taken under consideration:

- The metal hydride is homogeneous and isotropic.
- The reactor has uniform temperature and pressure distribution.
- The ideal gas law characterizes the gas phase.
- Hydrogen introduced to the system is of constant pressure and constant flow.
- The volumetric parameters of the solid, the reactor and the gas phase are kept constant.
- At the initial time of the absorption reaction the reactor temperature is assumed to be equal to the cooling water temperature: $T_{in}=T_{wa.}$
- At the initial time of the desorption reaction the heating water temperature is assumed to be equal to the reactor temperature: $T_{in}=T_{wd}$.
- The initial amount of metal hydride in absorption is $m_{MH}=0$ as there is none hydrogen yet reacted with the solid.
- The initial amount of metal hydride in desorption is almost $m_{MH}= m_S$ as the hydrogen has fully reacted with the solid.
- The amount of hydrogen being introduced to the system during absorption at the initial time is equal to the constant flow rate amount that is $m_{H2}=0.1$ g/s.
- The amount of hydrogen being desorbed out of the system at the initial time is equal to the constant flow rate amount that is set equal to $m_{H2}=0.05$ g/s.

The assumption that uniform pressure and temperature distribution were present in the tank, allowed the exclusion of equations that describe the distribution of these parameters. A simpler model is promoted allowing the description of energy and mass balances through ordinary instead of partial differential equations. Also, the average values of composition and temperature are used instead in the energy and mass balances equations. In reality, the pressure, the composition and the temperature distributions are not uniform across the system. In this project, it is more important to model an accurate and of facile comprehension system rather than an in depth representation that can lead to wrong results. Additionally, forming a simple model that serves as a baseline pointing

towards a generally accepted direction, before constructing a more complex one, can be beneficial.

Hydrogen mass balance

In the absorption case, gaseous hydrogen is pumped in the metal hydride tank. Hydrogen is absorbed by the metal hydride. At some point, the amount of hydrogen that can be stored within the MH in solid form is reached and the extra hydrogen pumped in the system after this point is stored the tank in gaseous phase. In the desorption case, gaseous hydrogen flows/ pumped out of the tank. Hydrogen is desorbed from the MH and the MH is converted back to solid. At a certain point, no more hydrogen can be released from the MH to the tank and no more hydrogen is available in the tank in gaseous phase (See Appendix 1).

The hydrogen mass balance equation is used to describe the amount of hydrogen in gas phase within the metal hydride tank per unit time. That provides us with an insight of how the rate of absorption/ desorption changes as time passes. The absorption reaction refers to the conversion of solid into metal hydride as hydrogen is being absorbed and the reverse stands for the desorption case. The higher the rate of absorption the lower the amount of gaseous hydrogen within the system and the higher the rate of desorption the higher the amount of gaseous hydrogen within the system. Because each MH reacts in a different way with hydrogen and the according stoichiometric coefficient of the reaction must be taken under consideration.

Metal Hydride mass balance

From the previous equation, relevance between the rate of reaction and metal hydride formation is represented. The metal hydride (MH) mass balance allows the determination of the amount of MH produced or reduced per unit time. As the rate of absorption increases, the rate of solid converted to metal hydride increases as well, leading to a positive proportionality between these two parameters. In the desorption case the contrary is taking place. It important to state that the rate of reaction depends on the amount of solid available in the absorption case and on the amount of MH in the desorption case. As the mass of the solid/MH increases, the amount of substance available to be converted increases leading to higher conversion rates (See Appendix 1).

Hydrogen energy balance

The absorption reaction is exothermic and desorption endothermic. For this reason, the temperature variation is an important variable of the sorption reactions. To describe the rate of change of temperature per unit time, a hydrogen energy balance is composed; the introduction of hydrogen to the system is the reason why the reactions are temperature dependent. The temperature change is proportional to the mass of gaseous hydrogen in the system and the mass of solid available. In the absorption case, the temperature change per unit time depends also on the amount of gaseous hydrogen introduced to the system per unit time due to its lower initial temperature. In both cases, the temperature depends on the overall heat transfer between the refrigerating/heating water and the metal hydride, and the reaction rate that takes place. It is important to investigate the various heat transfer phenomena in more depth so that to be able to identify and have a better visualization of the impact of each component on the system (See Appendix 1).

The absorption process is an exothermic reaction, and the reaction rate describes the rate that heat is introduced per unit time. To enhance the absorption process heat must be removed from the system. The heat exchanger is in contact with the system, it removes heat by circulating water of lower temperatures than the ones that dominate in the system. In addition, the inflow of H_2 to the system introduces lower temperatures, compared to the ones pre-existing in the MH tank, lowering in this manner the temperature of the system.

The desorption process, is an endothermic reaction, and the rate of the reaction describes the rate that heat is removed from the system per unit time. To enhance the desorption process heat must be introduced to the system. The heat exchanger provides the necessary heat to the system by circulating water of higher temperatures than the ones that dominate the system.

Reaction Kinetics

The rate law depends on the concentration of chemicals that take place in the reaction. The driving force is the difference between the pressures of absorption/desorption to the equilibrium pressure. That difference shows the rate at which hydrogen is actually able to react and be absorbed/desorbed by the solid/MH that results to an incline in the pressure of the system along with a change in temperature. In the absorption process, MH is formed from solid and ratio proportionality must be utilized to denote the impact of that variable. In the desorption case solid is formed from MH and the same ratio proportionality must be utilized. The reason why the ratio must be closer to unit value and not to zero in contrast to the high amount of solid/MH present in the initial step is that during absorption/desorption MH/solid is formed (See Appendix 1).

Equilibrium Pressure

This system pressure's depends on the temperature and hydrogen metal hydride to solid ratio. For this reason an equation that describes pressure composition isotherms or PCIs should be used for the approximation of the equilibrium pressure. The equilibrium or plateau pressure will be optimally represented using van't Hoff relation. This theorem states that the equilibrium pressure of an ideal hydride depends solely on the temperature variable. To take under consideration the material behavior of each case the constant slope term is taken under consideration (See Appendix 1).

Heat transfer equation

The rate of heat removed from or provided to the system by the heat exchanger must be further explained and the variables associated with the procedure must be more thoroughly depicted. For this system, it is assumed that the metallic water tube walls are too thin to have an impact on the heat transfer and for that reason heat losses associated with them are ignored. The heat transfer characterization is broken down to two parts. The first part describes the heat transfer between the metal hydride tank and the water of the heat exchanger. The second one describes the variation of the temperature of the outflow water. The heat transfer is defined by the difference of the heat gained or lost by the system. More specifically, heat is lost or gained by the metal hydride system to the inlet and outlet cooling or heating water. There is a continuous loss or gain of heat depending on the sorption process until the water exits the system due to the comparatively elevated or lower temperatures of the MH system. The variation of temperature of the water outlet profile is a very important parameter of the system that affects the reaction rate of the model because of the amount of heat transfer variations from or towards the system per unit time. The advantage of this equation is that we can actually set the input temperature

of the circulated water, providing the ability to manipulate the rate of heat transfer required in each case and consequently the rate of hydrogen produced or stored (See Appendix 1).

Additional Equations

The ideas gas state equation is used to represent the relation between the different critical variables in the system that are described.

The hydrogenation capacity equation is used as a reference point that allows a visualization of the amount of hydrogen present in the MH with respect to time (See Appendix 1).

6.2.2. Fuel cell PEM model

Anode equations

Hydrogen balance equation

In the anode part of the fuel cell, there is the variable inflow of hydrogen. From that hydrogen, a certain amount is diffused through the membrane to react and the rest flows out of the system. For simplification reasons it is assumed that at the anode there is only hydrogen as we assume that there is always just enough amount of humidity on the membrane to allow an efficient diffusion of ions. Thus, the excess amount of hydrogen present in the anode defines the pressure created at the anode for our system. The outflow

of hydrogen depends on the difference between the atmospheric and anode's pressure present. The higher the pressure in the system is, the higher the amount of hydrogen being present and flowing out (Appendix 1).

Cathode equations

Mass balance

In the cathode part of the fuel cell, there is a variable inflow of air in the system where in this case we are going to assume that no nitrogen is present and that there is interaction only with the amount of oxygen introduced. From the amount of oxygen introduced, a part of it reacts with hydrogen ions and electrons and the rest flows out. As in the anode case, the humidity level on the membrane is assumed to be just enough to allow an efficient flow of ions through and thus saturation pressure is considered negligible and ignored.

The rate of the reaction that determines the consumption rate of hydrogen and oxygen depends on the current variable which is set to increase with time to produce results for the whole spectrum of the system's operability (Appendix 1).

Partial pressure of species

It is assumed that there will always be just enough water vapor on the membrane, so for one more time it is assumed that negligible vapor pressure is created. As a result, the pressure at the cathode depends only on the amount of the oxygen present, thus any pressure increase in the cathode depends on the excess inflow of oxygen in the system that

does not react. To be realistic the value of the partial pressure of oxygen is multiplied with 4.72 whose product is assumed to represent the total pressure created in the system. The reasoning behind 4.72 is that oxygen takes up 20% of the air and nitrogen almost 80%, so that value is used to represent the total pressure created by the theoretical amount of air that would be present to provide that amount of oxygen and be able to keep the system simple and accurate. The flow rate of oxygen out of the system follows the same law as the hydrogen in the anode case.

Stack Voltage

Due to the low cell voltage (1.2 V) it is a requirement to stack many cells to produce the required energy but in our model only one cell is used. The main characteristics of a fuel cell are found in a polarized curve. Figure 23 represents a fuel cell polarization characteristic where voltage is plotted against current density. The stack voltage is determined by the difference between the ideal Nernst voltage, that decreases as the current provided increases, and the voltage losses such as the activation, ohmic loss and concentration or mass transfer losses that can be better depicted in Figure 23 (Appendix 1).

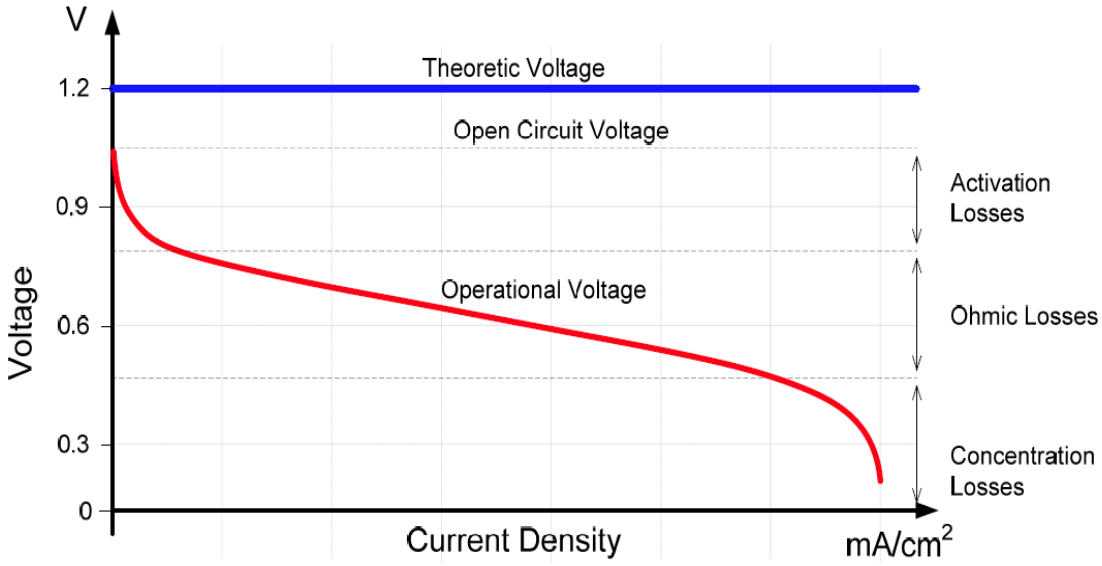

Figure 23: Theoretical/Nernst voltage Vs operational voltage (Ziogou, 2013) (Kirubakaran, Shailendra, & Nema, 2009).

The graph provides a very good prediction of the available voltage for each current case and it is an essential part of the PEMFC profile. That initial period when the system is warmed up is called activation polarization, the voltage losses are associated with the slowness of the chemical reaction that takes place on the surface of the electrode (Fuel Cell). Activation losses are shown on the left side of the operational voltage-current density graph. In our case, the formulas included in Appendix 1 take into consideration the concentration amount of oxygen accumulated on the surface of the catalyst's layer at the cathode and other experimentally defined parametric coefficients (Appendix 1).

As the current density increases, the ohmic losses become more dominant. The linear part of the line represents the ohmic polarization, a characteristic of the ohmic nature of the system is that takes place when the current density increases, causing the voltage to drop (Kirubakaran, Shailendra, & Nema, 2009). The fuel cell's operability is at its highest within the linear region when alternating the internal resistance of the cell stack for various loading and hydrogen pressures conditions (Kirubakaran, Shailendra, & Nema,

2009). Internal resistance of various components causes the ohmic polarization. More specifically, ohmic losses are associated with the resistance of the membrane to flow of ions through the material of the electrode, the resistance of the electrolyte to flow protons through and the resistance of the cell hardware and of various other interconnections to flow electrons. The voltage drop at the main part of the curve is proportional to the current density (Ziogou, 2013) (Fuel Cell) . When the current density is low, the losses associated with the ohmic nature do not have a great impact on the system.

At very high current densities, the voltage decreases significantly due to lower gas diffusion efficiency. This characteristic is associated with the over flooding of water in the catalyst (water is concentrated on the catalyst) that causes mass transport losses, that lead to a decrease in the reactant concentration at the surface of the electrode as the fuel is used. This part of the graph is called concentration polarization (Kirubakaran, Shailendra, & Nema, 2009). The mathematical formulas (Appendix 1) relate the conductivity of the electrolyte to the porosity of the gas diffusion layer. At the point of maximum current density, the concentration of the fuel on the surface of the catalyst is very close to zero, due to the fact that the reactants are utilized immediately when they become available on the surface (Ziogou, 2013), (Fuel Cell).

Thermodynamic balances

In a thermodynamic model, energy balance equations are used to portray the comportment of the temperature of the fuel cell. Not all the energy produced is converted to useful electricity. Energy is provided to the system depending on the amount of fuel at the anode and oxygen at the cathode that are taking place in the reaction. These energy profiles as well as the heat produced by the resistance of the system are excluded from our model due to simplification reasons. The components that are taken under consideration are; the energy and heat produced by the exothermic chemical reaction and the amount of energy that is actually converted to electrical power. Heat losses are associated with the

amount of heat radiated to the surrounding environment and the heat lost to the environment through convection. The described equations can be found at Appendix 1.

Due to the excess amount of heat produced during the fuel cell operation, only part of the energy can be converted into useful power and the rest energy is produced in the form of heat, as a result the temperature of the system increases. This comparatively increased temperature of the system to the surrounding environment causes heat losses to it. The heat losses are caused by radiation and convection. Convection energy losses are categorized into heat losses due to natural convection and heat losses by the cooling system (heat exchanger) that is used to preserve the temperature of the fuel cell (FC) within a desired temperature range (Ziogou, 2013).

The baseline model is produced using the model builder platform gPROMS that introduces all the relationships required as described. The model takes under consideration all the physical equations explained. The hydrogen can only flow in and out of the metal hydride tank and fuel cell from the one end as it is in the commercial cases.

6.2.3. Proportional integral (PI) control model

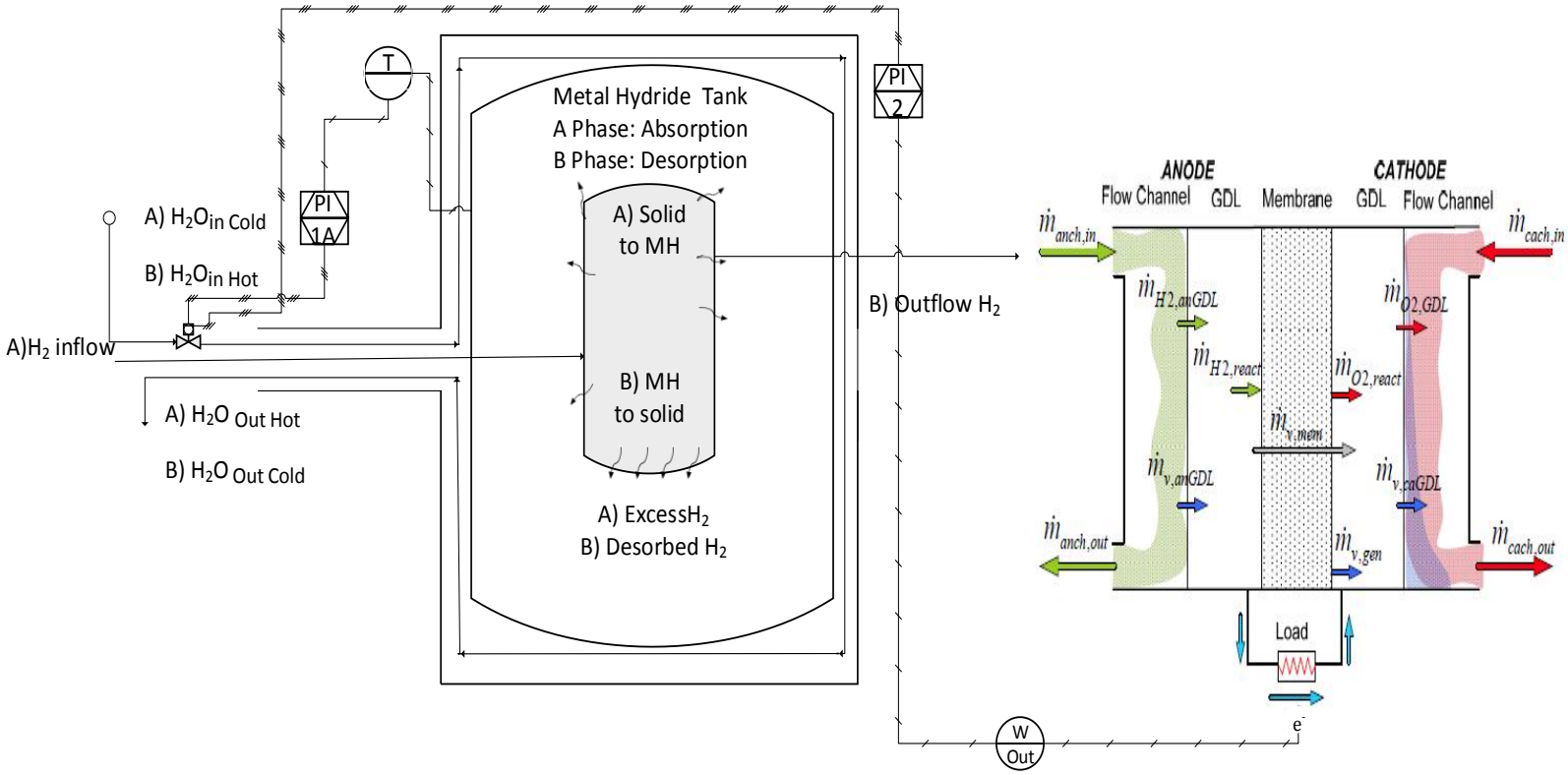

Figure 24: PI control over the MH tank and fuel cell model.

In the model, the different characteristics are measured such as: temperature, pressure, heat and mass transfer with respect to time, to determine the impact to the system. That allows a better understanding of the behavior of the system. The PI control is used to maximize the absorption rate or in other words to minimize the filling time of hydrogen in the metal hydride tank. The next goal of the PI controllers is to meet the demand in hydrogen of the fuel cell. The PI control is responsible to make sure that enough hydrogen is supplied (desorbed) to produce the necessary amount of current desired at a constant rate. Two PI controllers are necessary to accomplish this task, and the whole system along with them is presented on Figure 24.

PI 1 operates during the fueling process where absorption takes place, the engine is turned off and there is no energy demand. The PI 1 controller tries to regulate the temperature of the metal hydride tank making it its control variable. In the MH tank the temperature is the variable that has the highest impact on the process due the fact that both reactions (absorption and desorption) are temperature dependent and for that reason, for the reaction rate to be over a certain level the temperature of the system must be monitored and regulated. The mean to control the temperature of the system is through the flow rate of water in the heat exchanger that in other words is defined as the manipulated variable. One reason why the PI 1 controller is added is that there are instants when more hydrogen can actually be absorbed if the reaction rate was higher leading to faster fueling/filling of the MH tank. For that reason, PI 1 monitors the temperature of the MH tank, and it decreases the flow of water in the heat exchanger when the temperature is getting close to the set point temperature, and increases the flow of water in the heat exchanger when that error increases. The second reason why PI 1 controller is used is to accommodate with a safety precaution against operating in extreme conditions. When hydrogen is supplied to the system the temperature can increase rapidly. If the temperature of the MH tank is not well monitored and regulated accordingly, the system can have safety issues associated with the incapability of the heat exchanger to bring the temperature of the unit within safe values.

The PI 2 controller operates during the operation of the engine where there is need for power. The need in power is translated in a need for hydrogen by the fuel cell and the PI 2 tries to regulate the rate of flow of hydrogen form the MH tank to the fuel cell. PI 2 controller depends on the amount of voltage that is demanded by the fuel cell. The voltage is

the controlled variable and must be met as close as possible for its various, non-constant values. The manipulated variable is the amount of water that flows in the heat exchanger to allow an efficient rate of desorption to take place. The error created is associated with the theoretical amount of voltage required by the fuel cell and the actual amount that is produced by the fuel cell. PI 2 is vital to the system, as the initial model does not guarantees that the MH tank releases the correct amount of hydrogen to the fuel cell when needed. There are two scenarios: too much or not enough hydrogen can be released to the fuel cell. A high amount of hydrogen release causes a safety issue as the accumulation of hydrogen in gaseous form leads to elevated pressures in the system. If not enough hydrogen is released then not enough voltage is produced and thus the vehicle cannot operate properly. The control operates as following; when the voltage output is higher than the amount demanded, the rate of water flow in the heat exchanger decreases, decreasing the rate of desorption, decreasing the flow of hydrogen out of the MH tank. In the case where the need for voltage is higher than the one provided, the rate of flow of water in the heat exchanger increases, leading to higher reaction rates, allowing more hydrogen to flow out of the MH tank system towards the fuel cell. Another important impact of the PI 2 controller is that it provides a constant flow of hydrogen from the one system to the other. The importance arises from the fact that the fuel cell just like any kind of engine requires a constant amount of fuel to produce a certain amount of work over a period.

7. CASE STUDY

In the model, each sorption reaction operates for 120 seconds. In the combined case scenario, there are three pairs of sorption reactions taking place, starting and finishing with a desorption reaction representing a total of 840 seconds period. The model starts and finishes with the desorption reaction as it is assumed that the tank is initially full and it must be left empty in the end. The 120 seconds period is an outcome of this study. This period is enough for both absorption and desorption reactions to reach almost zero reaction rate having almost the entire solid and MH utilized accordingly. During the absorption reaction if the process was to continue for more than 120 seconds, from the pumped in hydrogen almost none would be further absorbed by the solid, forming a MH, as there would be only a very small amount of solid present. As a result, the hydrogen would be stored in gaseous phase within the tank leading to an increase in the pressure of the system. In the desorption reaction, within this period almost all of the MH has emancipated its hydrogen and the MH is converted back to solid. In addition to the depletion of MH, is the depletion of hydrogen in the MH tank. These characteristics signify the end of the process. In the case that desorption was to operate for more than 120 seconds no more hydrogen would flow out of the system or if so that would be of insignificant amounts. It is important to state that limitations in the chemical reaction are taken under consideration in both cases. This is depicted by the existence of a remnant of unreacted MH and solid present, thus the theoretically capable amount of absorbed and desorbed hydrogen is never reached.

8. RESULTS

8.1. Absorption of MH tank modeling results

In the model, the initial high rate of reaction in Figure 25 is because initially there is a high amount of solid available and no MH. As more H_2 is stored, more solid is converted to MH and the rate of reaction decreases. The rate of the reaction is negative as hydrogen is absorbed and MH is produced.

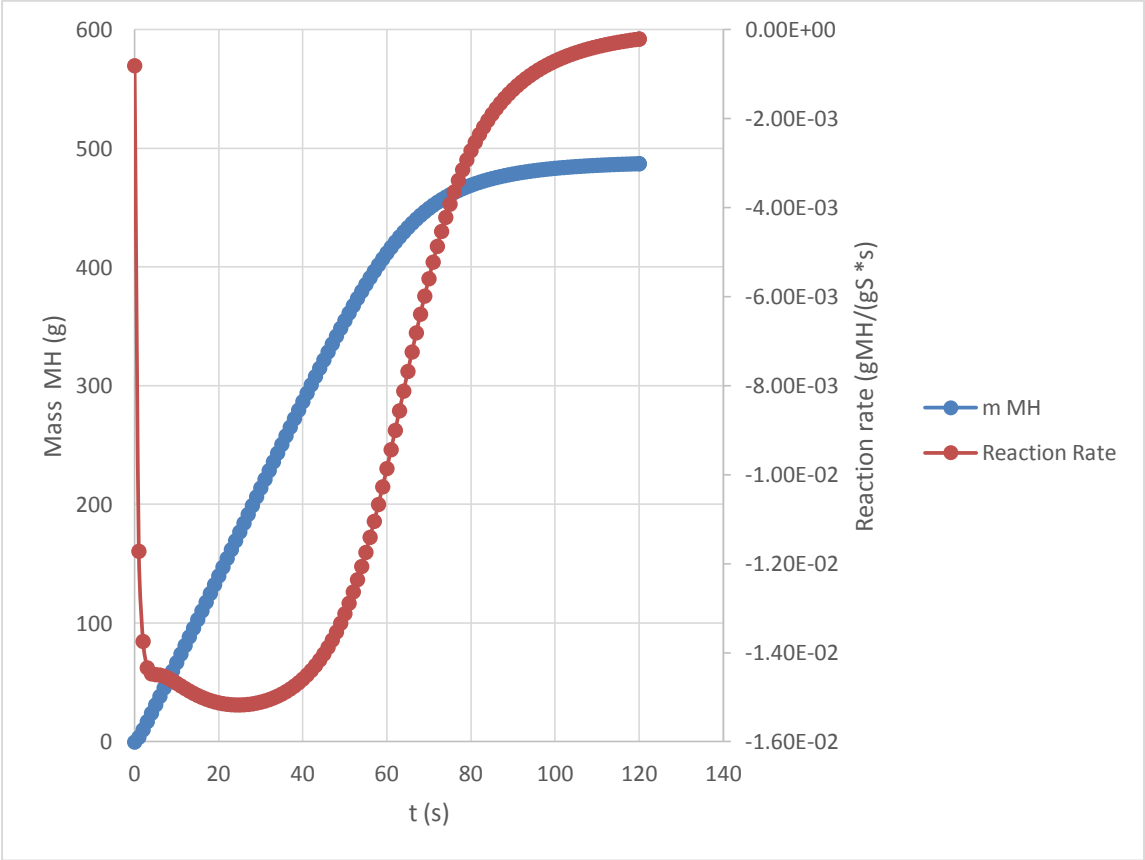

Figure 25: Mass of MH with reaction rate Vs time.

The model takes into account the none ideality of the chemical reaction as there is always some mass of solid that does not react. For that reason, some of the hydrogen is not absorbed by the solid and kept as gas in the tank. As the reaction proceeds, the rate of the reaction declines and thus the rate of absorption, but the amount of hydrogen that flows in the system is kept the same. Gradually, the amount of hydrogen stored in gaseous phase in the tank increases. That causes a greater increase in the pressure of the tank than when it was stored in the MH as can be shown at Figure 26. At some point, almost no solid is converted to MH, shown at Figure 25, and now the hydrogen pumped in is stored only in gaseous form leading to build up pressures, Figure 26, and at that point it is decided for the reaction to be terminated.

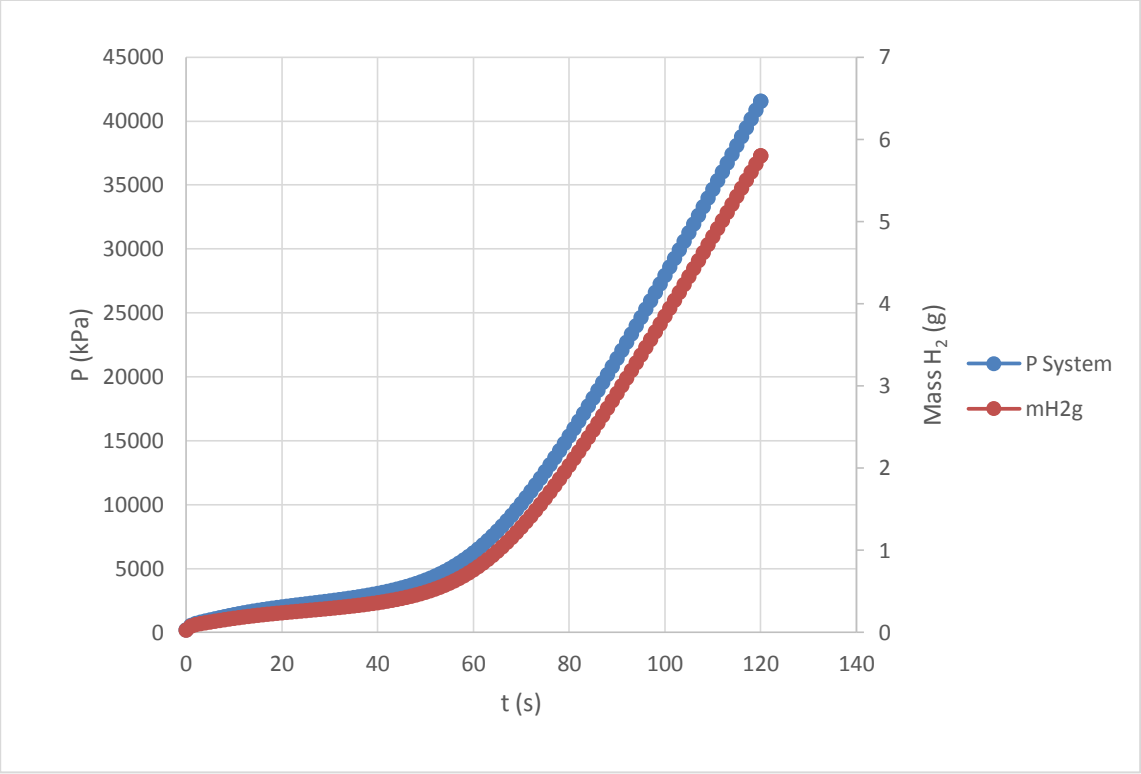

Figure 26: Pressure and hydrogen gaseous mass Vs time.

The pressure variable is positively correlated to the temperature value and a decrease or increase affects that parameter accordingly. In the beginning of the process, the hydrogen is being stored on the surface of the MH (α-phase) (Berube, Radtke, & Gang,

2007). Increasing the concentration of hydrogen in the α-phase increases the H-H interactions, which start to play an important role, leading to the next phase, named beta phase. This phase is associated with volumetric expansion, change of the crystalline structure and the formation of a nucleation energy barrier (Berube, Radtke, & Gang, 2007).

The production of heat during absorption causes an increase in the system's equilibrium temperature. An increase in the temperature though inhibits the reaction rate and for this reason, cooling water from the heat exchanger flows around the tank. The temperature of the water is 298 K and is sufficiently low to prevent a great increase of the temperature of the system by absorbing the excess heat as can be depicted in Figure 27. The heat transfer from the tank to the water plays a vital role on deciding the set temperature. In the beginning of the process, more hydrogen is absorbed and slowly the absorption rate decreases as explained before. As Figure 27 shows, the high initial rates create a rapid increase in the temperature and high heat exchange rates with the cooling water. The heat exchange follows closely the temperature pattern of the system but there is some time lag associated with the time required for heat to convect to the water. As the water flow rate in the heat exchanger stays the same and the rate of reaction decreases, the system gradually cools down until the reaction eventually stops as the full capacity is reached by the metal hydride for the current conditions.

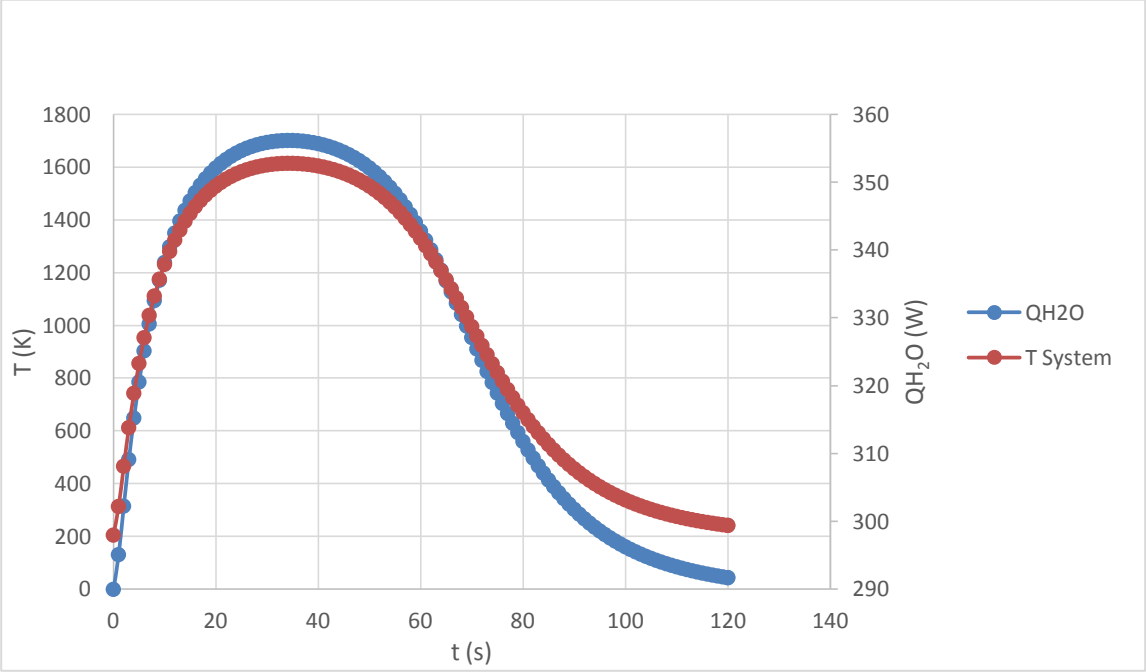

Figure 27: Temperature and heat absorbed by the heat exchanger's water Vs time.

8.2. Desorption of $LaNi_5$ tank modeling results

At time zero, there is no heat introduced in the system from the heat exchanger. As soon as the temperature of the water flowing in the heat exchanger is increased, desorption reaction spikes. At this initial point there is very high reaction rate due to the abundance of the MH present, Figure 28. The model takes some time to provide the necessary heat to the system and then reaction rate suddenly spikes. That peak is associated with the fact that the necessary heat was provided when the system was still in great abundance in MH. The reaction rate decreases very fast as the MH amount is now decreased and the easiness of gaining hydrogen out of the MH decreases as most of the surface MH is converted to solid. As the process continues, more hydrogen is desorbed and more MH is converted into solid leading to an even lower rate of reaction as can be seen in Figure 28.

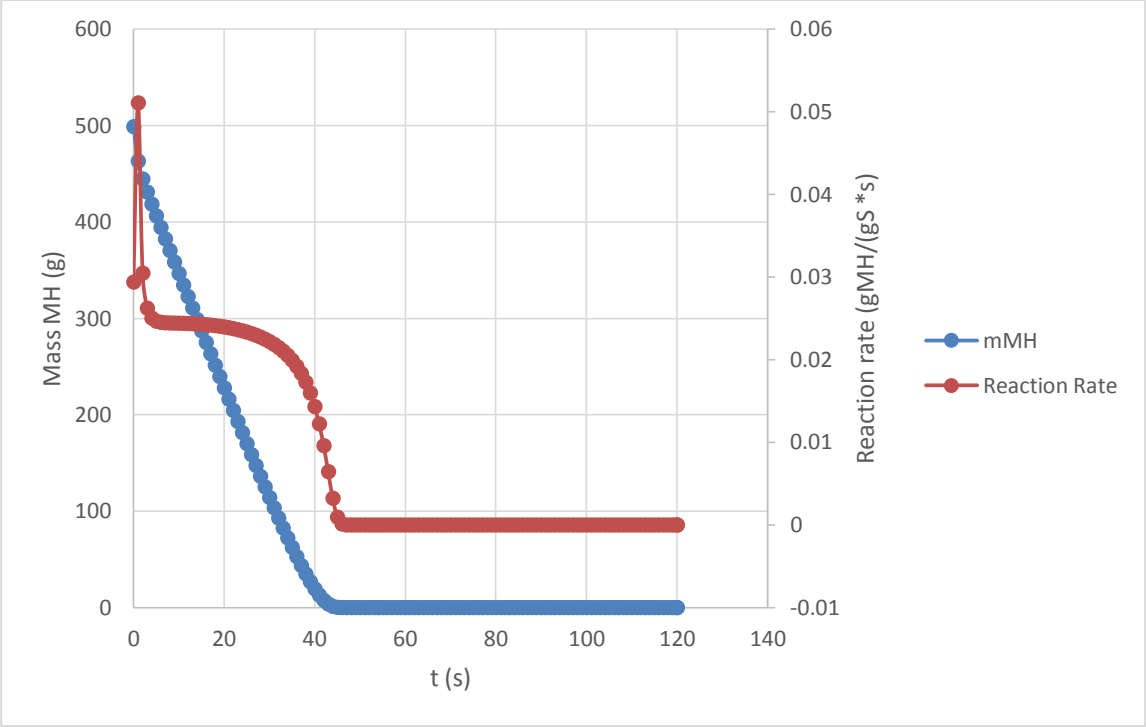

Figure 28: Mass of MH with reaction rate Vs time.

The chemical reaction is not ideal and some of the hydrogen is not desorbed and as a result there is always going to be some MH left behind. As the reaction proceeds more and more hydrogen is desorbed but the rate of outflow of hydrogen is regulated and set to be at a constant value, which is lower than the rate of desorption. For that reason, an increase in the tank pressure is witnessed as can be seen at Figure 29. As the reaction rate decreases and the hydrogen is kept pumped out at a constant flow, such that the outflow rate is greater than the amount desorbed within the tank, the available gaseous hydrogen in the tank decreases leading to lower pressures, Figure 29. At some point there is almost no mass of MH, no reaction, low pressure and small amount of hydrogen in gaseous form. These conditions signify the end of the desorption process. See Figure 28 and 29.

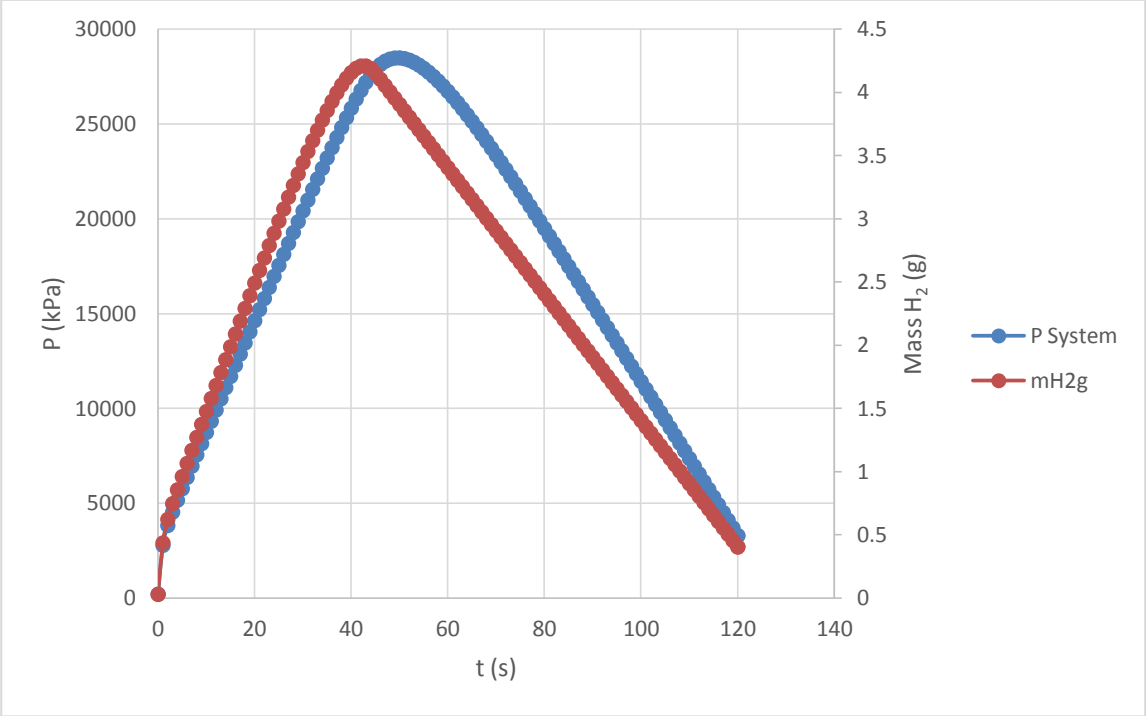

Figure 29: Pressure and hydrogen gaseous mass Vs time.

The pressure variable is positively correlated to the temperature variable. An increase in the pressure from excess hydrogen desorbed causes an increase in the temperature of the system. Desorption is an endothermic reaction which means that a heat increase causes an increase in the rate of reaction. For that exact reason, a slight increase in the reaction rate is seen between 5-25 s in Figure 28.

Due to the endothermic character of the desorption reaction causing a decrease in the temperature, the reaction rate is inhibited. For this reason, the heating water of the heat exchanger that flows around the tank has a temperature of 340 K: high enough to prevent reaction rate inhibition by providing the necessary heat as can be seen in Figure 30. The heat transfer from the tank to the water plays a vital role on deciding the set temperature. In the beginning of the process, more hydrogen is desorbed and slowly the rate decreases as explained before. The high initial rates create a rapid decrease in the temperature, but the high heat exchange rates between the heating water and the MH tank penalizing the phenomenon as can be seen at Figure 30. In the first 50 s, most of the heat transfer between the heat exchanger and the MH tank takes place and is directly associated with the reaction rate.

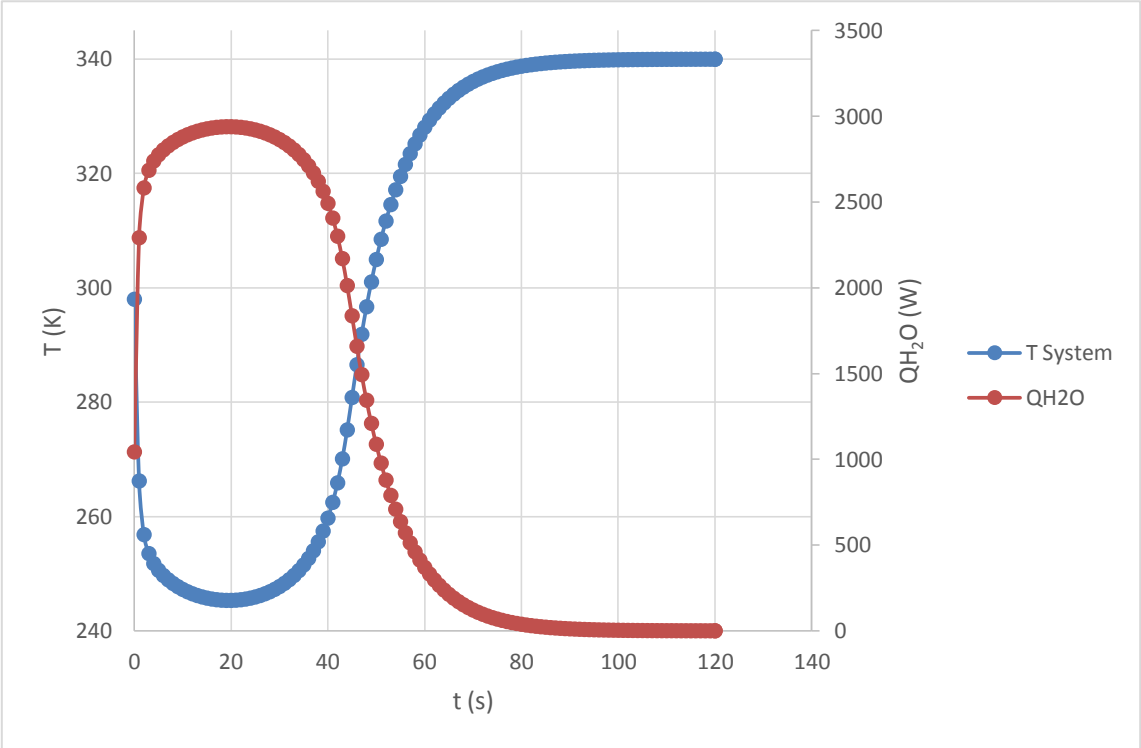

Figure 30: Temperature and heat absorbed by the heat exchanger's water Vs time.

The heat exchange curve values increases significantly and the curve that describes the temperature of the system decreases during this period of time. Just like in the

absorption case, in the desorption case there is some time lag associated with the time required for heat to convect from the heat exchanger water to the system. As the water flow rate in the heat exchanger stays constant and the rate of reaction decreases, the heat absorbed by the system decreases as well. Thus the heat exchanged deceases as shown in Figure 30. Due to the lower rate of reaction, the system gradually reaches a higher but constant temperature of 340 K as the heat exchanger keeps providing heat to the system until it reaches the set temperature. The reaction eventually stops as the hydrogen amounts stored in the MH tank is depleted for the current conditions. More but non-significant amounts of hydrogen can be further desorbed for higher temperature and pressure conditions, but that makes the system unsafe and thus these conditions are not investigated.

8.3. Absorption, desorption & PEM fuel cell connection results

8.3.1. Absorption and desorption connection results

In this model the absorption, desorption and the Fuel Cell models were connected. The first part describes the absorption connection. The two processes are switched to one another three times and the resulted data are provided. For that reason a binary variable is introduced that allows each process to alternatively operate every 120 s. The 120 s period was based on the results of the previous produced models. Within this time period there is more than enough time for the processes to reach completion, zero reaction rate and constant mass of solid and MH etc.

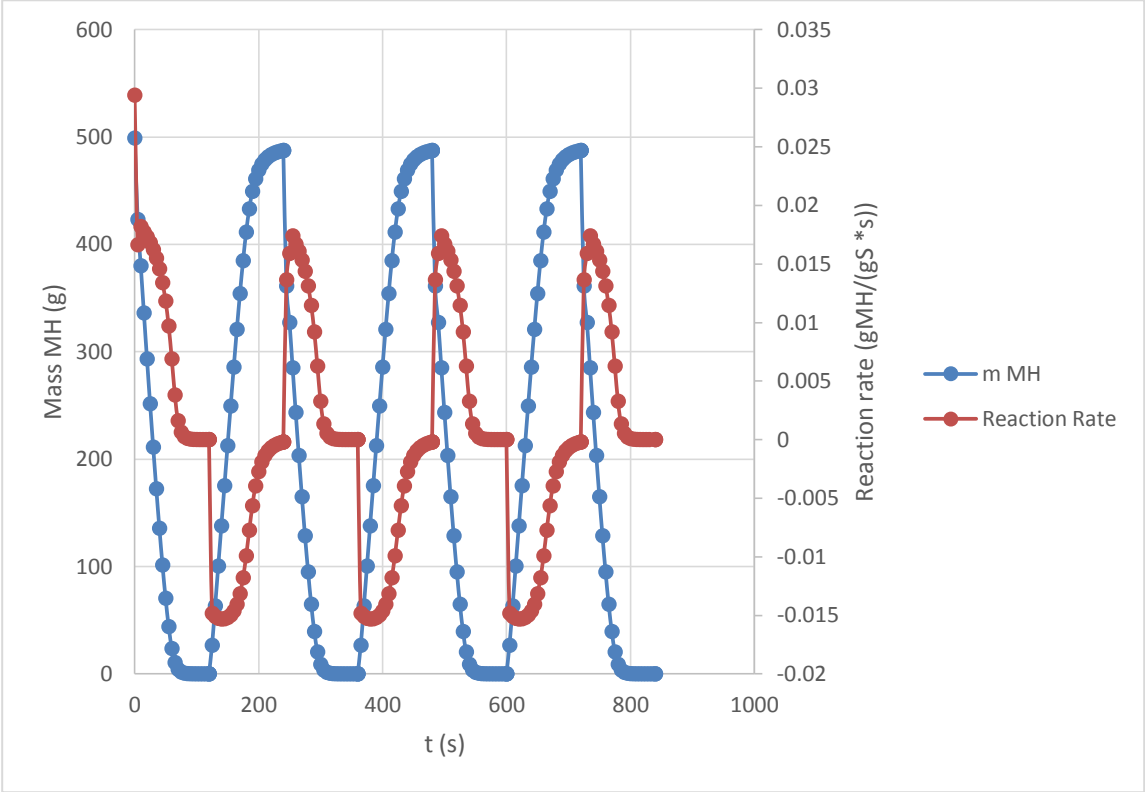

Figure 31: Mass of MH with reaction rate Vs time.

The model initiates at the desorption phase. During this phase as it has been described before and depicted again in Figure 31 the mass of the MH decreases as it is converted into solid. The mass of the MH starts to increase again when the absorption phase initiates at time 120. At the point of the switch, a very high reaction rate takes place but as the reaction continues that gradually decreases. In the graph desorption is associated with a positive reaction rate and absorption with a negative one. This change in sign is associated with the consumption and production of hydrogen and further of solid and MH. When solid and hydrogen is produced the model assumes a positive reaction rate, and when MH is produced a negative sign is introduced. In both cases, the reaction rate decreases reaching closer to zero as shown in Figure 31, which is in perfect agreement with the theory. Furthermore, the pattern of the slopes of the two curves are of similar manner showing the

close correlation between these variables proving for one more time the trustworthiness of the system.

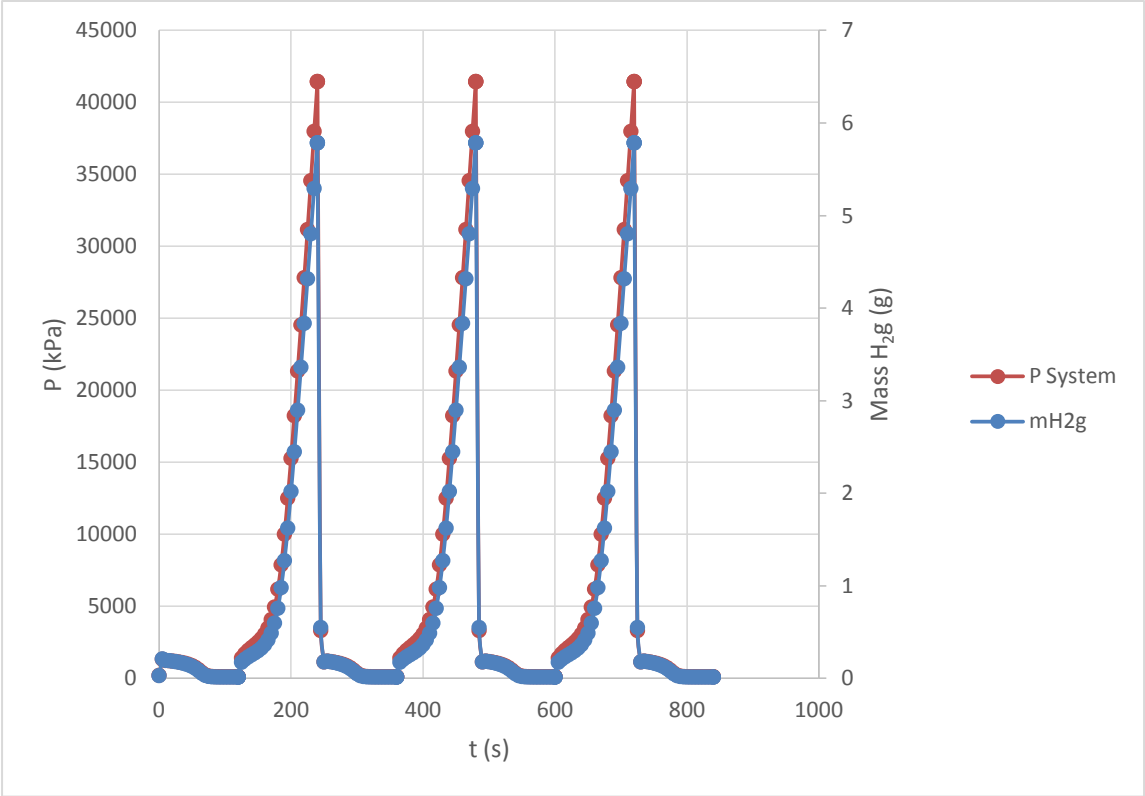

Figure 32: Pressure and hydrogen gaseous mass Vs time.

The initial high reaction rate of desorption is associated with the high amount of MH that is available and decreases as the pressure increases due to accumulated gaseous hydrogen, as can be seen in Figures 31 and 32. In the desorption phase, there is already available gaseous hydrogen, Figure 32. The pressure increases further as the currently desorbed H_2 from the MH is added to the gaseous hydrogen that was initially available. Yet that pressure starts to decreases as the gaseous H_2 flows out of the system. In the absorption case, the introduction of gaseous hydrogen in the system causes a dramatic increase in pressure. The initially lower rate of increasing gaseous hydrogen is associated with the fact that the MH allows lower operating pressures as it is absorbing most of the available hydrogen. As soon as the full capacity of the MH to H_2 is reached, the pressure of

the system increases proportionately to the gaseous H_2, resulting in major peaks that signify the end of the absorption reaction, Figure 32.

As the reactions are exothermic and endothermic, the temperature profile of the system is a vital parameter that should be analyzed. When the reaction of absorption or desorption proceeds heat is produced or absorbed by the system accordingly, inhibiting the rate of the reaction. For that reason, a heat exchanger is employed to regulate the temperature and allow greater reaction rates. Figure 33 represents that heat transfer between the system and the heat exchanger in accordance to the temperature of the system. The desorption phase requires heat to desorb hydrogen; the heat exchanger provides that heat through a constant water flow of 20 g/s at temperature of 340 K. In the beginning, due to the high reaction rate the temperature of the system falls below the system's initial temperature of 298. This leads to higher heat transfer values with the heat exchanger, Figure 33. As the reaction proceeds and the reaction rate decreases, the heat exchanger is capable of increasing the temperature of the system. This results to a decreased amount of heat-transfer. In the absorption phase, the water of the heat exchanger absorbs heat. A high amount of heat transfer occurs at the start of the reaction and decreases as the reaction proceeds. In the same manner as in desorption phase, the temperature of the system is affected more at lower reaction rates.

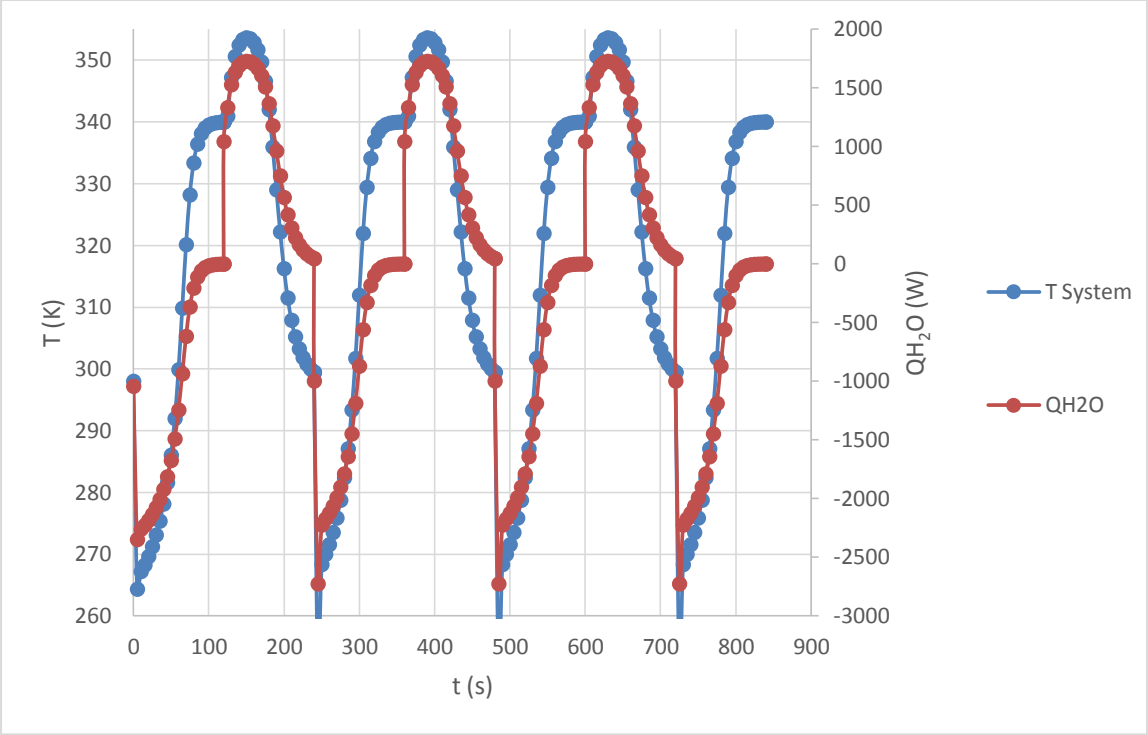

Figure 33: Temperature and heat absorbed by the heat exchanger's water Vs time.

The absorption case is when the system is being fueled with hydrogen and thus there is no desorption taking place and no hydrogen is emitted out of the MH tank to the fuel cell for the production of energy, see Figure 34. In the desorption phase though, hydrogen flows out towards the fuel cell to produce the desired power. The peaks in Figure 34 are correlated with the elevated pressure in the MH tank system during the absorption phase where extra hydrogen is pumped into storage as a gas. This stored hydrogen is rapidly released when the system is allowed to flow hydrogen to the fuel cell.

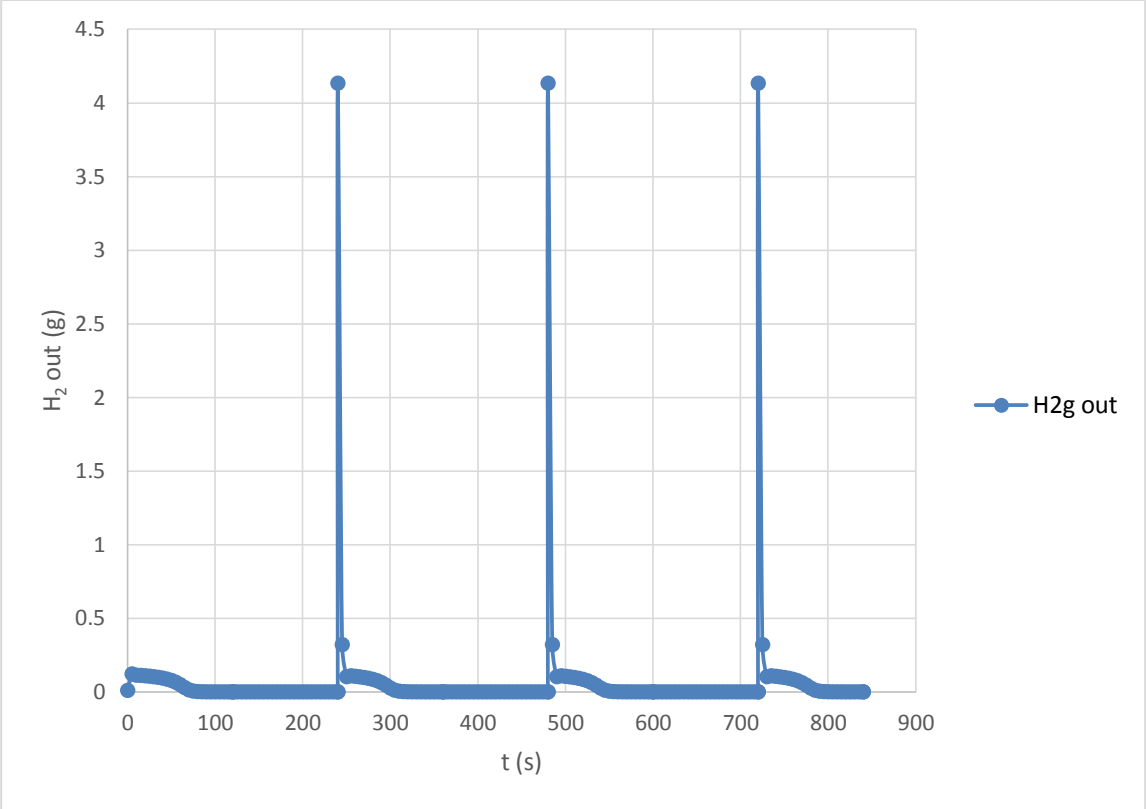

Figure 34: Hydrogen flow out from MH tank during absorption and desorption Vs time.

8.3.2. Desorption & PEM fuel cell connection results

The second part of the model is the connection between the desorption phase of the $LaNi_5$ tank and the proton exchange membrane fuel cell (PEMFC). This part of the model follows the same time principles as the absorption desorption part and it is used to describe the process that is utilized for the production of electricity from the desorbed hydrogen. During the desorption phase the fuel cell operates to produce energy, while it remains inactive during the absorption phase. During the desorption phase hydrogen flows from the MH tank to the fuel cell as shown in Figure 34. The initial peak on Figure 35 of this phase is associated with the high release flow of pressurized hydrogen gas from the MH to the anode area of the PEMFC. As the reaction proceeds, hydrogen is utilized and power is being produced leading to a decrease in its accumulation as shown in Figure 35 and 37. At the cathode part of the fuel cell, oxygen is pumped in at a constant rate during the desorption/

power production phase to meet the reaction needs and allow the production of liquid water. In a real time scenario, air is introduced to the system that is mainly composed of nitrogen and only partially by oxygen, but for simplicity, it is assumed that only oxygen is present.

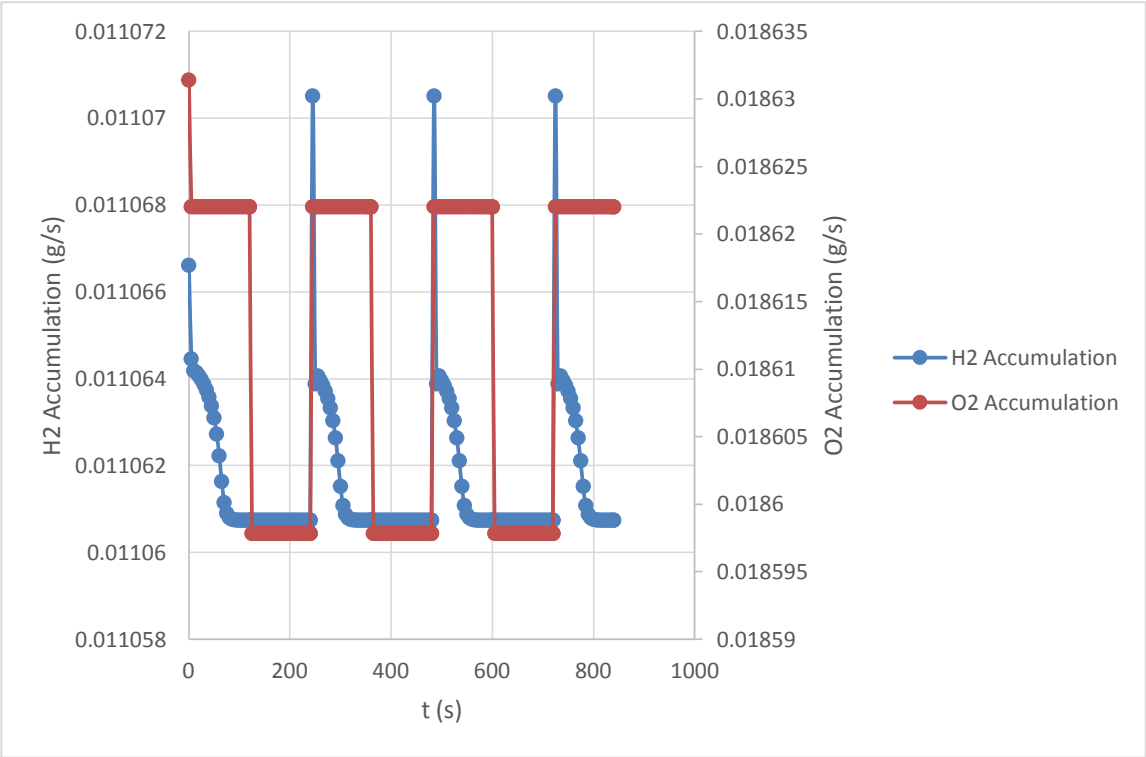

Figure 35: Accumulation of hydrogen and oxygen Vs time.

During the absorption phase there is no inflow of hydrogen. Thus there is no need for the presence of oxygen at the cathode. It is noticed that the accumulation of hydrogen does not reach zero, as there is always some on the surface of the membrane that still reacts and produces a certain amount of power. The accumulation of oxygen is even lower because when the phase changes and the inflow of oxygen becomes zero, that certain amount of remaining hydrogen is spent reacting with oxygen, Figure 36.

As hydrogen mass is being pumped in and out of the system, pressure conditions alternate that have an impact on the system i.e. the rate of reaction, see Figure 31. It is

important to sustain higher pressures in the anode part of the fuel cell so that a higher amount of hydrogen ions can pass through the membrane and react leading to higher currencies. In the model, it is assumed that in the anode there is only hydrogen vapor and in the cathode only oxygen as it is assumed that there is just enough vapor water on the electrode to allow an efficient diffusion rate through. For that reason no pressure is associated with the water accumulation in the system. In result, the anode pressure is identical with the hydrogen pressure and the cathode pressure similar to the oxygen pressure. As hydrogen is pumped in the system there is a high initial pressure created, as shown in Figure 36. The high pressure in the MH system during the absorption phase leads to a high initial inflow of hydrogen to the fuel cell and elevated initial accumulation during desorption. As the reaction proceeds and H_2 is consumed that pressure decreases, see Figure 36. During the absorption phase, when there is no inflow of hydrogen or oxygen, the pressures are constant and much decreased. The slightly higher value of anode pressure is associated with the higher accumulation of H_2.

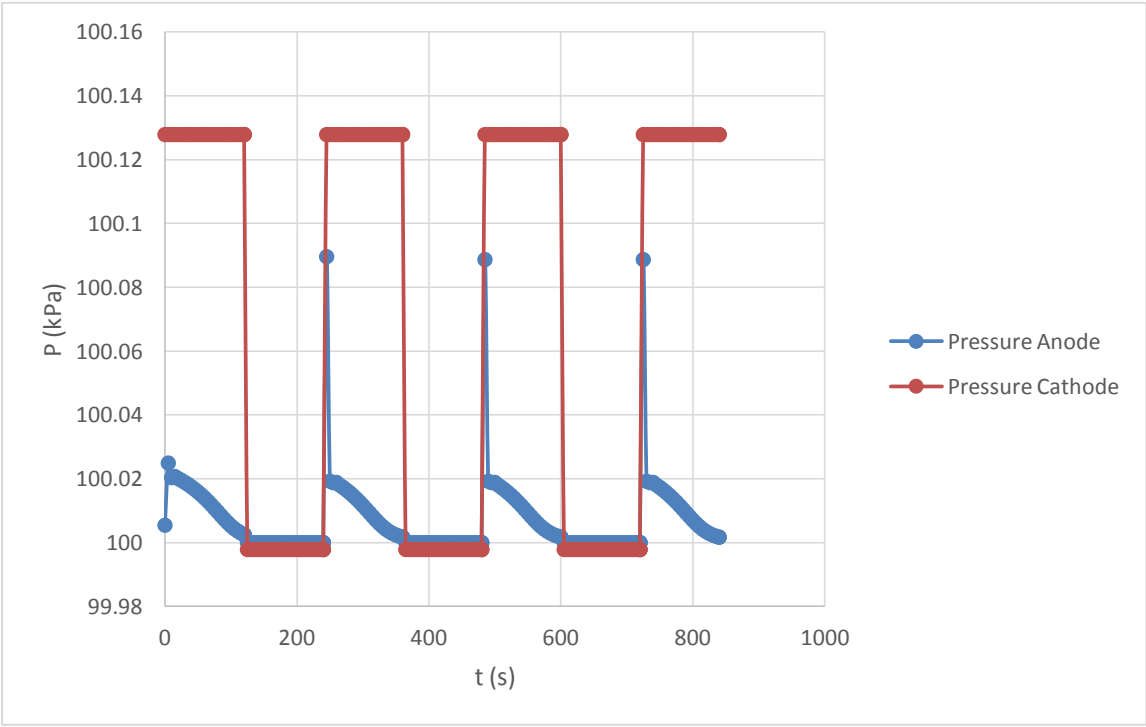

Figure 36: Pressure of anode and cathode Vs time.

Figure 37 is a better representation of the amount of the periodically produced power which has been discussed above.

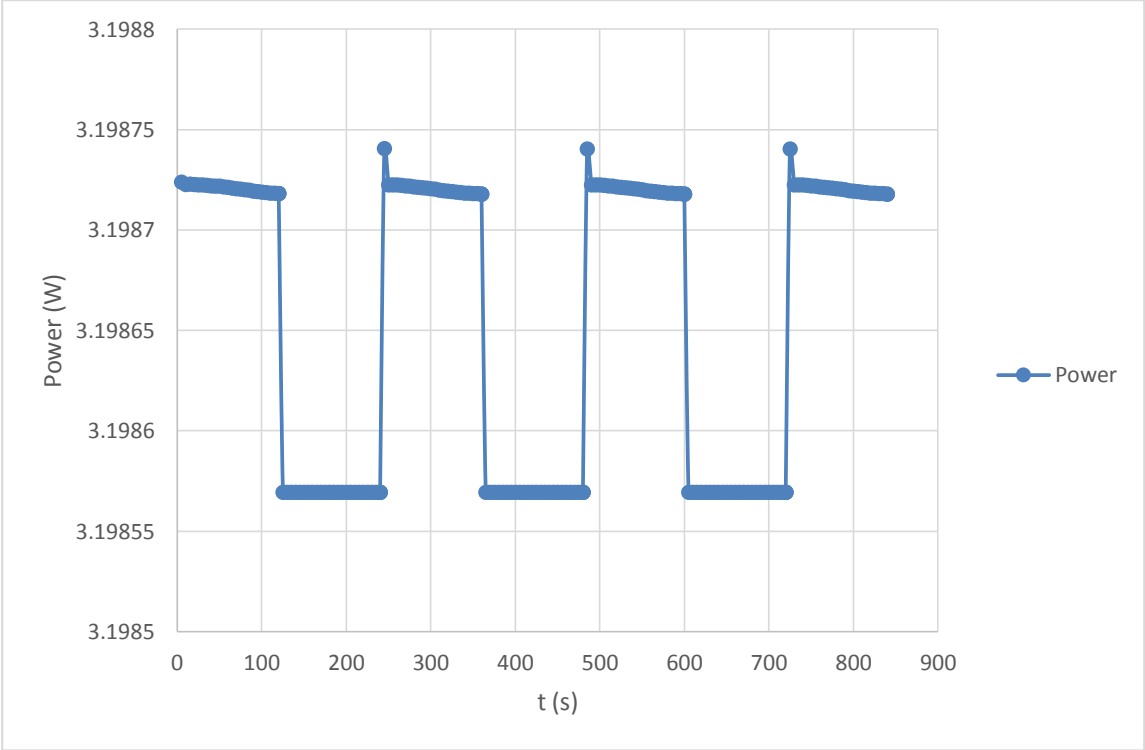

Figure 37: Power produced from the fuel cell Vs time.

The reaction that takes place in the fuel cell is exothermic leading to an increase in the temperature of the system. In Figure 38 the heat of reaction is shown and the peaks are another result of the initial amount of hydrogen that flows and reacts in the fuel cell when it is rapidly emancipated from the MH tank. The values are justifiably low due to the low amount of operating current and voltage of the system that are 4 amp and 0.8 V.

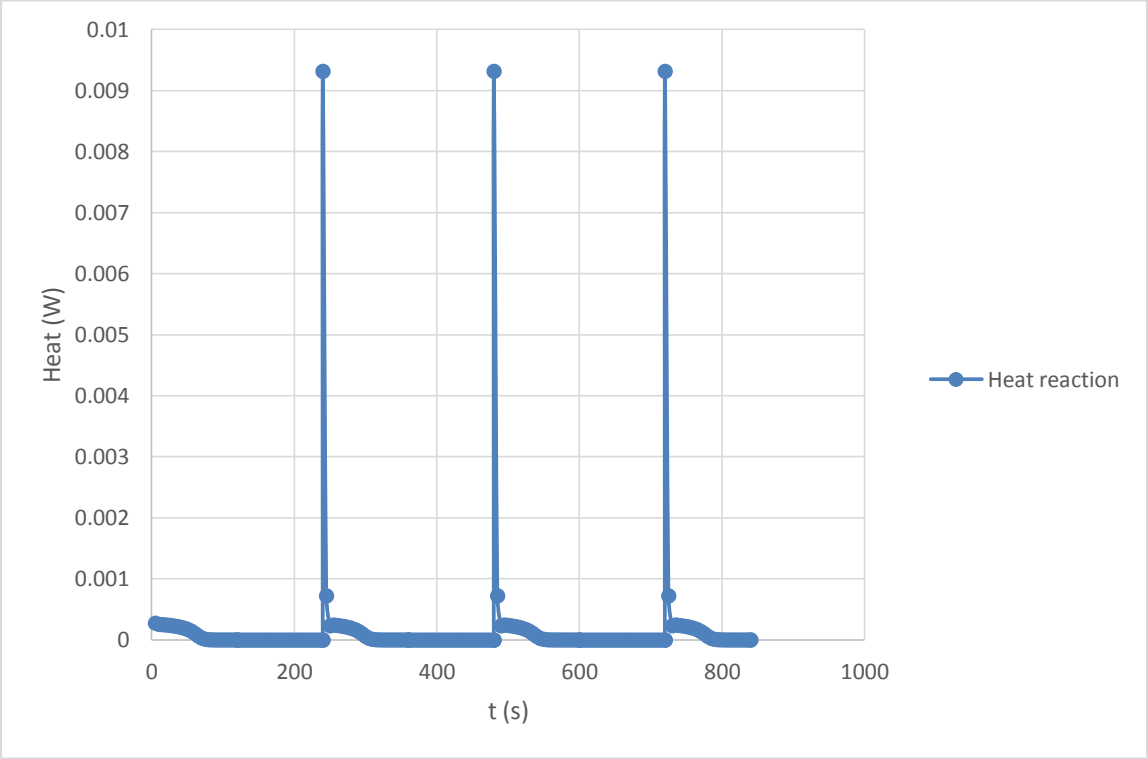

Figure 38: Power produced from the fuel cell Vs time.

It is interesting to further investigate the impact of the flow of the water in the heat exchanger to the overall system. More precisely have a comparison of how a change in the water flow can affect the temperature of the system during desorption and absorption as well as the filling and empting of the system with respect to time. The results are presented in Figures 39 and 40. Three different flows of water 20, 60, 100 g/s were tested for proof of concept. Figure 39 shows the impact of that change to the temperature of the system. As the flow increases the temperature of the system stays closer to the set point temperatures (340 for desorption and 298 for absorption). In addition, it is noted that the temperatures reach these set point values within a smaller period of time when the flow increases.

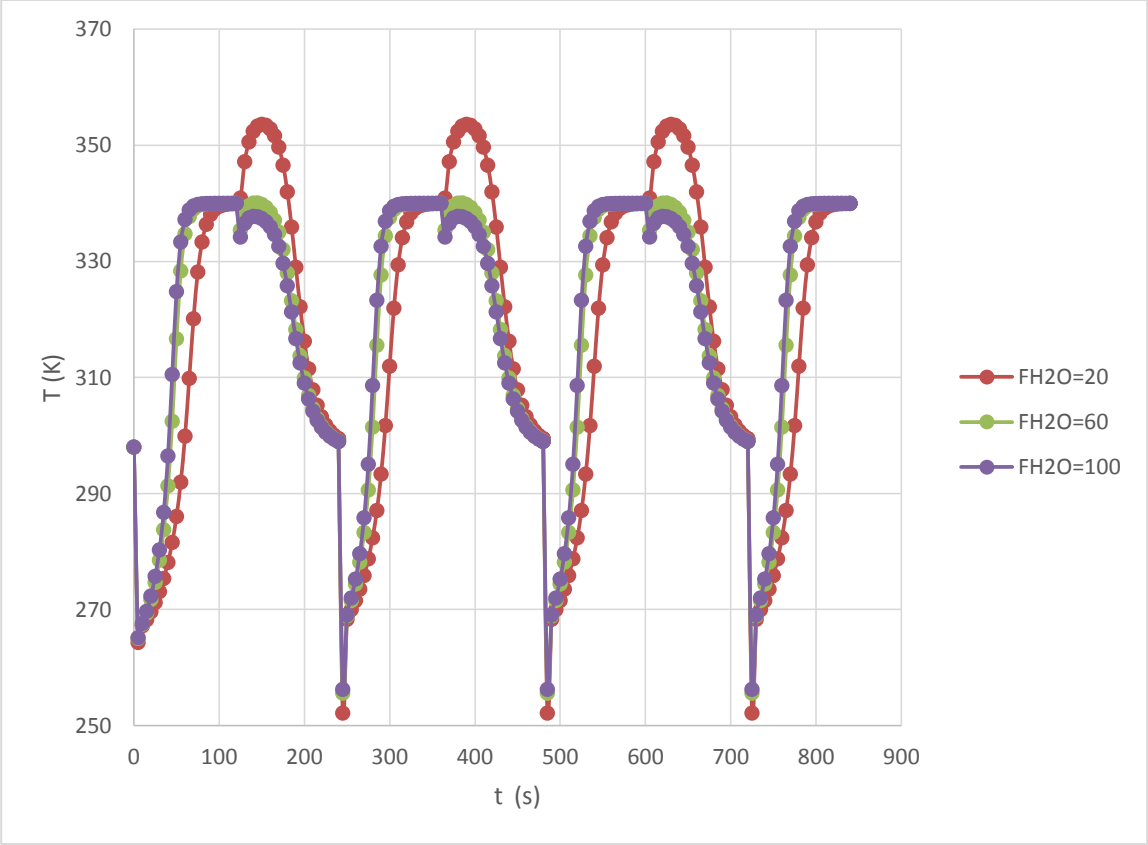

Figure 39: Impact of the flow rate of water within the heat exchanger in the temperature of the MH system in the absorption, desorption & PEM fuel cell Connected model case Vs time.

The rate of change of temperature of the system is improved with increasing flows, Figure 39. Thus, there should be higher rate of reaction of converting MH to solid and of solid to MH that implies higher filling and outflow rates. Figure 40 represents that concept. Indeed, as the flow of water in the heat exchanger increases the hydrogen storage capacity wt% in the solid is increased faster as shown in Figure 40. The same stands for the desorption case where hydrogen storage capacity decreases at a higher rates than the previous cases of lower flow rates.

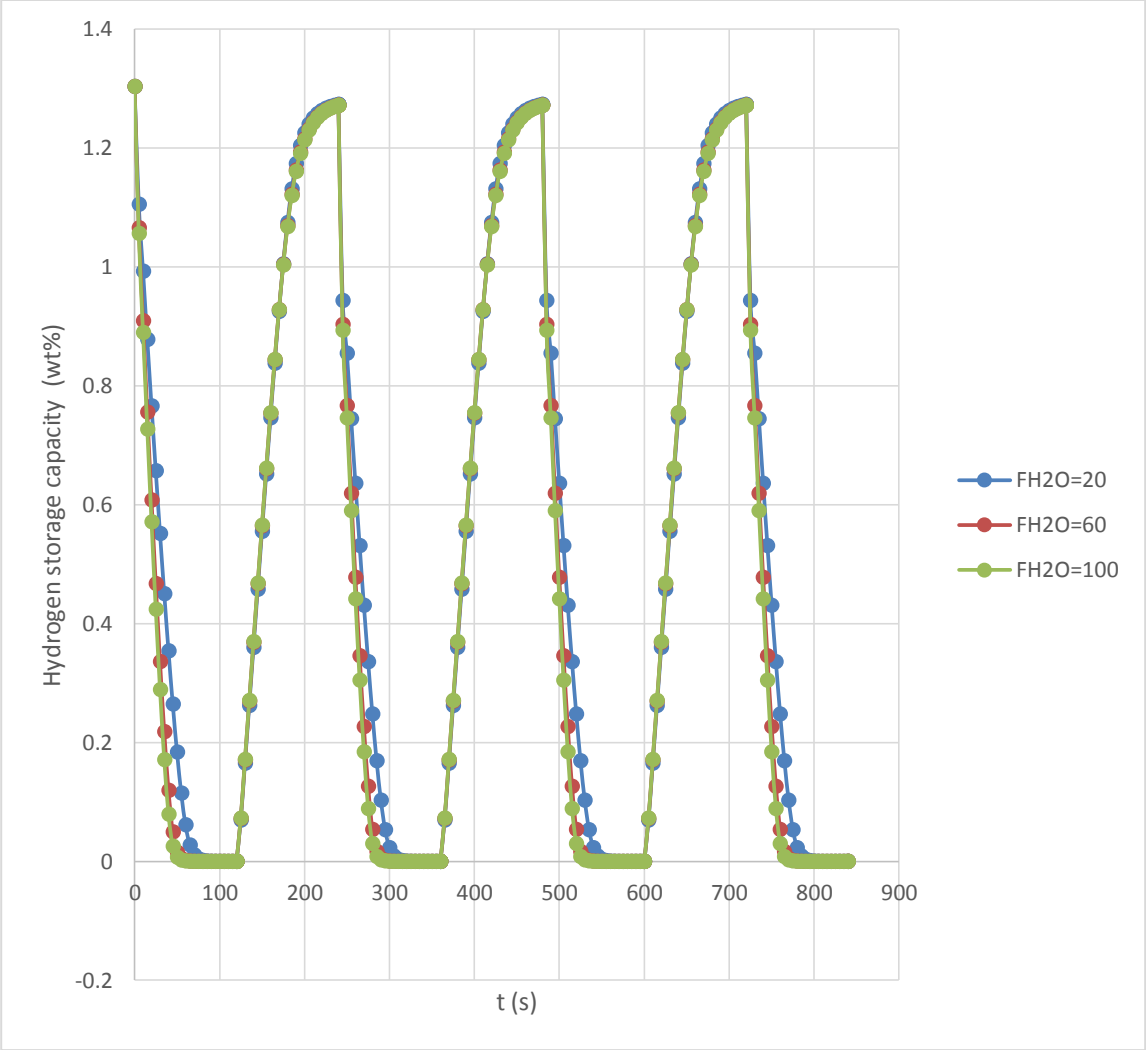

Figure 40: Impact of the flow rate of water within the heat exchanger in the hydrogen storage capacity (wt%) of the MH system in the absorption, desorption & PEM fuel cell Connected model case Vs time.

The impact of these results can also be depicted on the fuel cell technology. As the MH tank is better in responding to changes between the two phases, a certain improvement on the voltage and power produced in the fuel cell is expected as well. In Figure 41, it is shown that as the flow rate of water increases the fuel cell system gets a higher amount of voltage response within a smaller period of time showing in this way an increase in the fidelity of the system.

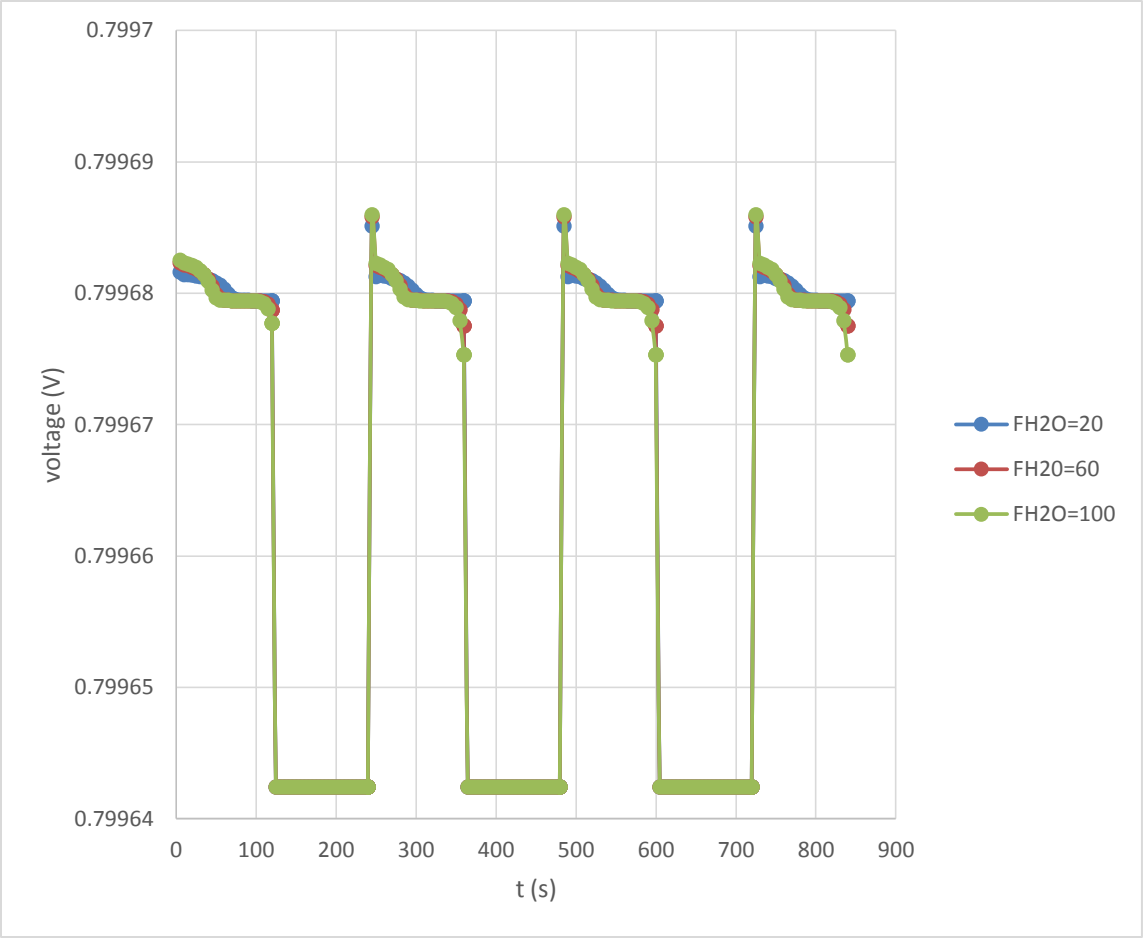

Figure 41: Impact of the flow rate of water within the heat exchanger in the stack voltage of the fuel cell in the absorption, desorption & PEM fuel cell connected model case Vs time.

8.4. PI control results

This part of the thesis describes the impact of the PI control to the system. In the PI control model the absorption and desorption temperatures of 289 K and 340 K of the water in the heat exchanger temperatures are the set points of the manipulated variables of the metal hydride system. As far as the voltage manipulated variable is concerned the set point is set to fluctuate between 0 V and 0.8 V depending on the phase of the system. During the absorption reaction (Times: 120-240, 360-480 etc.) there is no power production; thus, the voltage is set at 0 V and during desorption reaction (Times: 0-120,240-360 etc.) it is set at 0.8 V. The Kp and Ki values in the model were alternated in a process of trial and error until optimum values are reached that describe a model of higher efficiency, operability as well as safety compared to the previous case.

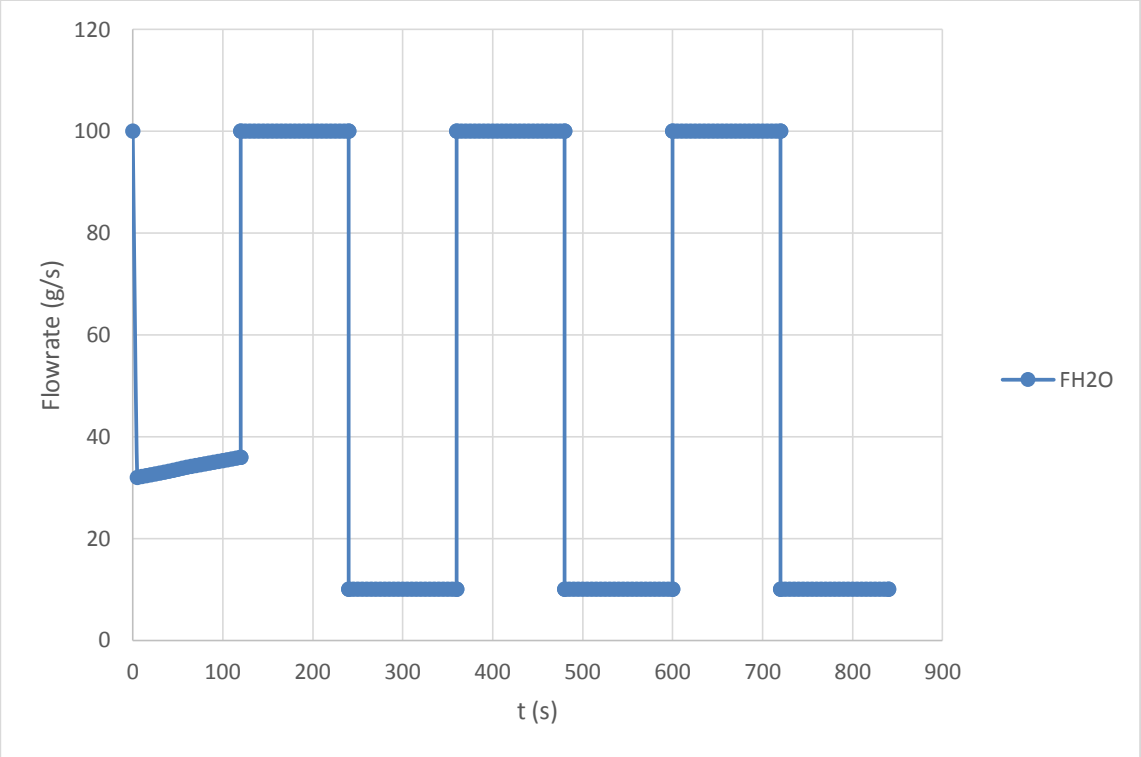

Figure 42: Flow rate of water within the heat exchanger of the MH system in the PI closed loop model case Vs time.

The PI control manipulates the flow of water in the heat exchanger depending on the phase that the system is operating at. Figure 42 shows that during the desorption case a

high flow is not required due to the elevated temperature of the water, which has a great impact on the system. In the case of absorption the flow rate is higher as the temperature of the water does not have such a great difference to the operating temperature. In contrast, the desorption case requires lower flow rates to lead to the desired results. In the PI model there are higher rates of heat transfer per unit time in contrast to the simple case. Such results would preclude the PI model from operating if the flow rates were of the same magnitude due to liability issues associated with elevated temperatures and pressures in the system. The PI model allows an alternation of the flow rate of the water in the heat exchanger, which unlike the simple method, is safer and more efficient. The safety character arises from the fact that this flow rate alternation has an impact on the amount of heat transferred per unit of water through the pipe. In the case of absorption for example, as the flow rate increases the amount of heat exchanged is greater than the simple case due to the greater quantities of water flow through per unit time. This can be seen in the PI control case results in Appendix 2. In that way the control can impact the temperature of the system by meeting the set points not only in a safer manner but within a shorter period of time as well, see Figure 43.

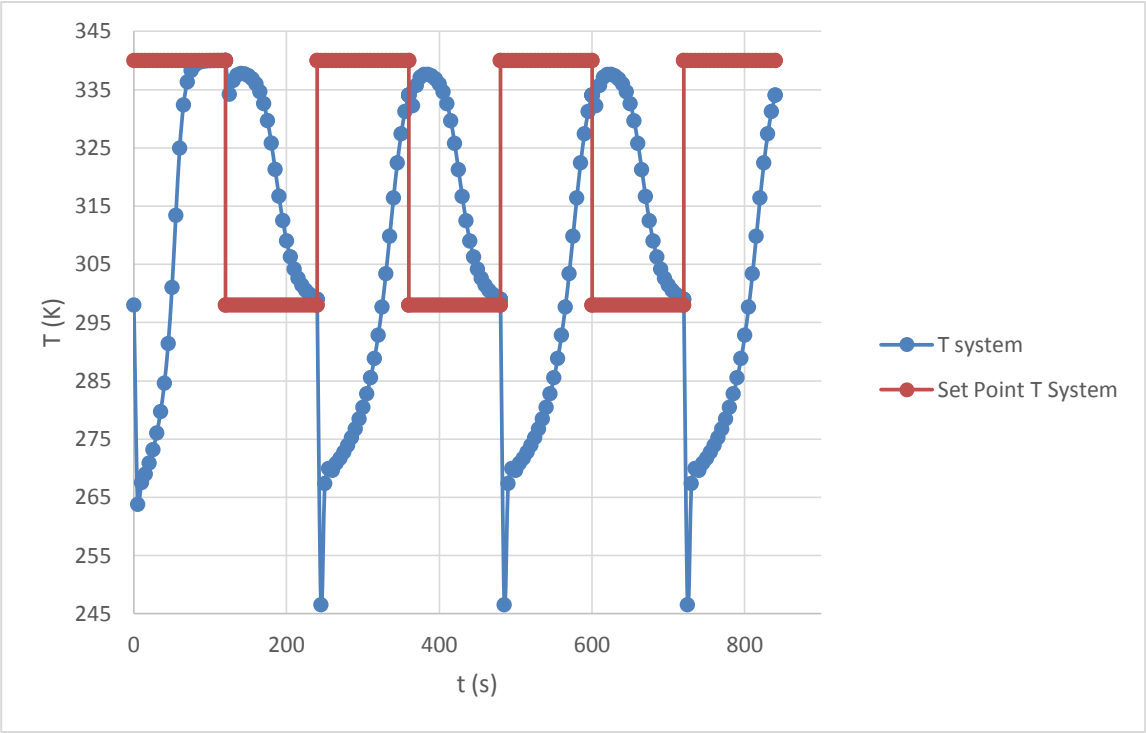

Figure 43: MH tank temperature and set point temperature in the PI closed loop model case Vs time.

The fact that the temperature of the system reaches the desired temperature faster than the simple case provides a major advantage in the process. It allows the fueling reaction to take place at a higher rate, see Figure 44, and can allow this technology to compete with the commercial cases. Desorption PI case has another great advantage in contrast to the simple case. The PI control through the higher heat transfer allows the system to react rapidly in any demand in energy. At any instance the model can be operated with higher fidelity as the reaction rate allows for production of the demanded energy within a smaller period of time as is shown in Figure 45.

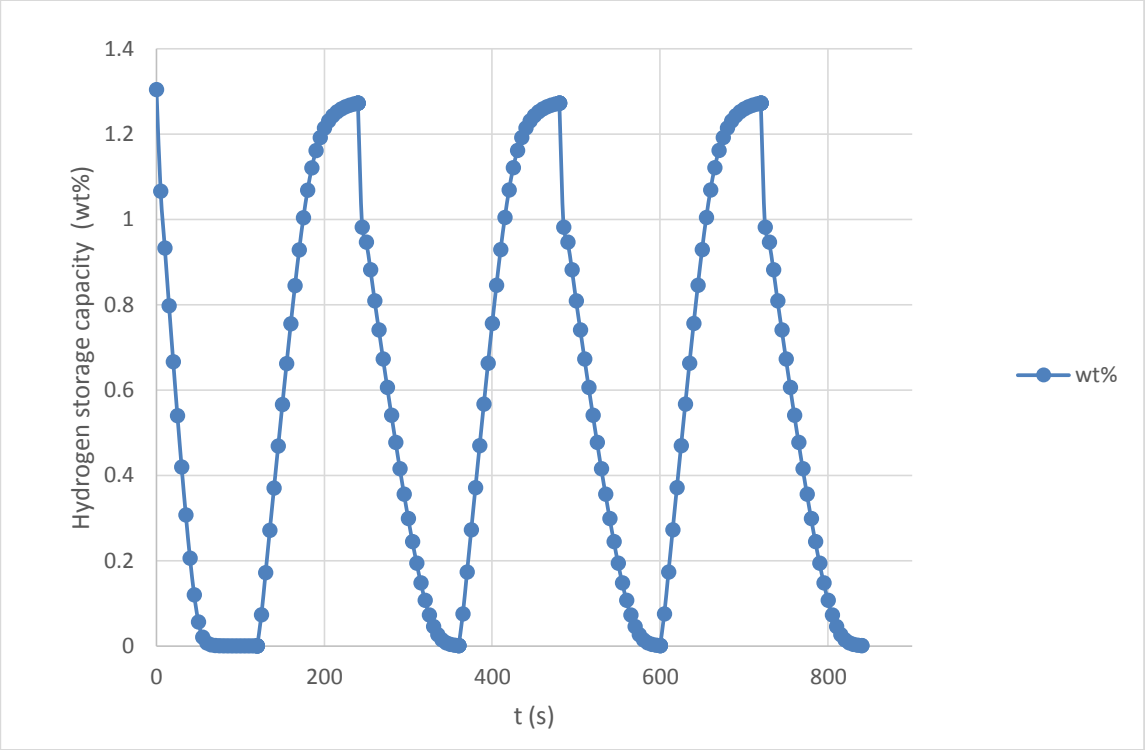

Figure 44: Hydrogen storage capacity (wt %) in the PI closed loop model case Vs time.

Figure 44 represents the rate of emancipation of hydrogen during desorption and the rate storage of hydrogen during absorption. The impact of the higher amount of heat provided during the desorption and taken away during the absorption phases allows higher rates of reaction that lead to a greater amount of released and stored hydrogen per unit time accordingly.

The voltage produced by the fuel cell is in accordance to the operation of the PI control, see Figure 45. The reason why the system does not lead to zero voltage production during the absorption phase is associated with the accumulation of hydrogen in the anode of the fuel cell. The peaks are associated with the fast initial flow of hydrogen from the MH tank to the fuel cell as a result of the stored gaseous hydrogen in the tank.

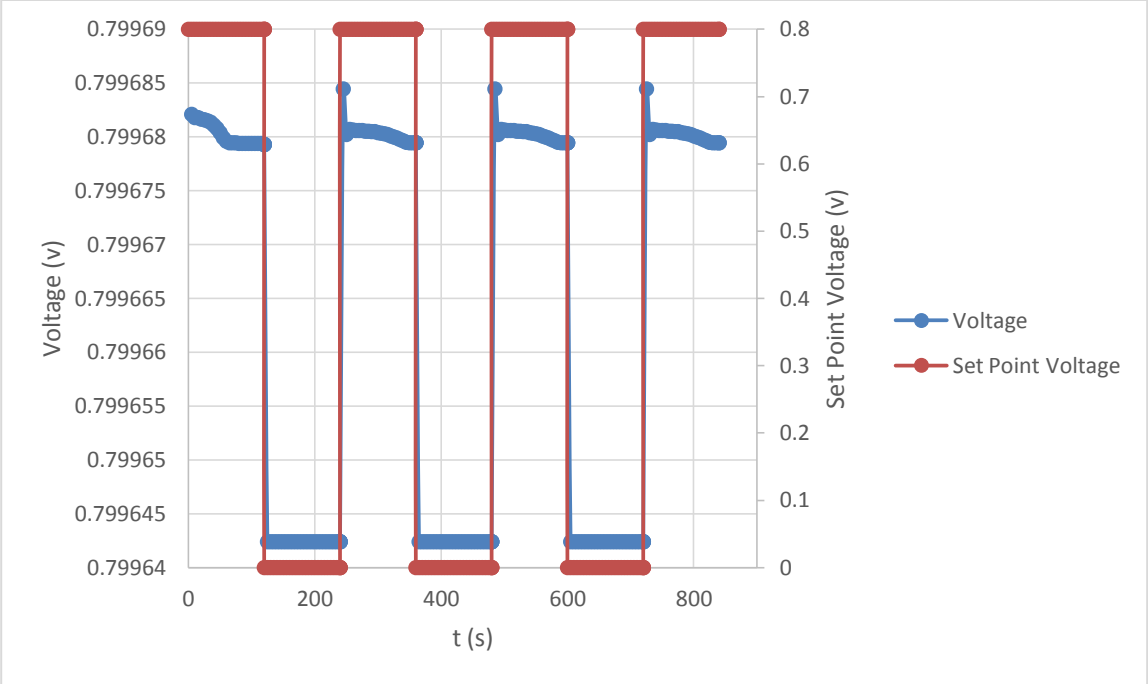

Figure 45: Voltage produced and set point voltage in the PI closed loop model case Vs time.

8.5. Results evaluation

The described operated tested PI model sufficiently met its target set points within a smaller operating time than the simple case. The temperature points are met without any fluctuations and the curves are steep adding trustworthiness to the response of the system to a change in the phase. Regarding the power needed, in the PI control case the voltage produced is sufficient and at a more constant rate than the simple case. However, the voltage may not reach zero power output during the absorption phase due to accumulation of hydrogen in the anode of the fuel cell, causing energy loss. Yet that can be because the scale of the system modeled is so small that such quantities cannot be properly utilized by the fuel cell. The system responds immediately to a change in energy demand, but the magnitude of the response is very small.

9. CONCLUSIONS

This section is an overview of the path taken as well as the important results derived from this thesis. The results are presented in parallel to the main contributions that allowed the formulation, representation and solution of the model.

9.1. Concluding remarks

This thesis is motivated by the need to derive a solution in mitigating the greenhouse gases emissions to the environment by human action and more specifically by their transportation. It is expected that the transportation sector will realize an exponential increase in demand of non-renewable energy resources in the future. In a mean to provide a solution that can mitigate the impact to the environment and the human quality of life without restricting the transportation factor, essential technologies must be utilized. This thesis was motivated from this exact need. More specifically, this thesis is combining and attempts to optimize already established models to produce a fully integrated dynamic energy model that describes the storage of a chosen fuel until its utilization for the production of power. More specifically the storage system describes a high pressure metal hydride (HPMH) tank where the fuel, hydrogen, is stored mainly in solid phase. The energy conversion technology chosen is a PEM fuel cell (PEMFC) system that converts the chemical energy into useful energy that can be further utilized by an automobile. The most important part of this thesis is the control in the operation of the system. The main issue associated with this hydrogen storage and utilization is the time taken to store the hydrogen in the tank and the rate of hydrogen provided to the engine. The role of the PI controls is to manipulate different variables that allow maximization of fuel storage and, depending on the power required by the engine, allow a steady rate of the desired amount of hydrogen outflow. The controllers form a higher fidelity system with greater safety precautions as the automatization operates in case scenarios that have been taken under consideration. Further, the controllers do not allow the system to operate out of certain pre-described threshold values. This thesis characterizes the operability of HPMH tank technology

combined with a PEMFC and how the utilization of PI controls can lead to supreme operating conditions and higher efficiencies.

Hydrogen, although a non-renewable fuel, can become a fuel with no GHG emissions when operated with the suggested technologies. Hydrogen can reach higher energy densities than the commercial fuels i.e. gasoline if stored accordingly. For that reason, in chapter 1 various hydrogen storage technologies were introduced and compared with one another. It was concluded that chemical storage of hydrogen in a high pressure metal hydride tank allows a higher energy density, lower weight, and lower volume take-up compared to other hydrogen storage technologies as well as the commercial cases. HPMH storage overcomes the pre-described issues by allowing a greater concentration of the fuel through solid form. Furthermore, the safety parameters associated with the properties of hydrogen in combination to the operation of the system are analyzed for each storage case. The findings present that HPMH is the safest one, making it preferable for a moving storage tank. These characteristics are associated with lack of moving parts, high hydrogen gas purity, compactness of the system and the fact that hydrogen when stored within MH cannot be extracted if sufficient heat is not provided. To determine the most effective for our non-stationary case MH an investigation of various parameters and procedures that affect their operability and lifetime took place. Through the research and comparison the optimal metal hydride $LiNa_5$ was chosen based on its competitive characteristics. $LaNi_5$ has high hydrogen density at lower weight, providing better chances to the energy system to complete with the commercial energy cases.

The next part of the thesis described the engine part of the model, the fuel cell. In this chapter of the thesis, the technology was compared to other energy producing technologies such as diesel engine, photovoltaics etc. and it was determined that fuel cells have the highest attainable efficiencies (Energy output per Chemical energy input) as the energy is released electrocatalytically compared to the commercial case where combustion has to take place. The main disadvantage is that it has comparative higher cost per unit of energy production. Yet, the fuel cell technology has advantages that can significantly impact our hesitance in using this technology stemming from its higher costs. More specifically, it has zero emission rates attaining sustainability and is silent—an important parameter when traveling in the cities where noise can be a negative externality to the lives of people. Also, it is scalable so it can be applied to different kinds of engines and it is rapid in its

installation making it preferable when time is an issue. Though different kinds of fuels could be used, the fact that hydrogen is used as our fuel and transportation is the field that the model will be implemented in, PEMFC or AFC must be used. An overall analysis was composed and determined that PEMFC allows the maximum power density and the lowest operating temperature that gives safety credits to the system. In addition, PEMFC has a rapid startup which is vital when operating an automobile and it is size and weight applicable assisting in the overall space and weight saving character of the system. These characteristics allow higher energy supply when required, better fidelity and better safety operating conditions. The disadvantages that are associated with the PEMFC is the comparative lower efficiency (40-45%) and its sensitivity to impurities of CO and H_2S.

After the utilized technologies are determined there is the need for the automatization of the system. That need is associated with higher efficiency and safer operating conditions. For that reason in chapter 4 the proportional-integral (PI) control is introduced. This controller is chosen based on its simplicity. More complicated controls can be based on this mindset, such as a model predictive control (MPC), and further improve the operability of the system. The impact of the control in the system by alternating the flow rate of water in the heat exchanger leads to higher absorbing and desorbing rates. That allows faster fueling rates of the MH tank and more rapid response to a voltage requirement by the PEMFC. The PI decreases the time required to fill the tank and at the same time increases the fidelity of the operating system as at any instant enough energy is supplied.

Chapter 5 contains the background of modeling of these systems. More specifically it described the conditions and the nature of assumptions that were taken under consideration that led to the next chapter's results. The mathematical relationships that have been illustrated in the section have been solved using a powerful modeling language specifically for the process industries named gPROMS. The uniqueness of this software arises from its duality on the language and graphical representations consistency. For these models, most of our numerical values were taken from the literature and the rest from the actual experimental apparatus that were available. The operating conditions were assumed identical as in the experimental and arithmetical work of Laurencelle and al (Talagañisa & Meyerb, 2011) and Ziogou (Ziogou, 2013) see Appendix 1. The different key variables were plotted in comparison to one another to represent the impact and result in a better understanding of the dynamic character of the system under various conditions.

The PI results indicated that the implementation of a closed loop model in the system leads to better results. It was concluded that indeed a fully integrated system of pairing a MH tank, fuel cell and with the assistance of a control is a viable solution that can be utilized in the future as a promising combination technology that is more friendly to the environment and of higher sustainability than the commercial cases.

9.2. Evaluation

The use of assumptions in the system allowed a higher level of simplicity as in some instances, the implemented models were just having an overcomplicating manner without a critical effect in the outcome. Although the existence of some parameters is known their true impact on the dynamic system is not always predictable as that depends on the system. For example, it is assumed that there is zero heat and time loses when heat is convected from the MH tank to the pipe of the heat exchanger and finally to the water of the heat exchanger. In some cases, this assumption can have significant impact on the case study of the system and thus it must be taken under consideration so that to better represent the actual system. Furthermore, different geometries of the actual system that is represented alternate the results of the model. A cylindrical MH tank is described by different equations compared to a rectangular one. Furthermore, it would be good in the model to have a valve between the HPMH tank and the PEMFC to allow a better regulation of the amount of hydrogen flowing from one system to the other. For simplification reasons, the accumulation of hydrogen in the tube before the valve was not taken into account in the model and no hydrogen accumulation equations were considered. A more realistic representation of the experimental model must include the rate of flow of ions from the anode to the cathode depending on the pressure and moisture level present due to their great impact on the PEMFC model. In the fuel cell it is assumed that there is just enough amount of water vapor available causing no increase of pressure nor flooding of the electrode which is a factor that inhibits the reaction rate. That moisture level variable must be taken into consideration in a more realistic model case scenario. In addition, the HPMH tank model representation would be great to have a temperature distribution analysis within the MH as to show at which radius there is higher change in temperature so that to have a better understanding of the MH system's operability. Furthermore, a thorough

analysis of the temperature of water in the heat exchanger must take place. It is important to state that there is no linear relationship between the temperature of the water and the temperature of the system for the amount of heat exchanged. For that reason different temperatures must be tested to find the optimum for each sorption process that maximizes heat transfer within the system and minimizes heat losses to the environment.

The optimal set point temperatures affect the PI control as well. Determining optimal SP temperatures for the water that flows in the heat exchanger system will allow improved flow rates of water from the heat exchanger. In our model, the flow rates take extreme values to meet the specified set points. Operating in such a high temperature during desorption does not guarantee that the outcome can be that great in the real system as there are associated heat losses to the environment that take place. For the desorption case, it would be optimal to have a higher fluctuation of flow rate of lower temperature water rather than a higher temperature that requires a minimum flow of water. The high temperature is associated with liability and efficiency issues as it is associated with higher risks of overheating and energy consumption. In the absorption case, the temperature of the water must be set at a lower point so that a higher fluctuation of flow rate would be allowed. In both cases such changes would allow the system to fluctuate the flow rate of water more, regulating better the process and improving the safety character of the operating system. This is due to the fact that the control through the heat exchanger can correct and protect better the system from extreme temperature values and sustain higher reaction rates when it operates below the extreme flow rate values and maximum heat exchange capacities.

In the real system more energy must be introduced as the different flow rate, temperature and pressure conditions in the system are not as ideal as modeled and thus the system must be studied for imperfections and limitation. Such issues arise from heat losses to the environment, as the surrounding temperature will have an impact on the operating conditions and the material resistance depending on their convection rates which will place limitations on the heat transfer phenomenon of the system. Further precautions in the system's model are associated with the rate of poisoning and degradation of the MH, the electrodes and the catalyst in the model. These conditions may depict differences on some of the modeled characteristics such as activation energy, enthalpy entropy etc.

For that reason, it is suggested to run the actual experiment that the model describes and then utilize the system's actual values such as enthalpy change, heat of reaction, mass and heat transfer coefficients. These values can be later implemented in the model and allow a more facile manner of counteracting the actual problems of the system as the model is a better representation of the actual operating system, with smaller error along the actual and modeled data.

This model represents a system that can highly change the image of the transportation sector as we know it today. This is possible as the system combines different characteristics that are not yet found in the market. More specifically, its installation is easier and more rapid, it is lighter in weight, it takes up lower volume, it has higher safety properties than the commercial case and it utilizes a fuel of higher energy density when stored in solid phase. That model can be utilized in the automobile industry for all kinds of automobile power requirements as it is easily scalable. In addition, the system can act as a new form of battery within the car. The car can produce and store hydrogen in the MH tank through electrolysis when less amount of energy is required than available allowing higher sustainability and operating time. The possibilities and applications are limitless and if it can be sufficiently modeled and efficiently operated and controlled, it can lead to solve one of the greatest energy sustainability problems associated with GHG emissions from non-renewable fossil fuels within the transportation sector.

BIBLIOGRAPHY

Berube, G., Radtke, M. D., & Gang. (2007, 05). Size effects on the hydrogen storage properties ofnanostructured meta l hydrides: A review. *International Journal of Energy Research* , pp. 637-663.

Brenda, G. L., Vijay, S. A., & Wei, J. W. (2004, 06 15). Mathematical Model of a Direct Methanol Fuel Cell. *Fuel Cell Science and Technology , 1(43)*, pp. 43-48.

Canha, L., Popov, V., & Farret, F. (2002). Optimal characteristics of fuel cell generating systems for utility distribution networks. Washington: IEEE.

Cheng, K., Sutanto, D., Ho, Y., & Law, K. (2001). Exploring the power conditioning system for fuel cell. Vancouver: IEEE.

Colominas, S., McLafferty, J., & Macdonald, D. D. (2009). Electrochemical studies of sodium borohydride in alkaline aqueous solutions using a gold electrode. *Electrochimica Acta-Elsevier , 54 (13) 3575-3579*.

Control, S. M. (2016). *Anatomy of a Feedback Fontrol System*. Retrieved 04 23, 2017, from Control Solutions Minnesota: https://www.csimn.com/CSI_pages/PIDforDummies.html

Cook, B. (2002). *Introduction to fuel cells and hydrogen technology.* Vancouver, Canada: Engineering science and Educational Journal.

Coors, W. (2003, 05 25). Protonic ceramic fuel cells for high-efficiency operation with methane. *Power Sources , 118 (1-2) pages 150-156*, pp. 150-156.

Corgnale, B. J., Hardy, D. A., Tamburello, S., Garrison, S. L., & Anton, D. L. (2012, 10). Acceptability envelope for metal hydride-based hydrogen storage systems. *International Journal of Hydrogen Energy* , pp. 14223-14233.

Dynamics, N. (2014). *SPECIFIC ENERGY AND ENERGY DENSITY OF FUELS.*

Eberle, U., Felderhoff, M., & Ferdi, S. (2009). Storage Hydrogen, .Chemical and Physical Solutions. *Angewandte Chemie International Edition* , pp. 6608-6630.

EG&G Technical Services, I. (2004). *Fuel Cell Handbook (7th Edition).* Virginia: U.S. Department of Energy .

EIA. (2013, 2 14). *TODAY IN ENERGY*. Retrieved 10 26, 2016, from www.eia.gov: https://www.eia.gov/todayinenergy/detail.php?id=9991

Endo, K., Matsumura, Y., & Kawakami, M. (2016, 04 20). Energy, Operation of metal hydride hydrogen storage systems for hydrogen compression using solar thermal. *Journal of International Council on Electrical Engineering* , pp. 65-71.

Energizer, B. M. (2016). *Nickel Metal Hydride (NiMH) Handbook and Application Manual.*

Energy. (2016). *HYDROGEN STORAGE*. Retrieved 10 26, 2016, from energy.gov: http://energy.gov/eere/fuelcells/hydrogen-storage

ENERGY.GOV. (2016). *CHEMICAL HYDROGEN STORAGE MATERIALS*. Retrieved 10 26, 2016, from http://energy.gov: http://energy.gov/eere/fuelcells/chemical-hydrogen-storage-materials

EnergyEIA. (2013). *EIA projects world energy consumption will increase 56% by 2040*. Retrieved 04 16, 2017, from eia.gov: https://www.eia.gov/todayinenergy/detail.php?id=12251

European, C. (2017). A roadmap for moving to a competitive low carbon economy in 2050. Brussels: European Commission.

Flamberg, S. R., & Denny, S. (2010). *Analysis of Published Hydrogen Vehicle Safety Research.* U.S. Department of Transportation, National Highway.

Fuel Cell, N. A. (n.d.). *Fuel Cell Theory*. Retrieved 05 14, 2017, from http://www.fuelcell.no/principle_fctheory_eng.htm

Glass, S. R., & Glass, G. (2000). *Hydrogen Gas Safety.* Los Alamos National Laboratory.

Hardy, D. L., & Corgnale, B. J. (2012, 10). Structural analysis of metal hydride-based hybrid hydrogen storage systems. *International Journal of Hydrogen Energy* , pp. 14223-14233.

Hart, D. (2016). More Than One Giant Leap: The Future for Fuel Cells. *Renewable Energy World* .

Heung, L. K. (2003). *Using Metal Hydride to Store Hydrogen.* Savannah River Technology Center.

Honeywell, D. (2000). *Design and Analysis of Feedback Systems.* Retrieved 05 25, 2017, from Caltech Department of Computing + Mathematics: https://www.cds.caltech.edu/~murray/courses/cds101/fa04/caltech/am04_ch8-3nov04.pdf

Huang, X., Zhang, Z., & Jian, J. (2006). Fuel Cell Technology for Distributed Generation: An Overview. Montreal, Quebec, Canada: IEEE.

Jamarda, R., Salomona, J., Martinent-Beaumonta, A., & Coutanceau, C. (2009). Life time test in direct borohydride fuel cell system. *Power Sources-Elsevier , 193 (2) pges 779-787*, 779-787.

Kirubakaran, A., Shailendra, J., & Nema, R. K. (2009, 12). A review on fuel cell technologies and power electronic interface. *Renewable and Sustainable Energy Reviews , 13(9) pages 2430-2440*, pp. 2430-2440.

Lamari-Darkrimb, M. H., & Sakintunaa, F. (2007, 06). Metal hydride materials for solid hydrogen storage: A review. *International Journal of Hydrogen Energy* , pp. 1121-1140.

Larminie, J., & Dicks, A. (2003). *Fuel Cell System Explained.* Sussex, England: John Wiley &Sons Ltd.

Maru, M. F., & HANS, C. (2001). Fuel Cells—The Clean and Efficient Power Generators. *IEEE , 89 PAGES 1819-1829*, pp. 1819-1829.

MICHAEL, E. W., VON SPAKOVSKY, M. R., & Nelson, D. J. (2001). Fuel Cell Systems: Efficient, Flexible Energy Conversion for the 21st Century. *IEEE , 89 (12) pages 1808-1818*, pp. 1808-1818.

Mishra, V., Yang, F., & Pitchumani, R. (2005, 02 16). Analysis and design of PEM fuel cells. *Power Sources , 141*, pp. 47-64.

Mozsgai, G., Yeom, J., Flachsbart, B., & Shannon, M. (2003). A silicon microfabricated direct formic acid fuel cell. Boston: IEEE.

Mudawar, T., Visaria, I., & Pourpoint, S. (2010, 04). Study of heat transfer and kinetics parameters influencing the design. *International Journal of Heat and Mass Transfer* , pp. 2229-2239.

Nehrir, C. W., & Hashem, M. (2007). Distributed Generation Applications of Fuel Cells. Clemson, SC, USA: IEEE.

Olsen, Z. A., & ZaluskiJ, O. (2001). *Structure, catalysis and atomic reactions on the nano-scale: a systematic approach to metal hydrides for hydrogen storage.* SpringerLink.

O'Sullivan, J. (1999). Fuel cells in distributed generation. Palo Alto: IEEE.

Payáa, M., Linderb, E., Corberána, & Laurienb, J. (2009, 04). Dynamic model and experimental results of a thermally driven metal hydride cooling system. *International Journal of Hydrogen Energy* , pp. 3173-3184.

PSE. (1997). gPROMS.

Pukrushpan, J. T., Peng, H., & Stefanopoulou, A. (2004). Control-Oriented Modeling and Analysis for Automotive Fuel Cell Systems. *Dynamic Systems, Measurement, and control , 126(1), 14-25*, 14-25.

Ragheb, M. (2011). *Hydrides alloys for hydrogen storage.* Retrieved 05 25, 2017, from http://mragheb.com/: http://mragheb.com/NPRE%20498ES%20Energy%20Storage%20Systems/Metal%20Hydrides%20Alloys%20for%20Hydrogen%20Storage.pdf

Rosaa, A., Valverdea, F., del Reala, A., & Arceb, C. (2013, 09 10). Modeling, simulation and experimental set-up of a renewable hydrogen-based domestic microgrid. *International Journal of Hydrogen Energy* , pp. 11672-11684.

Sakintunaa, F., & Lamari-Darkrimb, M. H. (2007, 06). Metal hydride materials for solid hydrogen storage: A review. *International Journal of Hydrogen Energy* , pp. 1121-1140.

Sandi, G. (2004). *Hydrogen Storage and its Limitations.* The electrochemical Society Interface.

Schüth, B. B., & Felderhoff, M. (2004, 09 21). Light metal hydrides and complex hydrides for hydrogen storage. *Chemical Communications* , pp. 2249-2258.

Soltani, M., & Bathaee, S. M. (2008). A new dynamic model considering effects of temperature, pressure and internal resistance for PEM fuel cell power modules. Nanjing: IEEE.

Swider-Lyons, K., Carlin, R., Rosenfeld, R., & Nowak, R. (2002). Technical issues and opportunities for fuel cell development for autonomous underwater vehicles. San Antonio: IEEE.

Talagañisa, G., & Meyerb, P. A. (2011, 10). Modeling and simulation of absorption–desorption cyclic processes for hydrogen storage-compression using metal hydrides. *International Journal of Hydrogen Energy* , pp. 13621-13631.

TPUB. (n.d.). *Instrumentation and contro*. Retrieved 05 25, 2017, from TPUB: http://nuclearpowertraining.tpub.com/h1013v2/css/Automatic-Control-System-112.htm

TZIMAS, F. C., PETEVES, S., & VEYRET, J.-B. (2003). *HYDROGEN STORAGE:STATE-OF-THE-ART AND FUTURE PERSPECTIVE.* Luxembourg: Petten, The Netherlands.

Valverdea, F., Rosaa, A., del Reala, A., & Arceb, C. (2013, 09 10). Modeling, simulation and experimental set-up of a renewable hydrogen-based domestic microgrid. *International Journal of Hydrogen Energy* , pp. 11672-11684.

Visaria, I., Mudawar, T., & Pourpoint, S. (2010, 04). Study of heat transfer and kinetics parameters influencing the design. *International Journal of Heat and Mass Transfer* , pp. 2229-2239.

Xu, H., Kong, L., & Xuhui, W. (2004). Fuel Cell Power System and High Power. *IEEE , 19 (5) pages 1250-1255*, pp. 1250-1255.

Yakabe, H., Sakurai, T., Sobue, T., Yamashita, S., & Hase, K. (2006). Solid Oxide Fuel Cells as Promising Candidates for Distributed Generators. Singapore: IEEE.

Ziogou, C. (2013). *Modeling, Optimization and Control of an Integrated PEM Fuel cell System.*

APPENDIX 1

Nomenclature

t	Time, s	MW	Molecular weight, $gmol^{-1}$
m	Mass, g	R	Universal gas constant, $J\ mol^{-1}\ K^{-1}$
f	Hydrogen flow, gs^{-1}	*Subscripts*	
r	Reaction rate, $g_{MH}\ g_s^{-1}\ s^{-1}$	sl	Plateau slope coefficient
T	Temperature, K	a	Absorption
P	Pressure, kPa	eq	Equilibrium
A	Heat interchange area, m^2	H_2	Hydrogen
V	Volume, m^3	MH	Metal hydride
U	Overall heat transfer coefficient, $W\ m^{-2}\ K^{-1}$	s	Solid
ΔH	Enthalpy, $J\ mol^{-1}$	g	Gas
ΔS	Entropy, $J\ mol^{-1}\ K^{-1}$	w	Refrigerating water
C	Kinetic constant, s^{-1}	in	Inlet
E	Activation energy, $J\ mol^{-1}$	SC	Stoichiometric coefficient
Cp	Specific heat, $J\ g^{-1}\ K^{-1}$		
wt%	Hydrogen capacity in weight percent		

A 1.1. Mathematical formulas of the MH model

A 1.1.1 Hydrogen mass balance

For the absorption reaction the equation that describes the gaseous hydrogen conversion is:

$$\frac{dm_{H_2 g}}{dt} = f_{inH_2} - rm_s \frac{MW_{H_2} \times SC}{MW_{MH}}$$

For desorption:

$$\frac{dm_{H_2 g}}{dt} = -f_{outH_2} - rm_s \frac{MW_{H_2} \times SC}{MW_{MH}}$$

A 1.1.2.Metal Hydride mass balance

For the absorption and desorption reaction the equation that describes the solid mass conversion is:

$$\frac{dm_{MH}}{dt} = rm_s$$

A 1.1.3.Hydrogen energy balance

For the energy balance equation, it is assumed that the temperature of the solid and the gas phases are of the same temperature. Consequently, the energy balance in the reactor for the absorption case can be illustrated by a lone equation:

$$(m_{H_2g} \times C_{pH_2} + m_S \times C_{pS}) \times \frac{dT}{dt} = f_{inH_2} \times C_{pH_2} \times (T_{in} - T) + A \times U \times (T_w - T) - \Delta H \times rm_s \times \frac{SC}{MW_{MH}}$$

For desorption:

$$(m_{H_2g} \times C_{pH_2} + m_S \times C_{pS}) \times \frac{dT}{dt} = A \times U \times (T_w - T) - \Delta H \times rm_s \times \frac{SC}{MW_{MH}}$$

A 1.1.4.Rate of Reaction

In the literature, numerous expressions take under consideration various parameters of the system to represent the rate of the reaction such as pressure, temperature and concentration per unit time. An issue is introduced when a general and yet accurate correlation of the reaction rate per unit time is required. This is due to the non-constant value of the reaction rate value over the reaction period. The root of this variation is that the rate of the reaction depends on many distinct reactions of the metal with the hydrogen within or on the surface of the metallic material. The equation that satisfy these criteria for the absorption reaction is:

$$r = C_a \times e^{-E_a/R \times T} \times \ln\left(\frac{P_a}{P_{eq}}\right) \times \left(1 - \frac{m_{MH}}{m_s}\right)$$

For desorption:

$$r = C_d \times e^{-E_d/R \times T} \times \left(\frac{P_d - P_{eq}}{P_{eq}}\right) \times \left(\frac{m_{MH}}{m_s}\right)$$

A 1.1.5.Equilibrium Pressure

Based on the theory a PCI or pressure composition isotherm, the equilibrium pressure depends on temperature and on hydrogen to metal ration value. A good way of

modeling the equilibrium pressure is through the Van't Hoff's relation. Van't Hoff's theory suggests that the plateau pressure must only depend on the temperature. Attempting to make the relation more realistic, the slope constant of the material applied is taken under consideration. The equilibrium pressure is then being characterized by a function of hydrogen concentration and temperature. For the absorption, the equation is expressed as:

$$P_{eq} = e^{\left(\frac{\Delta H_a}{RT} - \frac{\Delta S_a}{R} + sl \times \left(\frac{m_{MH}}{m_s} - 0.5\right)\right)} \times P_o$$

For desorption:

$$P_{eq} = e^{\left(\frac{\Delta H_d}{RT} - \frac{\Delta S_d}{R} + sl \times \left(\frac{m_{MH}}{m_s} - 0.5\right)\right)} \times P_o$$

A 1.1.6.Complementary Equations

The ideal gas state equation is:

$$m_{H_2 S} = \frac{P \times V_g}{R \times T} \times MW_{H_2}$$

The Hydrogen capacity in weight percent is describes as:

$$wt\% = \frac{m_{MH}}{m_s} \times \frac{MW_{H_2} \times SC}{MW_{MH}} \times 100$$

A Table 1: Parameters used in computations.

Parameter	Absorption	Desorption	Units
Material	$LaNi_5$	$LaNi_5$	
A	0.01552	0.01552	m^2
V_g	1.7375×10^{-4}	1.7375×10^{-4}	$m^3{}_{H2}$
U	2500	2500	$W\ m^{-2}\ K^{-1}$
m_s	488.98	488.98	g_s
P_o	100,000	100,000	Pa
T_{in}	298	298	K
ΔH	$-30{,}478$	30,800	$J\ mol^{-1}{}_{H2}$
ΔS	-108	108	$J\ mol^{-1}{}_{H2}\ K^{-1}$
E	21,170	16,420	$J\ mol^{-1}{}_{H2}$
C	59.2	9.6	s^{-1}
Cp_{H2}	14.3	14.3	$J\ g^{-1}{}_{H2}\ K^{-1}$
Cp_S	0.355	0.355	$J\ g^{-1}{}_{S}\ K^{-1}$
R	8.314	8.314	$m^3 J\ mol^{-1}{}_{H2}\ K^{-1}$
MW_{H2}	2.016	2.016	$g_{H2}\ mol^{-1}{}_{H2}$
MW_{MH}	432	432	$g_{MH}\ mol^{-1}{}_{MH}$

A Table 1 Continued: Parameters used in computations.

Parameter	Absorption	Desorption	Units
SC	2.76	2.76	$mol_{H2}\ mol^{-1}{}_{MH}$
m_{H2O}	0.41024	0.41024	g
sl	0.13	0.13	
F_{inH2}	0.1		$g_{H2}\ s^{-1}$
F_{outH2}		0.05	$g_{H2}\ s^{-1}$
Cp_{H2O}	4.184	4.184	$J\ g^{-1}{}_{H2O}\ K^{-1}$
phi	0.2	0.2	
T_{H2Oin}	298	303	K
F_{H2O}	2	2	$g_{H2O}\ s^{-1}$
Initial conditions			
m_{MH}	0	498.9811	g
m_{H2g}	0.02805	0.028051	g
T	298	298	K
T_{H2Oout}	298	298	K

A 1.2. Mathematical formulas of the Fuel cell model

A Table 2: Parameters used in computations.

Parameter	Fuel cell (PEM)	Units
No of cells	1	
Area act	0.0025	m^2
Vol Cath	0.000136	m^3
Vol Anod	0.000136	m^3
Gas const	8.314	$m^3 J\ mol^{-1}{}_{H2}\ K^{-1}$
Orifice const	0.0003629	Pa
Molar ms Oxy	16	$g\ mol^{-1}$
Molar ms Hydro	2.016	$g\ mol^{-1}$
faraday	96485	$Col\ s^{-1}$
E1	1.3205	
E2	−0.00312	
E3	0.000187	
E4	−0.000074	
E5	0.0033	
E6	−0.00000755	
E7	0.000785	
E8	0.000033	

A Table 2 continued: Parameters used in computations.

Parameter	Fuel cell (PEM)	Units
E9	0.06	
Ht cap stk	779	J g^{-1} K^{-1}
Ht cap Oxy	0.918	J g^{-1} K^{-1}
Ht cap water	4.1813	J g^{-1} K^{-1}
Ht cap Hydro	14.300	J g^{-1} K^{-1}
e	0.95	
Stack mass	1.38	g
sig	5.678×10^{-8}	
Area rad	355.27×10^{-4}	m^2
Assign		
Current	0.1 + 0.00375×Time	amps
Atm press	100,000	Pa
In ms Hydro	0.03	g s^{-1}
In ms Oxy	0.01	g s^{-1}
Initial conditions		
stack_temp	298	K
acc_ms_Hydro	0.03	g s^{-1}
acc_ms_Oxy	0.01	g s^{-1}

A 1.2.1. Anode Equations

A 1.2.1.1. Hydrogen balance equations

$$\frac{d\, acc_{ms_{Hydro}}}{dt} = in\_ms\_Hydro \; - \; out\_ms\_Hydro \; - \; Rxtd\_ms\_Hydro$$

$$par\_press\_Hydro = \; gas\_constant \; \times \; stack\_temp \times \frac{acc\_ms\_Hydro}{Molar\_ms\_Hydro \; \times \; Vol\_Anod}$$

$$anode\_press \; = \; par\_press\_Hydro$$

$$tol\_ms\_outA = \; 10 \times orifice\_const \; \times \; (anode\_press \; - \; atm\_press)$$

$$out\_ms\_Hydro \; = \; tol\_ms\_outA \times \frac{par\_press\_Hydro}{anode\_press}$$

A 1.2.2. Cathode Equations

A 1.2.2.1. Mass continuity or state equations

$$\frac{d\ acc_{ms_{Oxy}}}{dt} = in\_ms\_Oxy - out\_ms\_Oxy - Rxtd\_ms\_Oxy$$

$$Cat\_press = 4.72 * par\_press\_Oxy$$

A 1.2.2.2. Partial pressure of species in in cathode

$$par\_press\_Oxy = gas\_constant \times stack\_temp \times \frac{acc\_ms\_Oxy}{Molar\_ms\_Oxy \times Vol\_Cath}$$

$$tol\_ms\_outC = orifice\_const \times (Cat\_press - atm\_press)$$

$$out\_ms\_Oxy = tol\_ms\_outC \times \frac{par\_press\_Oxy}{Cat\_press}$$

A 1.2.3. Other mass flow

$$Rxtd\_ms\_Oxy = Molar\_ms\_Oxy \times \frac{current}{4 \times faraday}$$

$$Rxtd\_ms\_Hydro = Molar\_ms\_Hydro \times \frac{current}{2 \times faraday}$$

A 1.2.4 Stack Voltage

$$Stack\_voltage = (Nerst_{voltage} - Activation_{loss} - Ohmic_{loss} - conc_{loss})$$

$$Nerst_{voltage} = 1.23 + 8.5 \times 10^{-4} \times (stack_{temp} - 298) +$$

$$gas\_constant \times \frac{stack\_temp}{2 \times faraday} \times log(par\_press\_hydro \times par\_press\_oxy^{0.5})$$

$$Activation_{loss} = E1 + E2 \times stack_{temp} + E3 \times stack_{temp} \times \log(current)$$

$$+E4 \times stack\_temp \times log(Conc\_oxy)$$

$$Conc\_oxy = \frac{par\_press\_oxy}{5.08 \times 10^{6} \times e^{\frac{-498}{stack\_temp}}}$$

$$Ohmic\_loss = (E5 + E6 \times stack\_temp + E7 \times current) \times current$$

$$conc\_loss = E8 \times e^{E9 * current}$$

A 1.2.5. Thermodynamic

$$stack_{mass} \times Ht_{cap_{stk}} \times \frac{d\ stack\_temp}{dt} =$$

$$0.001 \times Heat\_rxn + P\_Elect - chem\_conv - Rad\_heat$$

$$Heat_{rxn} = in_{ms_{Hydro}} \times Ht_{cap_{Hydro}} \times \left(stack_{temp} - 298.15\right)$$

$$+ in\_ms\_Oxy \times Ht\_cap\_Oxy \times (stack\_temp - 298.15)$$

$$chem_{conv} = 0.01 \times 0.072 \times \left(stack_{temp} - 298.15\right)$$

$$+ 0.012696 \times (stack\_temp - 298.15);$$

$$P\_Elect = no\_cells \times stack\_voltage \times current$$

$$Rad\_heat = e \times sig \times Area\_rad \times (stack\_temp^4 - 298.15^4)$$

$$Curent\_Desnity = \frac{current}{Area\_act}$$

APPENDIX 2

A 2.1. Absorption

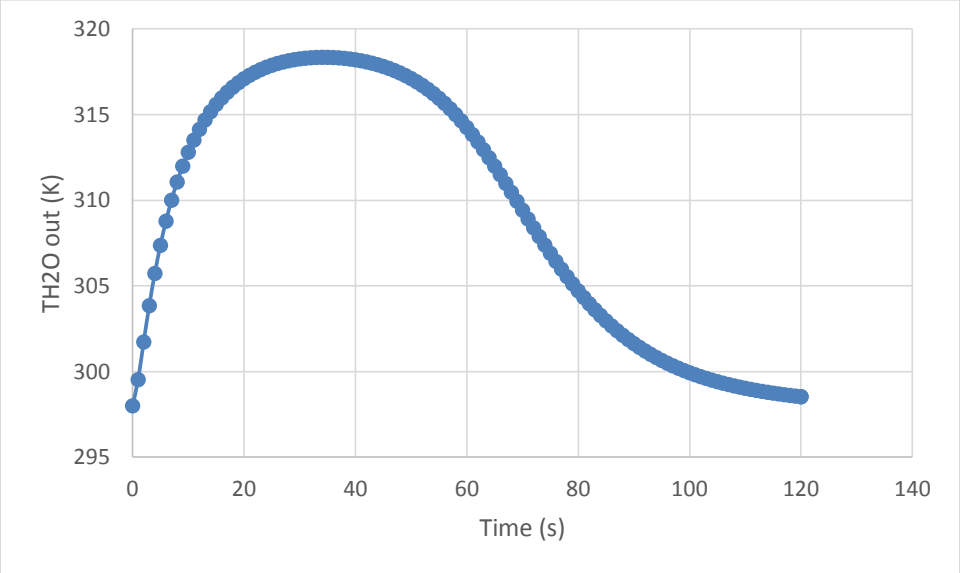

A Figure 1: Water temperature out from heat exchanger Vs Time

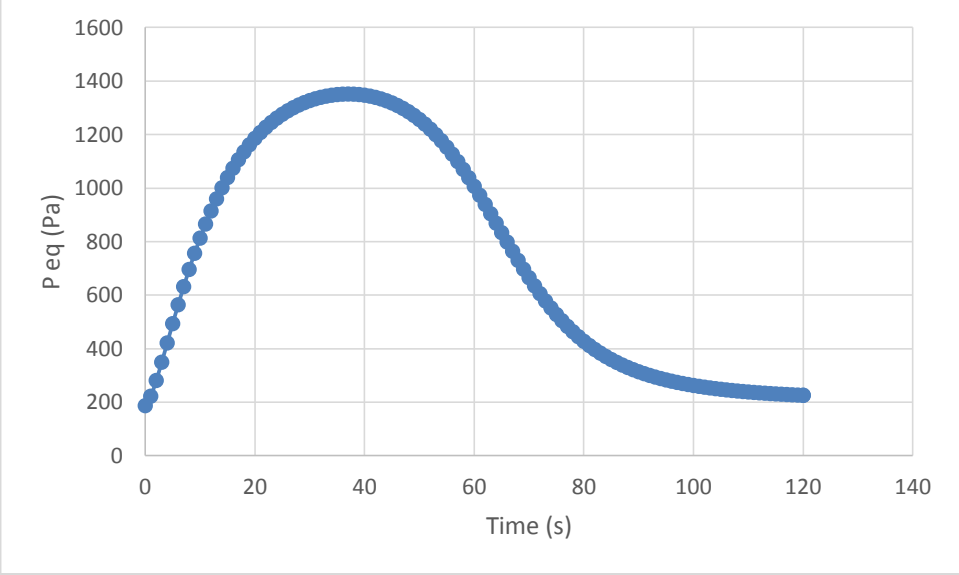

A Figure 2: Equilibrium Pressure Vs Time

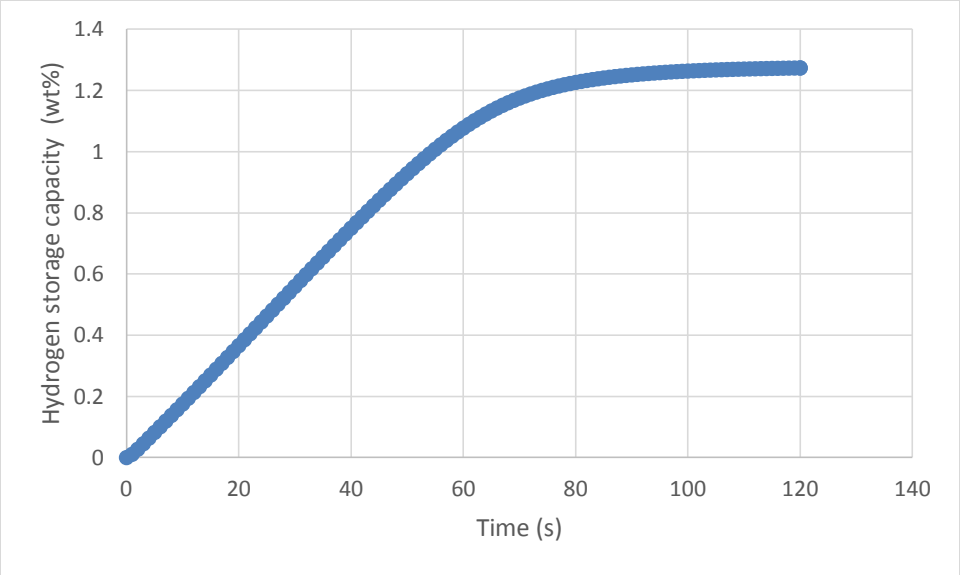

A Figure 3: Hydrogen storage capacity Vs time

A 2.2. Desorption

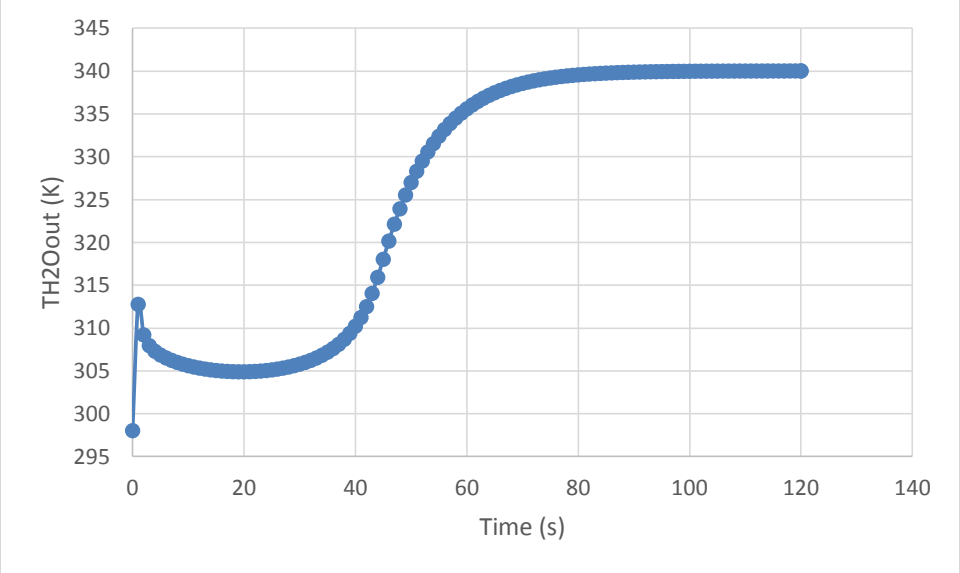

A Figure 4: Water temperature out from heat exchanger Vs Time

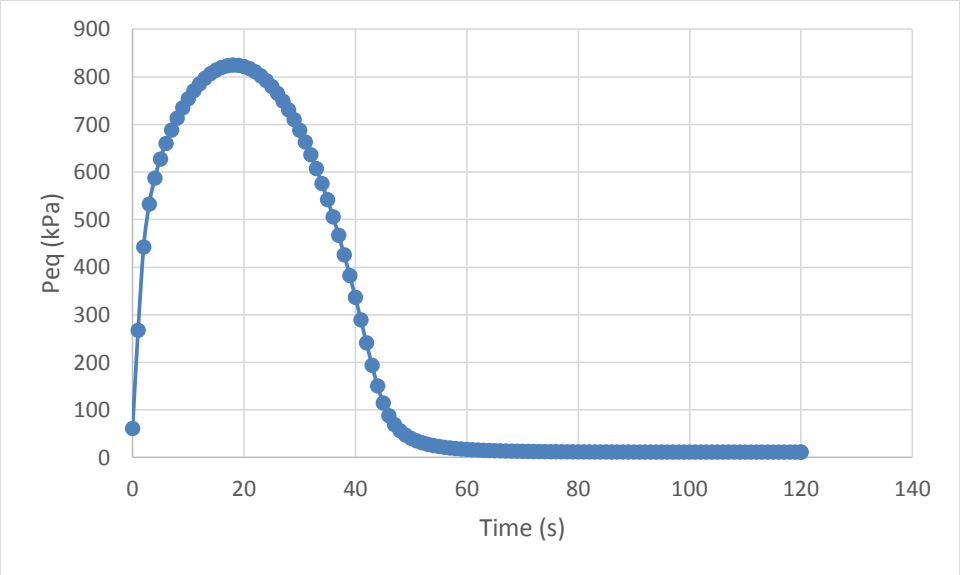

A Figure 5: Equilibrium Pressure Vs Time

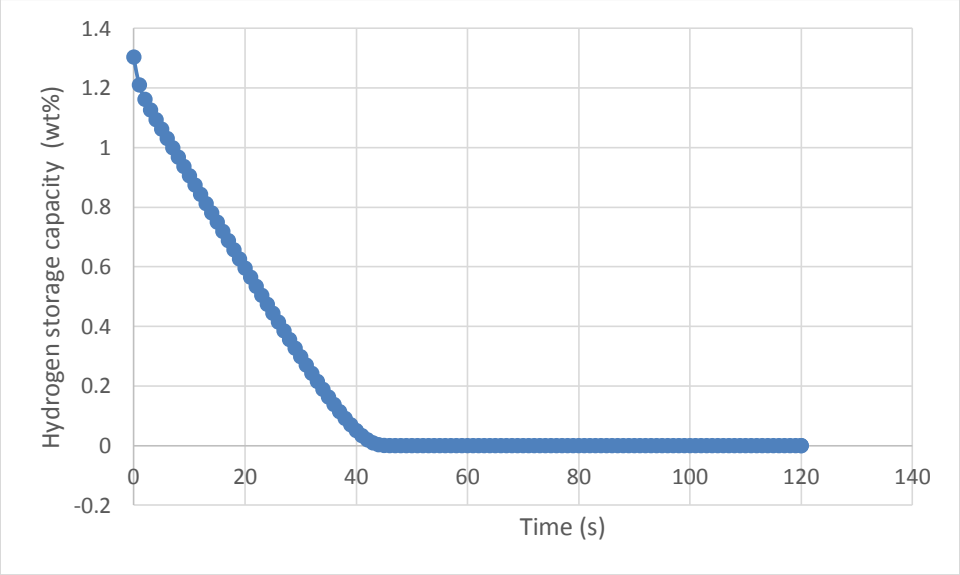

A Figure 6: Hydrogen storage capacity Vs time

A 2.3. Absorption Desorption Connection

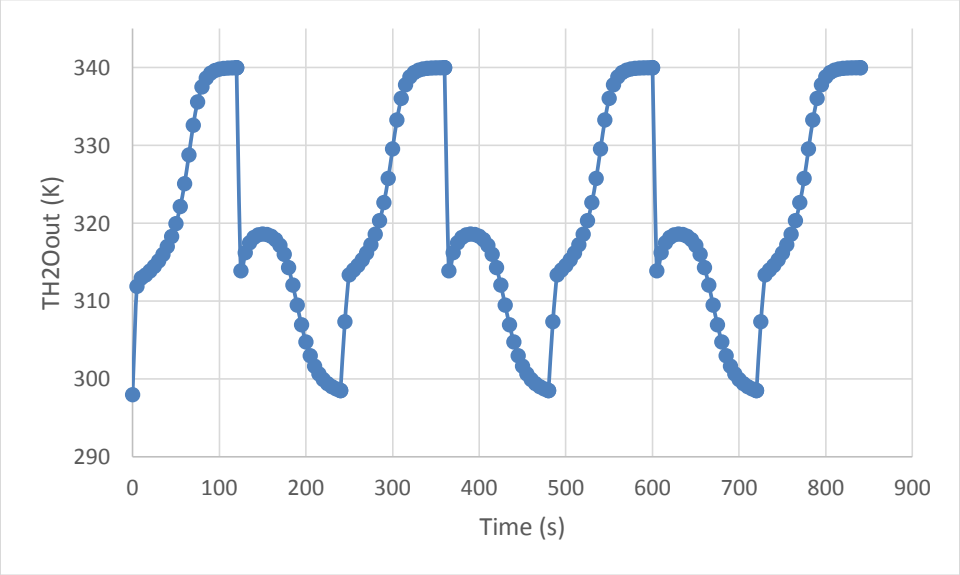

A Figure 7: Water temperature out from heat exchanger Vs Time

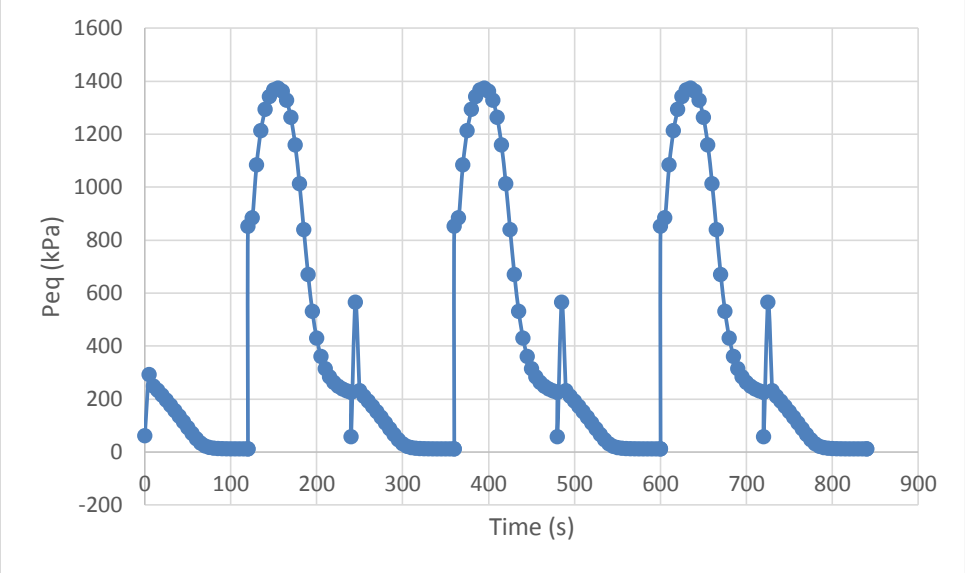

A Figure 8: Equilibrium Pressure Vs Time

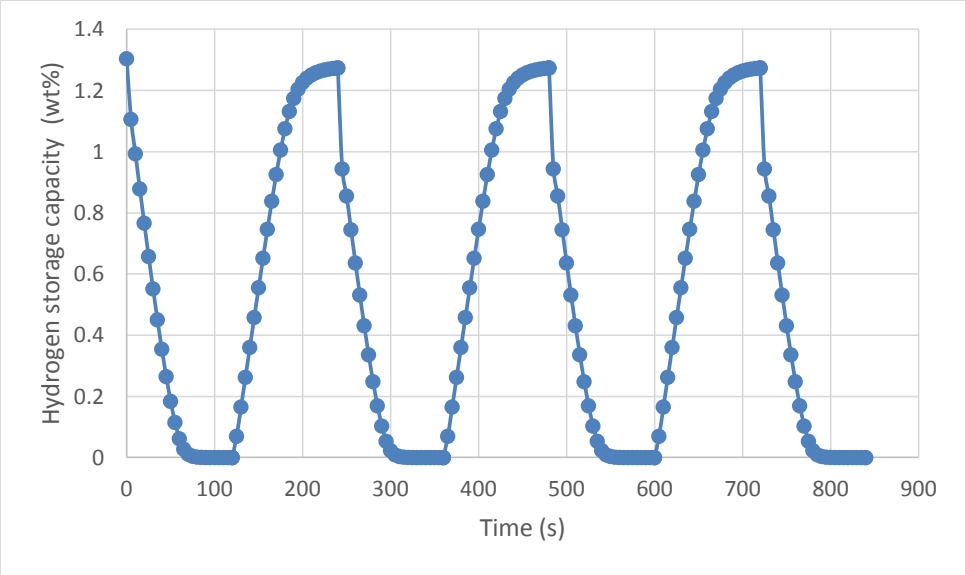

A Figure 9: Hydrogen storage capacity Vs Time

A 2.4. Desorption Fuel Cell Connection

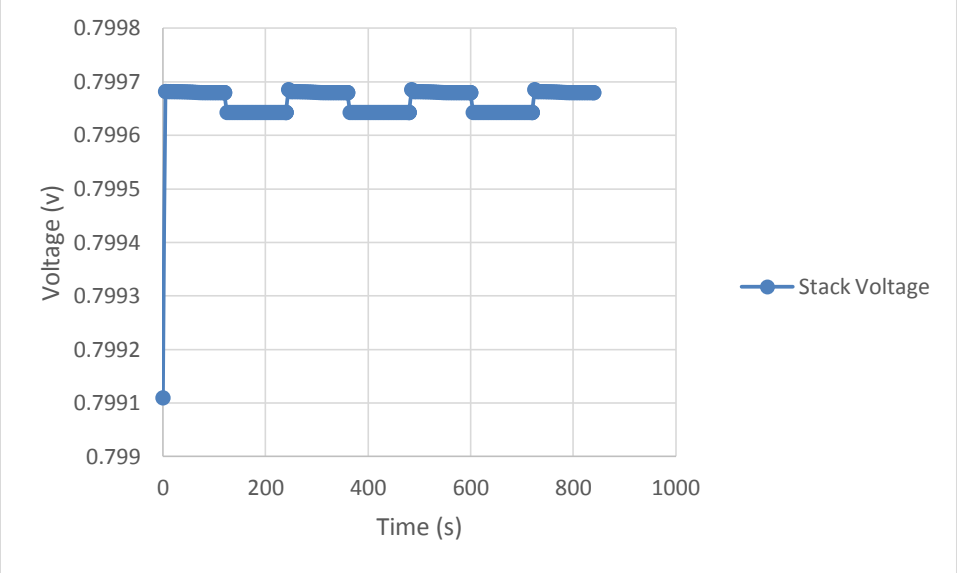

A Figure 10: Stuck voltage Vs Time

A 2.5. Closed loop PI control case results

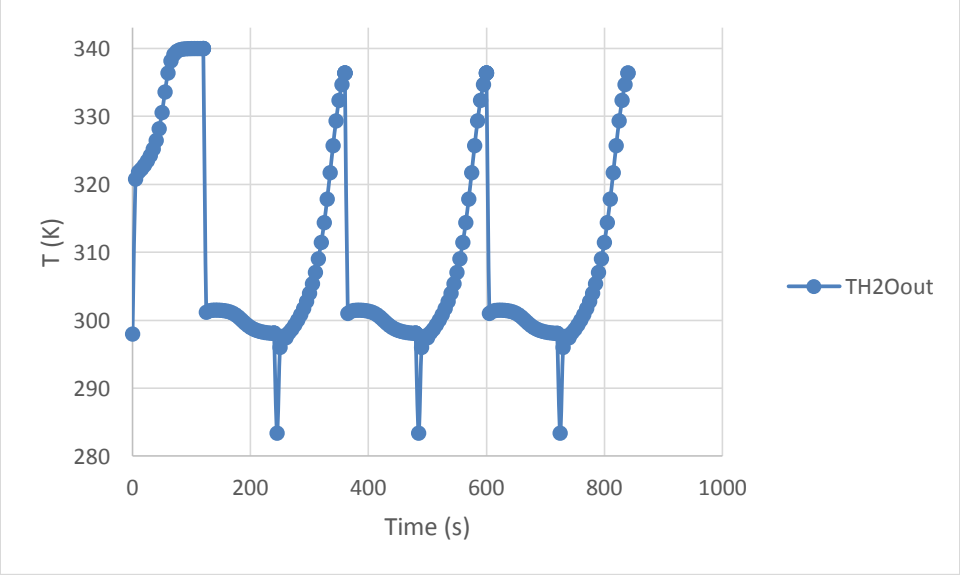

A Figure 11: Water temperature out from heat exchanger Vs Time